NASA TN D-1871

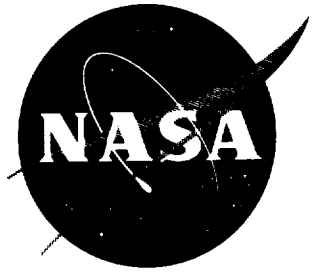

TECHNICAL NOTE

D-1871

EVALUATION OF INFRARED SPECTROPHOTOMETRY FOR COMPOSITIONAL ANALYSIS OF LUNAR AND PLANETARY SOILS

By R. J. P. Lyon

Prepared under Contract NASr-49(04) by
STANFORD RESEARCH INSTITUTE
Menlo Park, California
for

NATIONAL AERONAUTICS AND SPACE ADMINISTRATION

WASHINGTON April 1963

NATIONAL AERONAUTICS AND SPACE ADMINISTRATION

TECHNICAL NOTE D-1871

EVALUATION OF INFRARED SPECTROPHOTOMETRY FOR COMPOSITIONAL ANALYSIS OF LUNAR AND PLANETARY SOILS

By R. J. P. Lyon

SUMMARY

A preliminary feasibility study of infrared analytical techniques for the study of the lunar surface has been made, including absorption studies of 370 rock and mineral samples, and reflection studies of 80 rocks. Spectral information was collected in the wavelength range 2.5 to 25 microns (4000 to 400 cm^{-1}). Emittance spectra have been calculated from the reflectance data for several of the most important rock types.

Feasibility of absorption analysis has been established and this method is recommended particularly for use in manned laboratories.

The feasibility of near-normal specular reflection has also been established but its use also may be confined to manned laboratories because of the requirement that small, but highly polished flat surfaces must be prepared on the samples.

The feasibility of spectral emission needs to be studied further, particularly to determine the limits of applicability to materials with porous or powdery surfaces. Rocks of low porosity, and with reasonably flat surfaces are quite suitable for emission analysis, either from a stationary, surface-roving, or even an orbiting lunar vehicle.

These analytical methods are not dependent upon the crystallinity of the sample, and the composition of volcanic glasses, lavas, or crystalline rocks can be determined. The presence or absence of "water" can be determined, and its form, whether as bonded hydroxyl $(OH)^{-}$, or as loosely attached water molecules, can be defined.

TABLE OF CONTENTS

FIGURE

FIGURE

FIGURE

TABLE

SYMBOLS, ABBREVIATIONS, AND GLOSSARY

Symbols and Abbreviations

Ab	albite, plagioclase feldspar end-member
Al	aluminum
An	anorthite, plagioclase feldspar end-member
Aug	augite
cm^{-1}	reciprocal centimeters $= \frac{1}{\text{microns}} \times 1000$
En	enstatite, pyroxene end-member
Fa	fayalite, olivine end-member
Fe	iron
Fo	forsterite, olivine end-member
Hy	hypersthene pyroxene
H_2O^-	water lost on heating below 110^oC
H_2O^+	water lost on heating above 110^oC
KBr	potassium bromide
K-spar	potash feldspar
Lab	labradorite
NH_4^+	ammonium
O	oxygen
OH'	hydroxyl group
Oli	olivine
Q	quartz (as impurity)
Si	silicon
SiO_2	silica

Y	value for Al^{3+}/Si^{4+} substitution, which may range from 0 to 2
α	absorptivity
ϵ	emissivity
μ	microns
ν	frequency (in cm^{-1})
ρ	reflectivity

Spectroscopy Glossary

Absorbance, A. Logarithm to the base 10 of the reciprocal of the transmittance $A = \log_{10} (1/T)$. Equivalent to absorptance.

Absorptance is a property of a specimen; it is the ratio of the rate of absorption of radiant energy to its rate of incidence.

Absorption coefficient is a fundamental property of a material. It is a quantitative expression for the rate of decrease in radiant flux density in the direction of propagation of radiant energy through a material. Expressed mathematically,

$$W = W_0 e^{-ax} \qquad (I)$$

in which: W = flux density after passing through thickness x of the nonscattering material, W_0 is the flux density at zero thickness just after penetrating the surface (thus not including the reflected portion of the incident radiation), a is the absorption coefficient, and e is the base of natural logarithms.

Absorptivity is a special case of absorptance, it is a fundamental property of a material, and is measured as the absorptance of a specimen of the material that has an optically smooth surface and is sufficiently thick to be completely opaque.

Absorptivity, Molar: Product of the absorptivity, and the molecular weight of the substance.

Emissive power is the rate of thermal emission expressed as radiant flux per unit surface area.

Emissivity is a special case of emittance; it is a fundamental property of a material, and is measured as the emittance of a specimen of the

material that has an optically smooth surface and is sufficiently thick to be opaque.

Emittance is a property of a specimen; it is the ratio of its emissive power to that of a blackbody radiator at the same temperature and under the same conditions.

Extinction coefficient is a fundamental property of a material. It is a quantitative expression for the rate of decrease of radiant flux density in the direction of propagation of radiant energy through a material, due to both absorption and scattering. It is expressed mathematically by Eq. (I), in which case a represents the extinction coefficient.

Frequency: Number of cycles per unit time.

Infrared: The region of the electromagnetic spectrum extending from approximately 0.78 to 300 microns.

Micron: Unit of length equal to 10^{-6} meter.

Radiant flux is the rate of flow of radiant energy. It is analogous to current as applied to electricity.

Reflectance is a property of a specimen and is the ratio of the rate of reflection of radiant energy to its rate of incidence.

Reflectivity is a special case of reflectance; it is a fundamental property of a material, and is measured as the reflectance of a specimen of the material that has an optically smooth surface and is sufficiently thick to be completely opaque.

Scattering coefficient is a fundamental property of a material. It is a quantitative expression for the rate of decrease in radiant flux density in the direction of propagation of radiant energy through a material, due to scattering. It is expressed mathematically by Eq. (I), in which case a represents the scattering coefficient.

Spectral: Having a stated wavelength, or at a stated wavelength.

Spectrograph: Instrument with an entrance slit and dispersing device that uses photography to obtain a record of spectral range. The radiant power passing through the optical system is integrated over time, and the quantity recorded is a function of radiant energy.

Spectrometer, Optical: Instrument with an entrance slit, a dispersing

device, and with one or more exit slits, with which measurements are made at selected wavelengths within spectral range, or by scanning over the range. The quantity detected is a function of radiant power.

Spectrophotometer: Spectrometer with associated equipment, so that it furnishes the ratio, or a function of the ratio, of the radiant power of two beams as a function of spectral wavelength. These two beams may be separated in time, space, or both.

Thermal emission is the act or process by which radiant energy is emitted by a body as a consequence of its temperature only. This is frequently shortened to "emission".

Transmittance is a property of a specimen; it is the ratio of the rate of transmission of radiant energy to its rate of incidence.

Wavelength: The distance, measured along the line of propagation between two points that are in phase on adjacent waves—units A., $m\mu$, and μ.

Wavenumber: Number of waves per unit length. The usual unit of wavenumber is the reciprocal centimeter, cm^{-1}. In terms of this unit, the wavenumber is the reciprocal of the wavelength when the latter is in centimeters in vacuo.

Mineralogy Glossary

Acid rock	igneous rock with high percentage of SiO_2-rich minerals; light colored
Acmite	a pyroxene; usually $NaFeSi_2O_6$
Actinolite	an amphibole in the tremolite-actinolite series; approximate composition, $Ca_2(Mg,Fe)_5(Si_8O_{22})(OH)_2$
Albite	soda-plagioclase; usually $NaAlSi_3O_8$
Alkali halide	KBr, KCl, KI; materials used for pellets having no marked absorption in the wavelength under consideration
Almandite	a garnet; usually $Fe_3Al_2(SiO_4)_3$
α-alumina	form of alumina, Al_2O_3, with an ilmenite structure
α-β inversion	a change in the structure of quartz which occurs at about 573°C

α-cristobalite	low-temperature form of cristobalite (SiO_2); stable below 250°C
α-quartz	low-temperature form of quartz (SiO_2) stable below 573°C
Ammonium illite	illite with exchangeable NH_4^+ in the interlayer position
Ammonium zeolite	a zeolite with exchangeable NH_4^+
Amphibole	a mineral group with the general formula $(W,X,Y)_{7-8}(Z_4O_{11})_2(OH)_2$, where W is Ca or Na, X is Fe^{2+} or Mg, Y is Ti, Al, or Fe^{3+}, and Z is Si or Al
Analcite	a zeolite; usually $NaAlSi_2O_6 \cdot H_2O$
Anauxite	a form of kaolinite of uncertain composition
Andesite	a volcanic rock composed mainly of andesine plagioclase (An_{45}) and pyroxenes or amphiboles
Andradite	a garnet; usually $Ca_3Fe_2(SiO_4)_3$
Anorthite	calcic plagioclase; usually $CaAl(AlSi_2O_8)$
Anorthosite	a plutonic rock composed mainly of plagioclase
Anthophyllite	an amphibole; approximate composition, $(Mg,Fe)_7Si_8O_{22}(OH)_2$
Ash	volcanic debris of less than 4-mm diameter
Augite	a pyroxene; approximate composition, $Ca(Mg,Fe,Al)(Al,Si)_2O_6$
Australite	a tektite found in Australia
Bayerite	β-alumina trihydrate; an artificial product occurring in the Bayer process
Beidellite	an aluminum montmorillonite clay
Beryl	usually $Be_3Al_2Si_6O_{18}$ and commonly containing Na, Li, and Cs
Biotite	a mica; approximate composition, $K(Mg,Fe)_3(AlSi_3)O_{10}(OH)_2$; usually brown
Birefringence	double refraction; the difference between the greatest and least indices of refraction
Boehmite	usually AlO(OH)

Calcite	$CaCO_3$, with a hexagonal structure
Cassiterite	SnO_2 with a rutile structure
Chlorite	green micaceous mineral; approximate composition, $(Mg,Fe,Al)_6(Al,Si)_4O_{10}(OH)_8$
Chondrite	meteorite containing rounded bodies of silicate materials
Chrysocolla	usually $CuSiO_3 \cdot H_2O$
Clinoamphibole	an amphibole with monoclinic structure
Clinoenstatite	the high temperature form of enstatite with monoclinic structure
Clinohypersthene	the high temperature form of hypersthene with monoclinic structure
Clinopyroxene	pyroxene with monoclinic structure
Coesite	high density polymorph of silica (SiO_2) with a specific gravity of 3.2
Cordierite	approximate composition, $(Mg,Fe)_2Al_4Si_5O_{18}$
Cristobalite	polymorph of silica (SiO_2) with tetragonal structure at low temperatures and isometric structure at high temperatures
Cummingtonite	an amphibole; approximate composition, $(Fe,Mg)_7Si_8O_{22}(OH)_2$
Cyclosilicate	silicate structure formed by closed rings of tetrahedra each sharing two oxygens (Si_6O_{18})
Diabase	a rock of basaltic composition consisting mainly of pyroxene and plagioclase, but with a coarser texture
Diadochy	replacement of one atom with another in the same place in a crystal structure
Dickite	polytype of kaolinite containing two kaolin layers in the unit cell; usually $Al_4Si_4O_{10}(OH)_8$
Dioctahedral	octahedral layer in a mica or clay with only two of the three sites occupied, usually by aluminum
Diopside	a pyroxene; usually $CaMgSi_2O_6$

Ellipsoid (optical)	a surface formed by light wavefronts after the rays have traveled for unit time through a material
Enstatite	a pyroxene; usually $MgSiO_3$
Emerald	a gem quality beryl
Fayalite	olivine; usually Fe_2SiO_4
Feldspar	a group of aluminum silicates of potassium sodium, and calcium; abundant as rock forming minerals
Ferri-celadonite	a green mica; usually $KFe_2Si_4O_{10}(OH)_2$
Fe-sanidine	ferric iron analog of sanidine feldspar
Fe-microcline	ferric iron analog of microcline feldspar
Fire clay	structurally disordered kaolinite clay
Forsterite	olivine; usually Mg_2SiO_4
Fused silica	SiO_2in a glassy form
Gabbro	plutonic rock or calcic plagioclase and clinopyroxene
γ-alumina	Al_2O_3 with a spinel structure
Garnet	mineral group; approximate composition, $X_3Y_2(SiO_4)_3$, where X is Ca, Mg, Fe^{2+}, or Mn, and Y is Al, Fe^{3+}, or Cr
GeO_2-quartz	GeO_2 with a quartz structure
GeO_2-rutile	GeO_2 with a rutile structure
Gibbsite	usually $Al(OH)_3$; α-alumina trihydrate
Glass	a supercooled non-crystalline substance
Glauconite	a green micaceous mineral; approximate composition $K(Fe,Mg,Al)(AlSi_3O_{10})(OH)_2$
Glaucophane	an amphibole; usually $Na_2Mg_3Al_2Si_8O_{22}(OH)_2$
Goethite	usually $FeO(OH)$
Grandite	term for the garnet group grossularite, andradite, and occasionally uvarovite

Granite	a plutonic rock; mainly alkali feldspar and quartz; coarse grained and light colored
Grossularite	a garnet; usually $Ca_3Al_2(SiO_4)_3$
Gypsum	usually $CaSO_4 \cdot 2H_2O$
Halloysite	a kaolinite clay, generally with a tubular form
Hedenbergite	a pyroxene; usually $CaFeSi_2O_6$
Hornblende	an amphibole; approximate composition $NaCa_2(Mg,Fe,Al)_5(Al,Si)_8O_{22}(OH)_2$
Hypersthene	a pyroxene; approximate composition, $(Mg,Fe)SiO_3$
Idocrase	or vesuvianite; usually $Ca_{10}Mg_2Al_4(Si_2O_7)_2(SiO_4)_5(OH)_4$
Illite	a group of micaceous minerals, generally considered to be interlayed muscovite and montmorillonite
Inosilicate	silicate structure formed by chains of tetrahedra sharing two or three oxygens; examples are amphiboles and pyroxenes
Jadeite	a pyroxene; usually $NaAlSi_2O_6$
Kaolinite	aluminum silicate clay; usually $Al_4Si_4O_{10}(OH)_8$
K-spar	potash feldspar; a compositional term
Labradorite	a plagioclase feldspar intermediate between albite and anorthite; approximate composition, $(Ca,Na)(Al,Si)AlSi_2O_8$
Lava	volcanic rock; originally fluid
Lawsonite	usually $CaAl_2Si_2O_7(OH)_2 \cdot H_2O$
Li-biotite	lithium-bearing biotite
Li-phlogopite	lithium-bearing phlogopite
Lucite	plastic used for mounting specimens
Mare Imbrium	name of the largest "sea" on the lunar surface visible from the earth

Maria	or "sea"; a large, flat, dark area on the moon
Meteorites	extra-terrestrial material that has landed upon the earth; often composed of metallic and stony materials.
Microcline	potash feldspar with a triclinic structure; usually $KAlSi_3O_8$
Mineral oil	or Nujol; used as a mulling agent for sample preparation
Modal analysis	the mineralogical composition of an unaltered igneous rock, as contrasted with normative composition
Montmorillonite	a clay; approximate composition, $(K,Na,Ca)(Al,Mg,Fe)(Al,Si)_4O_{10}(OH)_2$
Mullite mortar	mortar composed of $Al_6Si_2O_{13}$, a synthetic mineral
Muscovite	a white aluminous mica; usually $KAl_2(AlSi_3O_{10})(OH)_2$
Nacrite	polytype of kaolinite containing six kaolin layers in the unit cell
Nesosilicate	silicate structure composed of independent tetrahedra
Normative analysis	a calculated mineralogical composition of an unaltered igneous rock using a group of "standard" minerals rather than those which might be present
Obsidian	a volcanic glass; typically of rhyolitic composition
Octahedral coordination	the six-fold coordination present at the center of an octahedron
Olivine	a mineral group; approximate composition, $(Mg,Fe)_2SiO_4$
Omphacite	a green pyroxene intermediate between augite and jadeite; approximate composition, $(Na,Ca)(Mg,Fe,Al)(Si,Al)_2O_6$

Opal	amorphous silica; usually $SiO_2 \cdot nH_2O$
Orthoamphibole	amphibole with an orthorhombic structure
Orthopyroxene	pyroxene with an orthorhombic structure
Paragonite	sodium-muscovite mica; approximate composition, $NaAl_2(Al,Si)_4O_{10}(OH)_2$
Peridotite	a non-felspathic plutonic rock consisting mainly of olivines
Perlite	volcanic glass; usually with a higher water content than obsidian
Pigeonite	a pyroxene intermediate between clinoenstatite and clinohypersthene
Phlogopite	a mica; approximate composition, $KMg_3(Al,Si)_4O_{10}(OH)_2$
Phyllosilicate	silicate structure of continuous sheets of tetrahedra each sharing three oxygens
Plagioclase	sodium-calcium feldspar; approximate composition, $(Na,Ca)(Al,Si)AlSi_2O_8$
Plutonic	deep-seated origin
Pollucite	cesium-bearing beryl
Polymorph	a substance which may crystallize in several distinct forms
Polytype	a stacking condition in micas wherein different orientations are maintained in successive layers
Potash feldspar	potassium feldspar; usually $KAlSi_3O_8$ of several structural types
Pyralspite	term for the garnet group pyrope, almandine and spessartite
Pyrex	a borosilicate glass
Pyrope	a garnet; usually $Mg_3Al_2(SiO_4)_3$
Pyroxene	a mineral group; approximate composition, $(W,X,Y)_2Z_2O_6$, where W is Ca or Na, X is Mg,Fe^{2+}, or Mn, Y is Al, Fe^{3+}, or Ti, and Z may be Si or Al
Quartz	SiO_2 with a hexagonal structure

Trioctahedral	octahedral layer in a mica, or clay with all three sites occupied, usually by Mg or Fe
Turquoise	copper phosphate
Tuff	a rock formed of compacted volcanic debris, usually less than 4 mm in diameter
Uvarovite	a garnet; usually $Ca_3Cr_2(SiO_4)_3$
Volcanic	of igneous extrusive origin
Wairakite	a zeolite
X-cut quartz	a quartz plate cut parallel to the optic axis and normal to X
Y-cut quartz	a quartz plate cut parallel to the optic axis and normal to Y
Z-cut quartz	a quartz plate cut perpendicular to the optic axis; a basal cut
Zeolite	minerals of the hydrous alumino-silicate groups; characterized by their easy and reversible loss of water
Zeolitic water	the water which may be easily and reversibly lost from a mineral

INTRODUCTION

For many years the predominant use of the infrared spectrophotometer has been for the structural analysis of organic materials. Recently it has been applied in the inorganic and mineralogical[1-4] fields, although its value as a quantitative tool[5] has been little utilized in compositional analysis of rocks.

The analysis of reflected infrared radiation from polished surfaces of minerals and rocks is an almost unexplored field, except for the works of Coblentz[6,7] and Pfund,[8] and classic studies of Simon and McMahon,[9,10] and Gardon[11] on the radiative cooling properties of glass slabs.

The spectral analysis of emitted infrared radiation has been given prominence of late, with the studies of nose-cone re-entry and the attendant problems of heat dissipation from refractory coatings. Again, however, the wavelength range of this interest is in the near infrared, 1 to 5 microns (10,000 to 2,000 cm^{-1}), and little investigation has been made in the region of diagnostic analysis for rock and mineral composition, i.e., the region of 10 to 25 microns (1000 to 400 cm^{-1}) and beyond.

With an eye to the ultimate application of infrared instrumentation in a system for remote mapping of surfaces like that of the moon, a need was felt for more complete understanding of the fundamentals of infrared spectra, either absorption, reflection, or emission, so that the complicating effects of compositional change within mineral species in a rock could be evaluated at the same time as the mineral content was determined.

From preliminary studies[2,4] it was felt that infrared analysis offered a tool of great potential value for compositional analysis of rocks and minerals. There were several immediate problems to be faced, however, before we could proceed to these goals. These problems can be readily imagined if one likens the state-of-the-art of infrared mineralogical analysis to that obtaining in the x-ray diffraction field about 30 years ago. Although there had been several broad surveys,[4,12,13] little had been done to examine the change of spectra with compositions

within mineral groups. Quantitative studies were rare and mostly related to determination of quartz, calcite and some clays; and rock analysis for mineral content (modal analysis) had only been briefly studied.

Almost without exception all the data pertained to absorption analyses, and sample preparation techniques were long, involved, and obviously not capable of being automatically performed under lunar conditions.

With the growing possibility of soft lunar landings, it was felt that samples could be presented to a spectrophotometer which was either fixed on or moving over the lunar surface. With further study it might be possible to suitably analyze infrared emission spectra from the lunar surface from an orbiting vehicle. Such surveys would be aided by the hard lunar vacuum, for on the earth the interference from atmospheric absorption plagues measurement of this type.

In January 1961 Stanford Research Institute (SRI) undertook a program of research with the following objectives:

1. To evaluate the absorption spectra of a series of assemblages of naturally occurring mineral phases under optimum laboratory conditions;

2. To evaluate the possibility of the use of an infrared spectrophotometer as a tool in a mapping system, on a moving surface vehicle or an orbiting space craft, using the reflected or emitted infrared radiation from the moon's surface;

3. To evaluate the possibility of instrumenting an infrared system compatible with operational specifications for a soft-landing spacecraft in the lunar environment.

CONCLUSIONS

A total of 370 infrared absorption analyses of selected rock and mineral specimens were run in the wavelength region 2.5 to 25 microns (4000 to 400 cm^{-1}). About 80 infrared reflection curves were prepared from polished surfaces of rock specimens over the same spectral region. A reasonably complete atlas of these curves (300) has been included in this report. Series of assemblages of these minerals, occurring naturally as rocks, or prepared synthetically as mixtures have been studied by these techniques.

The feasibility of infrared absorption analysis in an earth- or moon-based laboratory is clearly shown. The usefulness of near-normal specular reflection analysis to determine rock composition is also shown, provided one can secure a well-polished flat surface (about one-half of a square inch in size) on the specimen. By applying Kirchhoff's law, under thermal equilibrium conditions, one can calculate the spectral emittance curves of the (polished) surface at any given temperature. Such emittance curves are important prerequisites for the interpretation of the data from remote mapping[14,15] of the lunar surface.

It remains to be shown that infrared spectral emission analysis can be performed on lunar materials with porous or powdery surfaces. Solid materials with high porosity (or loosely packed powders) emit radiation close to that of a blackbody, and this bears little or no spectral information. However, rocks of low porosity, and with reasonably flat surfaces would be quite suitable for compositional analysis, either from a stationary, surface-roving, or even an orbiting lunar vehicle. Spectral emission of reasonable quality has been obtained[16,17] from sand-sized materials, with a mobile spectrophotometer using the emitted infrared radiation from quartz and gypsum sands. A fine dust layer such as has been predicted to be on the lunar surface would present a problem. However, bare rocks that are free from dust, such as those recently broken by meteorite impact, or cliffs and slopes too steep to hold a dust layer, should offer no problems of this type.

Grain size variations in rocks, ranging from those of a coarse volcanic rock to glassy lava with only random "molecules", do not present problems--in fact, the compositions of glassy materials can be readily deduced from infrared analysis data. The presence or absence of "water" may be determined, and its form, whether as bonded hydroxyl (OH)', or as loosely attached water molecules, can be defined by these analytical techniques.

The use of an infrared spectrophotometer as a tool in a lunar-mapping system has been evaluated. Operational specifications have been developed for such an instrument if placed upon an orbiting or surface-roving vehicle, and if utilizing the spectral emittance of infrared radiation of the lunar surface materials. Soft-landing, unmanned spacecraft could also utilize spectral reflectance analysis if small, highly polished surfaces could be prepared on samples under lunar conditions.

EXPERIMENTAL METHODS

A. Sample Acquisition

While some of the infrared analysis studies of minerals appearing in the literature are characterized by careful research a lot of the published data suffers from two faults--either the spectroscopist knew little or no mineralogy, or the mineralogist was not working with someone familiar with the technique of spectroscopy. There are even several cases in the literature of spectra for the wrong minerals being recorded, and impurities (e.g., quartz) are often to be noted in the spectra.

To avoid this a most concerted effort was made to secure samples, from research mineralogists, that they themselves were working upon. Most samples were inspected under the binocular microscope when received; and, if found to be impure, heavy density and magnetic separations were made to procure clean material for analysis. As only 10 to 15 mg were required for the absorption method, the material was sometimes handpicked for purity before analysis.

A study of this complexity could not have been performed without the assistance of a large group of mineralogists and geologists who supplied "standardized" samples. Acquisition of these 400 samples was made possible by the generosity of the people from all over the world who have responded to letters requesting analyzed materials for this new type of compositional analysis.

The rock samples (G-1 granite, W-1 diabase, and SY-1 syenite) are the powdered "standards" familiar to all who have performed emission spectrographic analysis. Unfortunately, no solid materials were to be had, and only "powder-mounts" in lucite plastic molds could be used.

The bulk of the rocks still require thin-section analysis before their true modes can be defined, but the samples covered a wide range of rock compositions. Several samples provided by R. C. Speed of Jet Propulsion Laboratories (JPL) were those on which he was performing

x-ray diffraction analyses. The meteorites came from a study collection of A. A. Loomis, also of JPL (see Table I).

B. Absorption Analysis

1. Sample Preparation

a. Potassium Bromide (KBr) Pellets

The discovery that a solid sample may be mixed at a low level of concentration with a powdered alkali halide, and then pressed into a clear solid disc or pellet for analysis has revolutionized the preparatory steps for insoluble materials. The KBr pellet technique has been shown by many[4] to be the most satisfactory method for handling rock and mineral samples for infrared analysis, and has been the principal method used for absorption analyses in this study.

The concentration of sample in the KBr is selected to yield the level of absorption of the infrared beam which produces almost full scale deflection in the region of interest. For silicates this is 9 to 10 microns, and from 0.15% to 0.25% is a suitable level.

Excellent infrared absorption spectra of minerals and rocks can be obtained with KBr discs containing about 1/4% of the sample in question. A well tested method of preparation involves hand grinding 10 mg of the sample with 10 drops of absolute alcohol in a 60-mm mullite mortar, until the alcohol evaporates. This reduces the grain size to below 5 microns (about 50% minus 2 microns) and minimizes effects[21] due to particle size. One and one-half milligrams of this preground sample are added to 1.00 gm of infrared quality KBr and blended in a dentists amalgamator (Wig-L-Bug). About 350 mg of the blend is weighed out to form a disc of the desired thickness, and pressed in a vacuum die. About 65 tons pressure per square inch is adequate to obtain permanently clear discs which have been stored and re-used years later.

It has been found necessary to grind the samples under alcohol because the structure of many minerals, particularly those containing

Table I

SAMPLES FOR INFRARED REFLECTION ANALYSES

Sample	Location and Description	Origin
Quartz	Oscillator plates (X-, Y-, Z-cuts)	SRI
Coesite and Stishovite	Meteor Crater, Arizona (residue from HF leaching of impacted Coconino sandstone)	D. E. Milton U.S. Geological Survey (USGS)
Granite	(Hard Hat) Nevada Test Site, Nevada. Medium grained granodiorite	N. Short University of California, Lawrence Radiation Laboratory (LRL)
Anorthosite	San Gabriel Mtns, Calif.	R. C. Speed JPL
Dunite	Twin Sisters, Calif.	
Rhyolite	Soledad, Calif	
Granite	Town Mtn., Calif	
Gabbro	San Marcos, Calif.	
Katmai ash	Katmai, Alaska	J. Whelan, Univ. of Utah
Gabbro, Stillwater	Stillwater, Montana	D. Jackson, USGS
G-1 Granite and W-1 diabase	Spectrographic standards	USGS
SY-1 syenite	Spectrographic standards	Canadian Spec. Soc.
Tektite (australite)	Victoria, Australia	C. Baker, Commonwealth Scientific and Industrial Research Organization (CSIRO)
Obsidian	Clear Lake, Calif.	G. Parks, Stanford University
Basalt, Kilauea Iki	Kilauea Iki, Hawaii, flow	C. Matthews, SRI
Basalt, Pisgah	Pisgah Crater, Calif.	W. B. Beatty, SRI
Meteorites (chondritic)	Various falls as below,	A. A. Loomis, JPL
Brüderheim	Alberta, Canada (1960)	
Potter	Cheyenne Co., Nebraska (1841)	
Ladder Creek	Greely Co., Kansas (1937)	
Haven	Kansas	

OH'groups in the lattice, can be altered in a few minutes by vigorous dry grinding. By using consistent preparatory grinding coupled with adequate blending, quantitative analyses[4,5] can be obtained with standard mineral specimens.

b. Other Possible Preparation Techniques

Nujol Mulls and Deposited Films. Hunt[1-2] described the use of deposited films of finely divided minerals on rock salt windows for infrared studies. Miller and Wilkins[18] compiled an excellent catalog of inorganic spectra obtained using mineral oil mull techniques. The value of the infrared spectra of minerals has been further demonstrated by a number of other workers in the field who used one or the other of these techniques or modifications of them.

The deposited film technique yielded excellent spectra beyond about 4 microns, but was relatively tedious and time consuming. There was a further possibility of modification of the composition of a mixture because of gravity separation of the components during settling. The mineral oil mull technique suffered from the presence of interfering absorption bands and lack of the desired degree of control for quantitative purposes.

Samples as Pastes on Aluminum Substrates. Uhlrich[19] in an article on uses of near-normal specular infrared reflectance gives a good review of methods for obtaining absorption spectra by reflection off an aluminum-mirror substrate. The infrared beam impinges almost normally, onto a thin clay coating, passes through to the mirror, is reflected back through the clay layer again, and emerges. The beam is then scanned by the spectrophotometer which produces an absorption spectra of the clay. Hannah[20] has found this method very useful when analyzing oxide coatings, paint layers, etc., on metals.

Attenuated Total Reflectance. A very new technique has been developed for obtaining an absorption spectrum by the reflection of an infrared beam at a prism-sample interface. This may yield a new lunar

preparation method, but as yet we have not adequately developed our understanding of the method. It will be difficult under lunar conditions, to attain optical contact between the sample and prism, without the use of immersion media, but more experience is needed at this stage.

2. Spectrophotometer Settings

The settings for the Perkin-Elmer 221 prism grating spectrophotometer are listed in Table II, for both prisms in the wavelength range 2.5 to 25 microns (4000 to 400 cm^{-1}).

Table II

SPECTROPHOTOMETER SETTINGS FOR INFRARED ANALYSIS

(Perkin-Elmer PE 221)

	NaCl Prism-Grating	KBr Prism
Wavelength	2.5 to 15 microns	10 to 25 microns
Wavenumber	4000 to 667 cm^{-1}	1000 to 400 cm^{-1}
Slit Program	927	945 - 2x (calibration) 910 - 2x (specimen)
Calibration Points	3737, 1600, 667 cm	993, 908, 419 cm
Gain	4	5
Attenuator Speed	11:00	11:00
Scan Time Setting	16	5
Suppression	7	7
Scale	1x	1x
Source Current	0.32 amp	0.32 amp

C. Reflection Analysis

The experimental techniques for reflection analysis are complicated by two factors--that of preparing a polished surface, and that of operation of the spectrophotometer. Standard polishing methods as used in the preparation of metallurgical specimens were used.

1. Sample Preparation

a. Solid Samples

A polished surface of the highest quality is prepared, over a flat surface about 1/2-in.^{2}. If the sample is a single crystal then the orientation of that polished face should be recorded, as it will clearly influence the spectrum obtained (see Section B, p. 35 and Fig. 47 for further discussion).

b. Powdered Samples

Powdered samples can be mixed with powdered lucite* and briquetted (as for a metallurgical specimen) and then polished in the standard manner. Obviously there will be less reflective surface of the sample in the beam than for a solid sample, and the reference beam may need attenuation to secure adequate response from the spectrophotometer. Figure 56 shows the first analyses we made for powdered dunite and gabbro samples compared with the spectra of their solid equivalents. The use of powdered samples is an important area for further development. "Synthetic" rock mixtures can be readily prepared and analyzed, or compared with those of unknown rock samples, by a simple matching process.

2. Spectrophotometer Settings

For infrared spectral reflection analysis it is necessary to attach a small mirror system in one beam of the spectrophotometer.[19] This mirror deflects the beam sideways onto the polished surface at an incident angle of almost 90 deg. The radiation when reflected by the surface is caught on a second mirror, and passes again along the original optical path into the instrument. The setting of these mirrors, the angle of attachment of the polished surface, and the attenuation of the reference beam are all parameters which must be kept optimum.

---

* A plastic must be used which has no reflection spectrum in this region.

D. Emission Analysis

We have tried only the briefest experiment in emission analysis, in which a powdered sample was heated to about 400°C outside a small metal furnace. The reference sample was carbon-black. The work is far too premature to be reported, but the spectral analysis of solid and powdered samples from 400°C down to ambient temperatures should be studied.

Discussion on p. 43 - 44 and 50 - 54 covers the most common method of obtaining emittance data--that of subtracting the reflectance of a polished surface, at thermal equilibrium, from the emission curve at that temperature for a blackbody.

E. Sample Parameters

1. Particle Size

The physical nature of the sample being studied by infrared analysis is very important, and this factor has been rather extensively but by no means exhaustively studied.

Duyckaerts[21] has drawn attention to several difficulties that are encountered when working with solid materials in making infrared absorption studies. Our experimental work[4] agrees with the conclusions of Duyckaerts that control of particle size is of vital importance. This control is necessary in absorption and reflection spectra measurements regardless of whether samples are handled as suspensions in KBr, as mineral oil mulls, or a deposited films.

The grinding method described in Sec. 1, p. 10 insures reproducibility of sample particle size. We have produced several thousand infrared absorption curves from all types of materials over the past seven years and have obtained good resolution of spectra. But particle size control clearly is a vital problem away from a manually operated (terrestrial) laboratory, where such sample preparation is not possible.

This is one reason why the emphasis in this laboratory has shifted to studies of reflection spectra[10,22] from polished slabs of minerals and rock surfaces where scattered radiation is at a minimum. To be of practical service to an orbiting spacecraft or even to a roving surface vehicle the technique must be able to produce diagnostic spectra without extensive preparatory steps. It is shown on p. 50 - 54 that thermally emitted infrared radiation has most of the spectral information as that in the absorption spectrum obtained from a powdered sample in a KBr pellet, or in the reflected spectrum from a polished face of the sample.

2. Orientation and Grain-Size

An important difference exists between an powdered sample and a single crystal of the material. As in x-ray diffraction, powdered samples present random orientations to a beam of radiation while a single crystal presents a unique orientation. A quartz plate cut normal to the optic axis (Z-cut) will show a different response from one cut parallel to the optic axis (X- or Y-cut).*

Because most infrared reflection studies of minerals (and gems) are made upon single crystals, one must determine the structural orientation of the crystal face (or cut-face) being examined. This is avoided in studies of glasses due to the relatively random internal orientation in liquids, and this condition may be approached in fine-grained, polycrystalline materials if their grain size is small relative to the area being irradiated (an area of about 1/2 x 1/4 in. in most spectrophotometers). Preferred orientation of the crystals should be avoided in the sample; otherwise spatial directions must be given. Most volcanic and intrusive rocks show no preferred orientation. Nonfoliated sediments and metamorphic rocks may show no preferred orientation, but those with planar structures will show preferred orientation effects.

* For a clearly drawn figure showing possible cuts in quartz crystals, and their code designations, see Berry and Mason,[29] p. 206.

3. Mineral Mixtures

a. Plagioclase Series Minerals

To explore the effect of changing composition upon spectra the plagioclase series was investigated. The plagioclase feldspars are often cited as examples of solid solution, wherein the composition may pass gradually from that of the sodic end-member, albite (Ab), to that of the calcic end-member, anorthite (An), in an unbroken series. We took the mineral labradorite ($An_{60}Ab_{40}$) and attempted to match its infrared absorption curve by mixing equal parts of albite (about An_9) and anorthite (about An_{85}) samples. The resultant curves are shown in Fig. 1. Curve 3244 is almost matched by the 50:50 mixture but differs in enough characteristics so that its "parents" can be identified. It is possible that if one annealed this mixture while still in the solid state enough disorder could be introduced so that the curves would match. This has been done by Laves and St. Hafner[23,24] on similar materials.

b. Simulation of Rocks by Mineral Mixtures

The analysis of a granite by infrared absorption has already been performed, but the comparable study of a basic rock, such as a basalt or a diabase presents many more difficulties. In granite quartz and microcline are two of the major components and show little compositional change from sample to sample. Their spectra thus remain constant. The composition of the other major component, plagioclase, often varies markedly from sample to sample, with an attendant variation in its infrared spectrum. As long as only one of the major minerals is capable of change then the mineral content (modal analysis) of the rock may be deduced. Future study may help in the computation for more complex variations.

It is this factor of spectral change with composition which negates any simple solution to determination of the mineral content of basic rocks. Basic rocks can contain as major components, olivine, plagioclase, and one or more pyroxenes. Every one of these minerals can change both in content in the rock, and in composition within its mineral series. In such crystalline solid solutions the composition of an intermediate member is usually expressed as the percentage of one end-member, e.g., olivines are expressed in terms of the amount of forsterite (Fo), as Fo_x. Similar nomenclature is used for the albite-anorthite series, An_x, and the enstatite-hypersthene series, En_x.

To study the problem, and to provide some examples for later solution with the computer, mixtures were prepared in proportions listed in Table III. Each mineral had been previously studied and its place in its own mineral suite identified.

Table III

MINERAL MIXTURES USED FOR ANALYSIS

One-Mineral "Rocks"	Two-Mineral "Rocks"	Three-Mineral "Rocks"
	(Fig. 2)	
(Oli) Olivine (Fo_{90})	66% Oli:34% Aug	
3210	50% Oli:50% Aug	
	34% Oli:66% Aug	(Fig. 4)
(Aug) Augite		1 Aug:1 Oli:1 Lab
3246		(33% each)
	(Fig.3)	
(Lab) Labradorite (An_{60})	66% Aug:34% Lab	
3244	50% Aug:50% Lab	
	34% Aug:66% Lab	

Absorption spectra for the 10 mixtures are shown in Figs. 2 to 4. Treating the W-1 diabase (Fig. 11) as an unknown, a reasonably good match is noted immediately with the 50% augite:50% labradorite or a 34% augite:66% labradorite curve. The basalts of Fig. 45 contain a little too much glass to clearly match any of the synthetics, but the 50% augite:50% labradorite curve would fit well if the basalt is

considered to be a "smoothed-out" equivalent of the synthetic mixture. The Pisgah Crater sample (3369 in Fig. 45) shows a closer fit due to a higher content of crystalline material.

The gabbro from Stillwater, Montana (3367 in Fig. 46) clearly shows the absence of olivine (see modal analysis, Table VIII) and again the closest fit is with 50% augite:50% labradorite. If the spectral differences between orthopyroxene and clinopyroxene are taken into account then the fit is better (see Figs. 21 and 22 for the two types of pyroxene).

4. Synthetic versus Natural Minerals

There is a growing awareness[25,26] that infrared absorption analysis often is more sensitive to short-range ordering of aluminum silicates than is x-ray diffraction. An excellent way to note this effect is by the use of synthetic minerals which, because of inherent difficulties in reaching equilibrium in times available in the laboratory, are prone to crystallize in a disordered state. When this involves aluminum/silicon (Al/Si) diadochy in the tetrahedral layers of silicate minerals, it is often undetectable by x-rays because of the similarities in scattering power between the two elements.

Infrared analysis is specifically sensitive to such substitutions, particularly those wherein a charge deficiency arises (Al^{3+} for Si^{4+}). But Stubican and Roy[27] were unable to note the effects of the Al^{3+}/Si^{4+} substitutions in a series of their synthetic chlorites either by x-ray diffraction, or by infrared absorption analysis. Using natural chlorite samples, however, one can show[3] this substitution in the strong 9 to 10 micron region quite readily. Following this initial study the same sensitiveness to Al^{3+}/Si^{4+} tetrahedral substitution was noted in the lepidolite (Fig. 34), muscovite, biotite, and phlogopite mica groups[25] and is strongly suggested in the pyroxene and amphibole groups whose absorption curves were obtained during this project.

Therefore, we studied as many synthetic minerals as we could obtain. Excellent spectral resolution was obtained for samples of kaolinite (Fig. 5), albite feldspar (Fig. 6), analcite (Fig. 7), and paragonite (Fig. 35), and with a group of iron analogs of aluminous-microcline and sanidine (Fig. 8).

In Fig. 5 the critical 1805 cm^{-1} peak for synthetic kaolinite is not as well resolved as for natural kaolinite; this same poor resolution is often found in the disordered kaolinites called fire-clays. But the resolution of the four OH'peaks in the stretching frequencies around 3700 cm^{-1} and in the Al-O-OH bending frequency at 935 to 911 cm^{-1} is excellent. In Fig. 6 the synthetic albite (3045) is clearly of the high-temperature form and thus should not resemble its low-temperature counterpart (KRC1498). This distinction is made on the lack of resolution of the following areas: 1138 to 1109 cm^{-1}, 1023 cm^{-1}, 788 to 720 cm^{-1}, and 474 to 460 cm^{-1}. A parallel exists with the synthetic K-spar (potash feldspar) in Fig. 8. Synthetic analcite almost matches exactly its natural form (Fig. 7) except for a lack of ordering in the 640 to 540 cm^{-1} region.

The differences between the two polymorphs of potash feldspar--sanidine (high temperature, disordered) and microcline (low temperature, ordered)--are clearly seen in Fig. 8. The region from 770 to 720 cm^{-1} is the best for indicating disorder in the feldspar lattice, and a definite peak change (from 648 to 639 cm^{-1}) occurs between the two forms.

The ferric-iron (Fe) analogs are seen in the top two curves in Fig. 8. The Fe-microcline clearly shows a well resolved spectrum indicative of a high degree of order in the lattice. The Fe-sanidine is quite disordered as deduced from the lack of resolution in its spectrum. The similarity between the two sets of analogs is striking in the 1100 to 900 cm^{-1} (Si-O) region. The substitution for Al^{3+} by Fe^{3+} led to the change of peak location from the 650 to 530 cm^{-1} region to about 514 cm^{-1} The 422 cm^{-1} peak is assigned[26] to a Si-O bond and consequently does not change position.

5. Analysis of Shock-Loaded Minerals

The study of the effects of planar shock waves generated by high-explosives has been under way for several years at the Institute. Several mineral specimens have been shock-loaded in the pressure region 350 to 600 kilobars and the materials collected and analysed by x-ray diffraction and infrared absorption analysis.

Two examples are given in Fig. 9. A sample of albite feldspar shock loaded to 600 kilobars produced a glass (specific gravity, 2.20 to 2.24; refractive index, 1.50). A loss of resolution in the spectrum comparable to the degree of disorder in some synthetic minerals (Figs. 6 and 8) is shown, particularly in the 796 to 719 cm^{-1} region. All detail is lost at 1140 to 1090 cm^{-1}, 582 cm^{-1}, and 458 cm^{-1}.

A similar pattern may be seen for quartz shock-loaded to 350 kilobars in a Mach-disc with cylindrically-converging shock geometry (3145), and to 600 kilobars with a flying-plate shock wave pattern (3015). With the exception of the 350-kilobar spectrum, where some quartz remnant may be seen, the patterns are those of a completely disordered glass. A similarity is shown to the opal structure rather than fused silica, based principally upon the absence of the 695 cm^{-1} peak.

Two higher density polymorphs of silica (SiO_2)--coesite (specific gravity, 3.2) and stishovite (specific gravity 4.5) were also identified and defined. A detailed discussion of this work can be found on p. 30 - 31.

6. Determination of Water in Minerals and Rocks

In the KBr-pellet technique, as used for the infrared absorption analysis of rock and mineral, "water" can occur either on the sample or adhering to the potassium bromide itself. It so happens that absorption peak positions for water adhering to the KBr, and the water adhering to most samples, are so nearly identical that the region of their respective

infrared absorption peaks overlap. Mineralogists and chemists distinguish two types of water by their reaction upon heating--one which is lost at or below 110°C (called H_2O^-) and one lost above 110°C, sometimes several hundred degrees higher (called H_2O+).

In a crystal, like alum or gypsum, there is water which is essential to the preservation of the structure, and this can be found to occur in "n" multiples of "H_2O." There is also "zeolitic water" which can be driven in or out of a sample in the temperature range of 100 to 250°C, without affecting the structure, and there are hydroxyl, or (OH)', groups of varying types bonded into varying positions within a crystal lattice. Excluding physically adhering water, or "moisture" (H_2O^-), which may be either on the KBr or on the sample, this type of infrared absorption analysis can distinguish each type of water, because of its different absorption peak position, dictated by differing degrees of hydrogen bonding in the different forms.

This is illustrated in a series of spectra* in Figs. 10, 11, and 12. In the top curve in Fig. 10 one can see the effect of water on a KBr blank disc and how it can be almost completely removed by vacuum drying (second and third curves from the top).

The spectrum for paragonite mica (undried) in Fig. 10 shows the moisture (shaded) and the two OH' peaks, which have a ratio of their absorbances of 1.48. After drying, the "moisture" at 3425 cm^{-1} has been removed, but the ratio between the two OH' peaks is almost the same (1.50).

---

* The spectra were analyzed on a PE 221 grating instrument linear in wavenumber, without any material in the reference beam. The excellent resolution of this region may be noted, but the peaks are much more spread out horizontally than one is accustomed to seeing with the prism presentation, which is usually linear in wavelength.

A slightly different case is shown for the lower three spectra in Fig. 10, which have both moisture (H_2O^-), at 3425 cm^{-1}, and (H_2O^+) existing in a "disordered" form, at 3610 cm^{-1}. This water is akin to zeolitic water and does not show the characteristic peak of the OH' as in the mica.

Figure 11 shows zeolitic water lost on drying, but with the continued presence of ammonium (NH_4^+) ion in the sample. The ammonium illite also possesses a sharp OH' band at 3632 cm^{-1}.

The synthetic kaolinite sample in Fig. 11 shows a beautiful resolution of four OH' peaks between 3694 and 3621 cm^{-1} but without any peak at 3435 cm^{-1}. This is further confirmed (in Fig. 5) at 1530 cm^{-1} where "moisture" normally shows clearly as a wide band if a similar band occurs at 3435 cm^{-1}. Kaolinite thus has OH' but no H_2O in its analysis.

Some acid volcanic rocks, called perlites, are of great interest for their possible occurrence upon the lunar surface. On the earth's surface they may contain up to 10% water which may be removed if the sample is heated to about 800 to 1000 C. Commercially this is called "expanding"--or "frothing"--Perlite, as it expands to several times its original bulk upon the evolution of this water content as steam. It is in great demand for lightweight aggregates, but on the lunar surface it may be a source of water for astronauts.

In Fig. 12 the top two spectra show a possible 2% to 5% water in the rock (stippled area) which is not camouflaged by that present on the KBr disc, itself. It is this OH' water, observed at higher wave numbers (3515 cm^{-1}) than the moisture, which is retained to higher temperatures. It is clearly discernible in the spectra of the black perlite and apparently absent in that of the gray perlite.

So far we have not found the water contents of rocks and minerals to appear in reflection spectra, but more study is needed. The reflecting power of a solid increases rapidly in the vicinity of the absorption

due to a strong vibrational frequency and the reflection spectra should be as predicted from the corresponding absorption patterns (see Fig. 48).

7. Analytical Reproducibility

One is always troubled with the reproducibility of any analytical method, and the observed total variance between repeated analyses of the same sample should be carefully scrutinized. In previous studies[4] we have statistically determined the variance due to the several steps in grinding the specimen to a standardized fine grain size for absorption analysis. This part of the variance is quite small, and the biggest portion of the error between duplicate samples lies in the accuracy of weighing the 1.5 mg of sample to make up the 0.15% KBr disc.

It is clear, also, that the total variance is small, as may be seen in hidden duplicates, prepared under different code numbers, and shown as Figs. 13, 14, 17 and 24. The total variance may be defined as the sum of the partial variances due to the following operations:

1. Sample mixing in original bottle
2. Weighing 1.5 mg of the sample
3. Mixing with the 1.00 gram of KBr.
4. Disc preparation
5. Instrument settings
   a. Absorbance adjustments
   b. Wavelength adjustments
6. Estimation of final wavenumbers for peak position.

In general peak position can be defined to ± 2 cm^{-1}. This is a fairly simple problem compared with that of estimating reproducibility of analysis of a solid sample, as in reflection or emission analysis. Here orientation, grain size, and re-location of the specific area on the sample all pose major problems. One accepts the instrumental reproducibility of ± 2 cm^{-1} and relates all the other differences to sampling variances. The peak positions in reflection analysis are reproducible but their amplitudes are dependent upon surface features. Most polishing equipment does not produce as flat a surface as that of the quartz

oscillator plates, and the reference beam of the spectrophotometer usually must be attenuated about 40% to ensure an adequate signal from the instrument. This "electronic" magnification does not affect peak wavelength in any way.

F. Quantitative Treatment of the Data

A field which has been barely touched during this data gathering phase, is that of the quantitative treatment of the rock spectra. With absorption data[5] the problem is relatively easy. For the purpose of measurement, a base-line is drawn tangentially to the points of minimum absorbance (maximum transmittance) on the curve. With most silicate minerals and rocks this base-line runs from about 1200 cm^{-1} to about 800 or 750 cm^{-1}. The base-line absorbance at any wavenumber within this range is considered to be the difference between the absorbance value read from the curve and that read from the line at that wavenumber. These base-line absorbances are additive. Standard spectrophotometric techniques may be followed and simultaneous equations developed from which the concentrations of several individual components are calculated.

We are considering the computer programming that would be necessary to directly determine the mineralogical modal analysis of a rock from its absorption curve.

For the lunar orbiter experiment we would obviously be working with emission data, and further complications would be introduced by the available spectral resolution, the digital conversion of data, and the down-grading of data by the spacecraft telemetry. Clearly much remains to be done in this area.

Initial results from the first portion of the current study were given in the Interim Report,[28] and show how minerals with simple spectra may be readily differentiated at selected specific wavenumbers.

The compilation of mineral absorption spectra in the region 2.5 to 25 microns (4000 cm^{-1} to 400 cm^{-1}) has been carried out using both the NaCl and KBr prism optical regions. A file of approximately 1050 infrared absorption curves prepared over the past three years from 410 "standardized" mineral specimens were used for the compilation. These samples are mainly silicate minerals and represent materials on which full chemical analysis of superior quality has been performed and/or materials whose detailed x-ray diffraction and optical character are known.

It was deemed essential to perform this initial detailed study of purified single minerals, before undertaking mixtures, so that a basic understanding of the sample spectra might be obtained. Figure 15 shows that the spectra of minerals in a mixture are additive, and characteristic absorbance peaks may be defined even when mineral percentages in the mixture are low.

A. Typical Results in the Silicate Mineral Groups

The modern basis for crystallography[29] relies upon a realization of the importance of the silicon-oxygen tetrahedron in its various linkage-patterns in forming the basic framework of the silicate minerals. We find that it is logical to group silicates of a similar basic framework, using the ratio of the silicon and oxygen atoms as the common denominator. We find the nesosilicates, with isolated SiO_4 tetrahedra (Mg_2SiO_4 or Fe_2SiO_4) at one end[13] of the wavelength scale, and the tektosilicates, with frameworks of SiO_4 tetrahedra but with all oxygens shared and yielding (Si_2O_4) units at the other end. In addition, as one progresses toward the framework silicates there is increasing substitution of Al^{3+} for Si^{4+} in structures which form ($AlSi_3O_8$) groupings.

The following structural classes are accepted for the silicate minerals:

1. Nesosilicate - independant tetrahedra (SiO_4)
2. Sorosilicate - 2 tetrahedra sharing one oxygen (Si_2O_7)
3. Cyclosilicates - closed rings of tetrahedra each sharing two oxygens (Si_6O_{18})
4. Inosilicates - continuous chains of tetrahedra
   a. Single chains, sharing 2 oxygens (SiO_3)
   b. Double chains, sharing alternately 2 and 3 oxygens (Si_4O_{11})
5. Phyllosilicates - continuous sheets of tetrahedra each sharing 3 oxygens (Si_4O_{10} or $AlSi_3O_{10}$)
6. Tektosilicates - continuous framework of tetrahedra, each sharing all 4 oxygens ($AlSiO_4$ or $AlSi_3O_8$)

This classification is clearly shown by infrared analysis, for the covalent portion of the (Si-O) and (Al-O) bonds prove to be very sensitive to infrared detection. In fact this method of analysis, above all others, offers the greatest hope for solving some of the problems of the ordering of Al-O and the Si-O tetrahedra, and the amount of Al^{3+}/Si^{4+} diadochy.[25]

1. Nesosilicates

a. Olivine

The olivines show very simple spectra comparable to many of the inorganic anions, with peaks changing wavenumber in a predictable manner as their cation metal changes (Figs. 16 and 17). Almost every detail of the spectrum persists unchanged from sample to sample but careful calibration will show marked wavenumber changes, as shown in Table IV.

This mineral group has recently been the subject of an exhaustive study by Duke[30]. The slight departures from complete independence of the tetrahedra in the solid crystal were used by him as the reason for modifying the theoretical absorption peak positions to match observed values.

Table IV

PEAK POSITIONS IN THE OLIVINE GROUP

Sample	Absorption Peaks (cm^{-1})						
Forsterite, Mg_2SiO_4	983	950	888	838	605	504	410
Fayalite, Fe_2SiO_4		947	873	829	558	482	410

b. Garnet

The garnet minerals may be divided into two main groups--the aluminous "pyralspites" with a general formula of $R_3^{2+}Al_2(SiO_4)_3$, and the calcic "grandites" with a general formula of $Ca_3R_2^{3+}(SiO_4)_3$. Within each group complete crystalline solution exists, but between the groups it is a rarity. Most of the samples in Fig. 18 are pyralspites, but the samples DEL 3 and DEL 5 are examples of this solid solution.

Spectral peak patterns are again constant within the two subgroups (Figs. 16 and 18) and vary in wavenumber with the cation metal, as shown in Table V.

Table V

PEAK POSITIONS IN THE GARNET GROUP

Mineral	Formula	Absorption Peaks (cm^{-1})							
Pyralspite									
Pyrope	$Mg_3Al_2(SiO_4)_3$	970	900	872	-	575	482	460	
Almandite	$Fe_3Al_2(SiO_4)_3$	970	902	880	638	570	480	455	
Spessartite	$Mn_3Al_2(SiO_4)_3$	955	892	870	632	562	472	452	
Grandites									
Grossularite	$Ca_3Al_2(SiO_4)_3$	915	860	840	618	-	540	470	450
Andradite	$Ca_3Fe_2(SiO_4)_3$	895	840	820	592	-	512	482	438
Uvarovite	$Ca_3Cr_2(SiO_4)_3$	900	840	825	609	-	540	455	425

2. Sorosilicates

The sorosilicate group is quite complex structurally and this is also shown by the infrared spectra. Idocrase (Fig. 19) has both (SiO_4) and (Si_2O_7) groups and is halfway between the nesosilicates and the sorosilicates. Lawsonite (Fig. 19) has 6-coordinated Al-O (and OH') groups, linked sideways by the Si_2O_7 groups.

3. Cyclosilicates

a. Beryl - $Be_3Al_2Si_6O_{18}$

Minerals of the beryl group--beryl, emerald, and the cesium-bearing pollucite--are very similar to one another and have very active spectra. Compositional changes may be defined in the 1015 to 1058 cm^{-1} region, as seen in Fig. 20.

b. Cordierite, $Al_3(MgFe)_2(Si_5Al)O_{18}$

Cordierite spectra are broadly comparable to beryl spectra but differ in the 800 to 700 cm^{-1} region in having fewer peaks. Substitution of Al^{3+} for Si^{4+} takes place in parallel with the diadochy of Mg^{2+} for Al^{3+} in the above structural formulas. Both substitutions tend to produce spectra characterized by fewer peaks.

4. Inosilicates

a. Single Chains - Sharing Two Oxygens (SiO_3)

Orthopyroxenes. The orthorhombic pyroxenes form the series hypersthene, $(Mg,Fe)SiO_3$,--enstatite, $MgSiO_3$; and compositions are usually expressed in terms of the enstatite end-member (e.g., En_{20} is 20 percent $MgSiO_3$). We analyzed a series of 21 orthopyroxenes and their spectra appear in Fig. 21, which shows the changing detail of an infrared spectrum with cation substitution.

Clinopyroxenes. The inosilicates also include a series $MgSiO_3$-$FeSiO_3$ (clinoenstatite and clinohypersthene), but samples of this

monoclinic group have only been found in meteoric material and are not readily available for study.

The common clinopyroxene, augite, which is to be found in almost all basic rocks, has a composition intermediate between diopside ($CaMgSi_2O_6$) and hedenbergite ($CaFeSi_2O_6$) with some aluminum as indicated below:

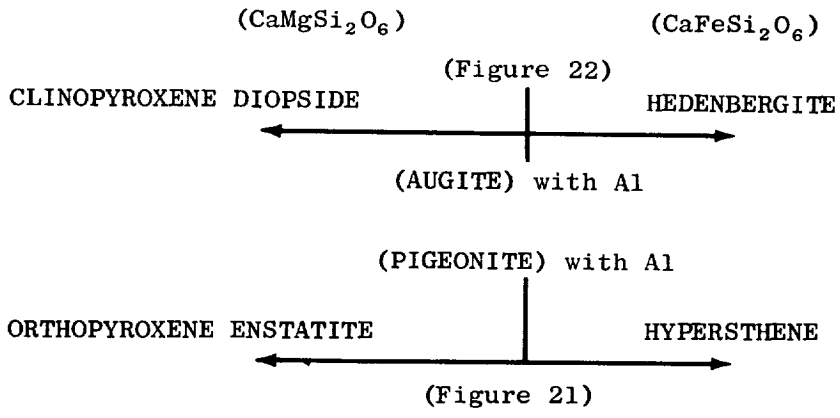

The mineral groups represented by augite and pigeonite are further complicated by a slight amount of Al/Si substitution in the tetrahedra. This is not known in the pure end-members of each series.

Augite is one of the most common rock-forming minerals in the basic rocks, basalt and andesite. A typical example is 3246, as used in the synthetic rock mixture shown in Figs. 3, 4, and 5. We have about 20 augites, but the detailed mineralogical analysis of this group was not completed in time for inclusion in this report. Two members of this mineral group, diopside and hedenbergite, are shown in Fig. 22.

Other clinopyroxenes--jadeite ($NaAlSi_2O_6$), acmite ($NaFe^{3+}Si_2O_6$) and omphacite--show a similarity of absorption spectra which corresponds to their similarity in basic structural formula (Fig. 22). A jadeite series is shown in Fig. 23, with which some of the omphacites in Fig. 24 may be compared for compositional similarity. Three acmites are shown in Fig. 25, but no analyses of their compositions are available.

b. Double Chains - Sharing Alternately Two and Three Oxygens (Si_4O_{11})

The amphibole group is chemically very similar to the pyroxene group but permits a much greater Al-Si diadochy in the Si_4O_{11} chains. Hydroxyl groups are an essential part of the structural formulas of the amphiboles and may be seen on the infrared spectra in the region around 3600 cm^{-1}.

The only orthorhombic member commonly found is anthopphyllite, $(Mg,Fe)_7Si_8O_{22}(OH)_2$, where Mg is greater than Fe. Aluminum often replaces silicon in the tetrahedra.

Amphiboles which have been studied are from the hornblende $[NaCa_2(Mg,Fe)_4Al(Al\ Si_7)O_{22}(OH)_2]$ series and the alkali amphibole series--glaucophane $[Na_2Mg_3Al_2Si_8O_{22}(OH)_2]$ and riebeckite $[Na_2Fe_3^{2+}Fe_2^{3+}Si_8O_{22}(OH)_2]$. Because of almost overwhelming complexities of possible substitutions these minerals are the most difficult with which to work. Multiple examples of these series are shown in Figs. 26 and 27. The cummingtonite $(Fe, Mg)_7\ Si_8O_{22}(OH)_2$ series minerals are represented by sample 3420 (Fig. 28) which was found in the same rock as the hornblende 3418. These are described in a recent paper by Vernon.[31] There is a suprisingly great similarity shown by these two samples, particularly when a larger group of hornblendes (Fig. 29) is compared.

The general relationships between the amphiboles are sketched on the following page, showing how hornblende is derived from actinolite by various atomic substitutions. The close similarity may be seen between actinolite 3247 (Fig. 28) and hornblende 3233 (Fig. 29), where all the peaks except the small peak at 920 cm^{-1} may be matched in the two spectra.

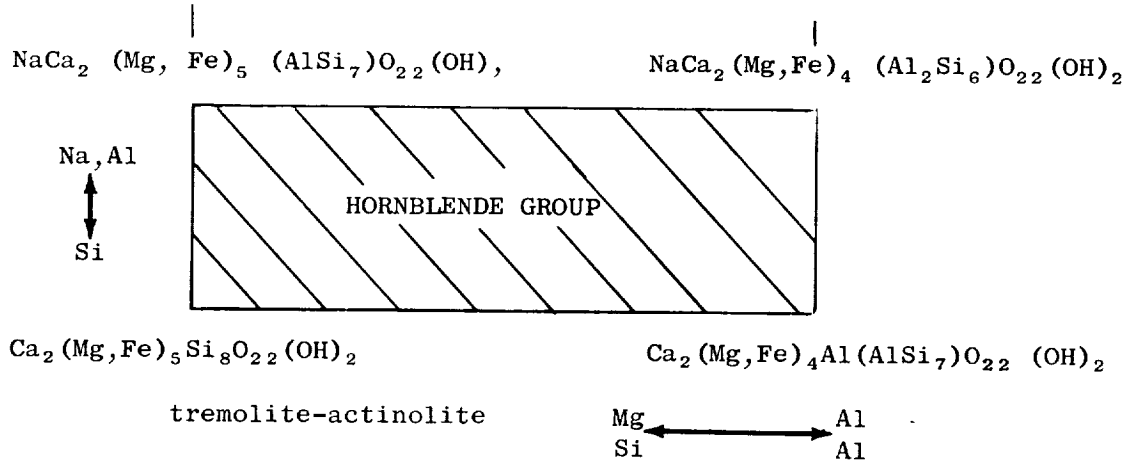

5. Phyllosilicates

a. Trioctahedral Layered Silicates

In talc, $Mg_3Si_4O_{10}(OH)_2$, a tetrahedrally coordinated layer is combined with an octahedrally coordinated layer of magnesium ions; this is the simplest example of the phyllosilicate group. Spectral assignments by Stubican[27] are as follows:

Trioctahedral phyllosilicates (Mg^{2+} and Fe^{2+}	
(Si-O) stretching	1100 to 900 cm^{-1}
(Si-O) "unassigned"	668 cm^{-1}
(Si-O-Si) bending	460 to 430 cm^{-1}

A spectrum for talc is shown in Fig. 30.

By varying the (Mg, Fe) composition of the octahedral layer we can form the biotite [$K(Fe,Mg)_3(AlSi_3)O_{10}(OH)_2$] and phlogopite [$KMg_3(AlSi_3)O_{10}(OH)_2$] micas, (see Figs. 31, 32, and 35). At the same time there is a marked change in the aluminum substitution in the basal tetrahedral layers. This is often called the "Y" number, from the formula

$$(4 - Y)Si^{4+} + Y\,Al^{3+} = 4(Si,Al)$$

where Y may have any value from 0 to 2. The resulting charge deficiency due to the Al^{3+} is balanced by the introduction of K^+ in the interlayer position.

b. Dioctahedral Micas

Muscovite, $KAl_2(AlSi_3O_{10})(OH)_2$ has two Al^{3+} ions for each three Mg^{2+} ions in the octahedral sheets, leaving a vacant site in the layer. Sheet stacking gives various possible types of symmetry. Assignments by Stubican[27] are as follows:

Dioctahedral phyllosilicates (Al^{3+} or Fe^{3+})	
(Si-O) stretching	1100 to 900 cm^{-1}
(Si-O-Si) bending	460 to 430 cm^{-1}

Muscovite spectra are shown in Figs. 31 and 33; Al^{3+}/Si^{4+} substitution in the tetrahedral layer can markedly vary the patterns. This substitution is very well shown by the series of lepidolites, $KLi_2Al(AlSi_3O_{10})(OH)_2$, shown in Fig. 34. Here a complete series in Al^{3+}/Si^{4+} diadochy has been examined with "Y" ranging from 0.18 up to 0.72. The marked change in the 1084 to 1130 cm^{-1} peak, and in the detail of the 992 to 962 cm^{-1} peaks has been previously reported[3,25] and is one of the best examples of this use of infrared absorption analysis in mineralogical studies.

The following varieties of mica may be obtained by atomic substitution in the muscovite structure:

muscovite, $KAl_2(AlSi_3O_{10})(OH)_2$	(Fig. 33)
paragonite, $NaAl_2(AlSi_3O_{10})(OH)_2$	(Fig. 35)
lepidolite, $KLi_2Al(AlSi_3O_{10})(OH)_2$	(Fig. 34)
glauconite, $K(Fe,Mg,Al)(AlSi_3O_{10})(OH)_2$	(Fig. 36)
ferri-celadonite, $KFe_2(Si_4O_{10})(OH)_2$	(Fig. 36)

c. Kaolinite, $Al_2Si_4O_{10}(OH)_8$

No substitution has been defined in the kaolin group, the members of which are considered to differ from each other only in the stacking of their plates. Most of the infrared spectra are quite similar, but the group members--kaolinite, dickite, halloysite and nacrite--may be distinguished. A kaolinite spectrum appears in Fig. 30.

There is a suggestion in the spectrum of halloysite, as distinct from that of any of the others of the group, that there is a certain amount of tetrahedral substitution of aluminum for silicon in the basal structural layers, similar to the case for the micas. A value of "Y" of up to 0.6 is suggested by direct comparison with the mica series. There is no other real evidence as yet to support this view, except that such a substitution would help to explain the tubular form of halloysite resulting from the misfit between the two layers in the structure (Bates[32]).

6. Tektosilicates

a. Quartz and its Polymorphs

Silica is the simplest of the tektosilicates and consists of a framework of SiO_4 tetrahedra with each oxygen linked to another in a neighboring tetrahedron. Silica can exist in various structural groups, several members of which are shown in Fig. 37; quartz and coesite retain the tetrahedral coordination, while stishovite shows the rutile (six-fold coordination) structure. Stishovite is considered to be the first mineral discovered in which silicon occurs with oxygen in a six-fold coordination (octahedral) instead of tetrahedral coordination.

Tarte and Ringwood[33] have recently drawn attention to the absence of SiO_6 octahedra in silicate minerals; however, on the basis of other work in XO_4 tetrahedral, and octahedral, groups, they predicted the infrared absorption frequencies for this octahedral configuration to be between 700 and 600 cm^{-1}. The stishovite[34] infrared absorption curve (Fig. 37) shows a major absorption at 769 to 628 cm^{-1}, effectively supporting their prediction. The data show a marked change in the position of the major absorption peaks when passing from the SiO_4 tetrahedral coordinations of quartz, coesite, and fused silica (1098 to 1077 cm^{-1}) to the SiO_6 octahedral coordination in stishovite (769 to 628 cm^{-1}; 949 to 885 cm^{-1}). A parallel to this has been recorded by Dachille and Roy[44]

for GeO_2- quartz and GeO_2-rutile structures, which show absorption peak shifts from 870 cm^{-1} for the "quartz" structure to 715 cm^{-1} for the "rutile" polymorph.

General assignments[35] for spectral peaks in quartz are:

(Si-O) stretching	1100 to 800 cm^{-1}
(Si-Si) stretching	800 to 600 cm^{-1}
(Si-O-Si) bending and distortion	460 to 430 cm^{-1}

b. Feldspar

The feldspars are a very complex group both compositionally and structurally, and to adequately cover this one group would be a complete study in itself.

The plagioclase group--albite, $NaAlSi_3O_8$, to anorthite, $CaAl(Si_2Al)O_8$,-- is treated in Fig. 38 which shows the marked structural break at An_{33} (and An_{66}) by changes in the infrared spectra. Only the low temperature plagioclases are shown. A detailed study of the calcic-plagioclases (An_{60} to An_{83}) is shown in Fig. 39. The diagnostic peaks are indicated by an asterisk. These samples traverse the structural break at An_{66}, but this is not so clearly revealed as that at An_{33}. The peak at 929 cm^{-1} begins to be a major peak immediately after the break and becomes dominant for An_{94}. Peaks at 663 and 755 cm^{-1} are also significant above the break at An_{66}.

B. Typical Results with Oxide Mineral Groups

Only two oxide mineral groups have been studied--Al_2O_3 and TiO_2. These are both of specific interest as they are known to be capable of fairly extensive substitution for Si^{4+} in the tetrahedral layers of silicates. Only aluminum oxide will be discussed.

The spectrum for γ-Al_2O_3 shown in Fig. 40 has a broad minimum from 825 to 580 cm^{-1}. The three most common hydrates of aluminum also show this minimum although it is generally narrower and forms a sharper peak

in the range 740 to 520 cm^{-1}. This is the wavenumber region where Al in six-fold (octahedral) coordination may be found on an infrared spectrum. When it is in four-fold (tetrahedral) coordination its absorption peak occurs at a much higher wavenumber. The parallel with silicon is tabulated below.

Form	Coordination	Peak Position
Alumina, γ-Al_2O_3	Six-fold	825 to 580 cm^{-1}
Alumino-silicates, $AlSi_3O_8$	Four-fold	1000 to 900 cm^{-1}
Stishovite, SiO_2	Six-fold	949 to 560 cm^{-1}
Quartz, SiO_2	Four-fold	1160 to 1080 cm^{-1}

C. Experimental Results with Rocks

Knowledge of single minerals has been extended to mixtures of minerals as found in rocks. Typical materials of presumed lunar origin (tektites) or of lunar accumulation (meteoritic chondrites, etc.) and over 80 rocks have been studied in the past six months. Many of the spectra from these rocks appear in Figs. 41 to 46. The rock types represented have also been tabulated in Table VI according to their composition and grain size.

The techniques of absorption analysis have formed the basis for the interpretation of the data from infrared reflection analysis of rock surfaces.[22] In turn this provides the key to the interpretation of infrared thermal emission spectra from hot (or warm) specimen sources. A series of absorption spectra (Fig. 41) for typical acid and basic rocks found on the earth's surface has been compiled.

The absorption spectra for three "acid" rocks (Katmai ash; Town Mtn., Calif., granite; and the Standard G-1 granite) are shown in the upper half of Fig. 41. For comparison the absorption spectra for three "basic" rocks, (Kilauea Iki basalt (1960); San Marcos, Calif., gabbro; and the Standard W-1 diabase) are shown in the lower half of the figure.

Table VI

ROCKS STUDIED BY ABSORPTION ANALYSIS

Rock Type	Sample No.	Figure No.
Acid, Fine-Grained Rocks		
Katmai ash	3199	41
Obsidian, Clear Lake	3358	41,42,52
Obsidian, Snowflake glass	3414	43
Obsidian, Snowflake crystals	3413	43
Obsidian	3393	43
Obsidian red	3360	43
Obsidian Konocti	3359	43
Obsidian	3381	43
Perlite, gray	3428	43
Opal, black woody	3301	42
Fused Quartz	3019	42
Acid, Medium-Grained Rocks		
Rhyolite, Soledad	3389	42
Tuff, Bishop	3388	42
Acid, Coarse-Grained Rocks		
Granite, Town Mtn.	3297	41
Granite, G-1 Std.	3165	41,44
Granite, Hard Hat	3306	44,52
Granite, Hard Hat	3307	44
Syenite SY-1	3368	44
Basic, Fine-Grained Rocks		
Basalt, Kilauea Iki (1959)	3298	41,45
Crystals from the above	3298	45
Basalt, Kilauea Iki (old flow)	3380	45
Basalt, Pisgah Crater	3369	45
Basic, Medium-Grained Rocks		
Diabase, W-1	3166	41,46
Basic, Coarse-Grained Rocks		
Gabbro, San Marcos	3296	41,46,52
Gabbro, Stillwater	3367	46
Gabbro, Mt. Hope, Md.	3375	46
Serpentine, San Luis Obispo	3384	45
Anorthosite, San Gabriel	3386	52

There is a definite similarity within the two groups as to the position of the absorption maximum around 1070 to 990 cm^{-1}. The acid rocks each approximate 1070 cm^{-1}, and the basic rocks approximate 990 cm^{-1}-- a shift of 80 cm^{-1}. This shift appears regardless of whether the rock being examined is glassy, crystalline, fine-grained, or coarse-grained. The peak shift is apparently dependent on the bulk composition of the rock, with the smaller peaks of the spectrum recording the presence of specific minerals.

Simple quantitative measurements can be made as long as adequate spectral resolution can be obtained in the resultant data. Characteristic spectral minima can be identified for each phase (quartz, olivine, etc.,) in a mixture when superimposed peaks due to two phases can be differentiated.

Thus there is at least a spectral shift of 80 cm^{-1} available on which to base experimental work. Absorption curves have not been prepared for olivine-rich dunites; but the minima[30] for olivine (Fo_{90}) is at 888 cm^{-1}, and the peak for a rock only of this composition should be close to this value, making a possible shift in the absorbance of around 180 cm^{-1} between obsidian and dunite.

INFRARED REFLECTION ANALYSIS OF MINERALS AND ROCKS

A. Previous Studies

The diagnostic use of infrared radiation, reflected from minerals and rocks, is a relatively unexplored field. Apart from the pioneering studies of Coblentz[6,7] (1906-1910) on minerals and inorganic surfaces and coatings, and of Pfund[8] (1945) on the use of infrared techniques for the identification of gems, such studies have been restricted to fused silicates and glasses. In addition, Coblentz was restricted in most of his studies to the 1 to 8 micron region, and Pfund to the 6 to 12 micron region of the spectrum, compared with the range of 2 to 25 microns available for use today with automatically recording spectrophotometers.

There have been several excellent studies on glasses, which are semitransparent in the infrared region. Simon and McMahon [10] and Gardon[11] have discussed the subject from the aspect of the fundamentals of radiative cooling of glass slabs and sheets. These workers and others like Saksena,[35,36] Sevchenko and Florinskaya,[37] and Matossi and Bronder[38] became interested in reflection measurements from polished surfaces of silicate minerals whose crystal structures were relatively well known. Minerals including quartz, tridymite, cristobalite, and some fused silicates were investigated by these techniques.

B. Infrared Absorption and Reflection for α-Quartz

Quartz oscillator plates, with their polished surfaces, make excellent samples for a study of infrared reflection; but because of the high absorption coefficient for quartz (particularly in the 9 to 10 micron and 21 to 25 micron regions), absorption spectra are usually prepared from a powdered sample mixed at low concentration (0.15%) in a KBr pellet. Absorption spectra for quartz and other SiO_2 polymorphs--coesite and stishovite--are shown in Fig. 47, and are covered in more detail on p. 30 - 31.

The techniques by which the reflection spectra used in this report were obtained have been described in Sec. C, p. 9-10. A certain amount of reference beam attenuation is needed with some samples, but this appears to be more a function of grain size of the crystals in the rock than of surface polish. The polish must be good, however, in order to get adequate reflection. The samples whose spectra are shown in Fig. 54 of dunite (3390), tektite (3257), and obsidian (3358) gave sufficient reflection without any attenuation of the reference beam.

Typical reflection spectra for quartz plates appear in Fig. 47. The X- and Y-cut plates show a marked difference from the Z-cut plates in the region of the 800 to 775 cm^{-1} doublet and in the details of the 500 cm^{-1} peak. Saksena[35,36] and Sevchenko and Florinskaya[37] have discussed the relation of the 775 cm^{-1} peak to the extraordinary optical ray and the 796 cm^{-1} peak to the ordinary optical ray of α-quartz. The Z-cut plate obviously shows only the 796 cm^{-1} peak, being an optically isotropic section through the crystal (circular section of the optical ellipsoid, with zero birefringence). Figure 48 has been redrawn from the paper of Sevchenko and Florinskaya as it serves to clearly show the relationship between absorption and reflection spectra.

A 45-deg rotation of the plate perpendicular to the plane of the infrared beam produces an effect most marked in the 515 cm^{-1} peak of the X-cut and Y-cut plates (Fig. 47). The Z-cut plate shows little or no effect upon rotation. No attempt was made to polarize the incident beam of radiation. No attenuation of the reference beam was required with any of these plates of quartz. The temperature dependence of reflection spectra is displayed for a quartz Z-cut plate in Fig. 49. This has been redrawn from the classic study of Simon and McMahon.[10] The structural change at about 543°C (or 816°K) is that of the α-β inversion which was accompanied by enough expansion to crack their specimen. The sharp doublet at 1180 and 1110 cm^{-1} is lost at this temperature, being replaced by the single peak at 1120 cm^{-1}, a characteristic of fused quartz spectra (Fig. 48).

The sharpening of spectral peaks as measured by their half-bandwidth, with decrease in temperature is most clearly seen in the 800-cm^{-1} peak. This may be quite a significant effect when spectra are obtained from the dark side of the moon, where the lunar temperature approximates 150°K.

C. Experimental Results for Rocks

Table VII lists the rocks studied by reflection analysis under this project. Rocks of the same composition will have the same spectra, with details dependent upon the degree of crystallization (Figs. 50 and 51).

The reflectance spectra for the group of rocks and meteorites presented in Figs. 54 and 55 show a progressive shift of 160 cm^{-1} (0.85 micron) in the spectral peaks around 920 to 1080 cm^{-1}. These samples range from acid rocks (obsidian, rhyolite, granite, tektite) through those of intermediate composition (andesite and diabase) to the basic and ultrabasic materials (olivine-bearing dunite and meteorite chondrites).

Most importantly the spectral peaks are again dependent upon bulk-composition and do not change in wave number with increasing grain size. Thus, whether a given chemical composition of rock is in the physical form of glass, felsite, fine-grained volcanic flow, or medium-grained or coarse-grained plutonic rock, its spectral maximum of reflection will remain fixed in wave number. As the crystallites form in the earliest stages of crystallization from a glass, smaller peaks will appear as modifications superimposed upon the spectral maxima or minima (see Fig. 54). These modifications increase in size as the crystals grow and as the rock loses its content of disordered silicate glass. The silicate spectrum changes from a simple bimodal curve to the multiple-peaked spectral curve typical of fully crystalline materials. Wave number will indicate the bulk composition, and the complexity of the curve will indicate the degree of crystallinity. Knowledge of the characteristics of individual peaks enable us then to calculate the mineralogical composition or "modal analysis" of the rocks.

It is clearly possible, therefore, to distinguish granite rocks from diabase rocks by infrared analysis, and in most instances, to obtain

Table VII

ROCKS STUDIED BY REFLECTION ANALYSIS

Rock Type	Sample No.	Figure No.
Acid, Fine-Grained Rocks		
Obsidian, Clear Lake	3358	53,54
Tektite (australite)	3257	54
Acid, Medium-Grained Rocks		
Granite, "fine-grained," biotite	3382	50,54
Rhyolite, Soledad	3389	54
Acid, Coarse Grained Rocks		
Granite, Town Mtn.	3297	50
Granite, Hard Hat	3306	50,52
"Quartz Diorite"	3373	50
Basic, Fine-Grained Rocks		
Basalt, Olivine, Pisgah	3369	51,54
Meteoritic Chondrites		
Brüderheim	3411	54,55
Ladder Cr.	3410	55
Potter	3409	55
Potter	3407	55
Haven	3408	55
Basic, Coarse-Grained Rocks		
Gabbro, Stillwater	3367	51,54,55,56
Gabbro, Mt. Hope, Md.	3375	51
Gabbro, San Marcos	3296	51,52
Anorthosite, San Gabriel	3386	52
Dunite, Twin Sisters	3390	54

quantitative results either by infrared absorption,[5] reflection,[22,10] or emission measurements.[16,17]

One of the most significant contributions of infrared technique regardless of the method of obtaining the spectral patterns, is its ability to analyze for amorphous materials such as glasses,[10] whether these be natural volcanic glasses like obsidian, or synthetic glasses like pyrex. Glasses possess molecular structure and thus show infrared

spectra whose patterns change with composition and progressive ordering (as in the beginning of crystallization). Glasses are to be treated, therefore, as separate phases whose infrared spectra appear in addition to those of any crystalline material present.

A series of fine-grained rocks were polished and infrared reflection spectra obtained in a manner similar to that described for quartz plates. Rock material adjacent to the polished face was powdered and KBr pellets (0.15%) prepared. Infrared absorption spectra were obtained as described earlier. The four pairs of spectra are compared in Figs. 52 and 53. (Sample locations are listed in Table II.) For detailed discussion we will confine ourselves to a study of the two spectra for the specimen of "Hard Hat" granite from the Nevada Test Site, shown as 3306 in Fig. 52a. The heavy line is the absorption spectrum for the powdered material; the dashed line is the reflection spectrum, which has been inverted for comparison. The general similarity in shape is clearly noticeable. There are important differences in the depths of particular peaks, e.g., the doublet at 794 and 775 cm^{-1} (due to quartz), which become most significant when one attempts to determine the mineralogical composition, or "modal analysis," of a rock. This is the most important difference between the absorption and reflection spectral curves. Obviously methods of analysis for absorption spectra,[5] will not produce a comparable analysis of infrared reflection data. It is clear that the difference is a fundamental one, due to the mechanism of reflection and absorption, rather than merely a slight difference in the samples--one a solid material, one a powdered material. The same effect can be seen in Fig. 48 for a α-quartz. We know the good degree of reproducibility for the KBr pellet technique;[4,5] but the difference shown here is some orders of magnitude greater.

Furthermore, all the rocks we have studied show these differences between spectra obtained by the two techniques. Perhaps more significant is the discovery that mineralogically and texturally similar rocks, with similar absorption spectra, will have similar reflection spectra, although for each sample the absorption and reflection spectra will show basic differences, characteristic of the two methods.

In a comparable manner spectra for anorthosite, gabbro, and obsidian specimens are also presented in Figs. 52 and 53. Unfortunately no reflection spectra are available for the labradorite sample (3244), but it has been closely matched by the reflection spectrum for the rock, anorthosite (3886), composed predominantly of labradorite.

With reflection spectra from a slightly wider range of rock compositions an even more marked peak shift of 160 cm^{-1} can be obtained, using surfaces polished on the rock samples. Figure 54 shows the spectral curves, from infrared reflection, of a series of rocks ranging from a tektite (australite) through granite, obsidian, and rhyolite, to basalt, gabbro, dunite, and a stony meteorite (chondrite). Clearly marked changes in the peak at 445 cm^{-1} and 550 cm^{-1} can also be noted in most of the samples.

The simplicity of the reflection spectra of Fig. 54 compared to the complexity of the absorption spectra of Fig. 41 again emphasizes the previous remarks with reference to the two analytical techniques.

As a further application, a series of chondritic meteorites (Potter, Brüderheim, Haven, and Ladder Creek) were prepared and their reflection spectra analyzed. These are compared with the reflection spectrum from a sample of Stillwater gabbro. The similarities are striking. This sample of gabbro (3367-55BEI) and its modal analysis were both kindly supplied by E. D. Jackson, of the U.S. Geological Survey. This is compared in Table VIII with the two modal analyses available for Ladder Creek and Brüderheim chondrites; both the samples and analyses were obtained by the courtesy of A. A. Loomis, Jet Propulsion Laboratory, California Institute of Technology.

Table VIII

COMPOSITIONS OF A GABBRO AND TWO CHONDRITES

Mineral Composition	Gabbro Stillwater, Montana 3367 (Mode)[a]	Chondrite Ladder Creek, Kansas 3410 (Norm)[b]	" Chondrite Bruderheim, Canada 3411 (Norm)[b]
Plagioclase	48%	10%	11%
Orthopyroxene	35	20[c]	32[d]
Clinopyroxene	17	6	6
Olivine	--	64[c]	51[d]
Total	100	100	100

[a]Mode--observed mineral frequencies

[b]Norm--Mineral content calculated from a chemical analysis of the rock

[c]Olivine and orthopyroxene calculated to be En, Fo_{68}

[d]Olivine and orthopyroxene calculated to be En, Fo_{76}

There is a broad similarity between the chondritic meteorites and the Stillwater gabbro as seen in Fig. 55; but a closer match may be obtained by making a comparison with the dunite (3390) of Fig. 54, particularly when we consider that the olivine in this sample is about Fo_{90}, and in the chondrites it is about Fo_{76} (as calculated). A change in the iron content, from Fo_{90} to Fo_{76} would move the peaks as shown in Table IX, to a closer match with the Brüderheim meteorite composition.

Table IX

OLIVINE PEAK POSITIONS SHIFTING WITH CHANGING IRON CONTENT
COMPARED WITH BRÜDERHEIM CHONDRITE

Minerals	Composition	Peaks, in cm^{-1}				
Absorption						
Forsterite	Fo_{95}	983	886	605	504	410
Olivine, 3320	Fo_{90}	981	884	603	502	412
(Calculated)	(Fo_{76})	(977)	(880)	(597)	(498)	-
Fayalite	Fo_5	947	873	558	482	410
Dunite, 3390	ca. Fo_{90}	985	883	605	500	405
Reflection						
Dunite, 3390	ca. Fo_{90}	922		525		420
" Brüderheim		921	883	510	493	405

D. Reflection Analysis of Powdered Rock Samples

One of the most difficult problems in reflection analysis arises when one attempts to quantitatively analyze the mineral components in a rock. In absorption analysis it is quite easy to mix up a "synthetic" rock and obtain its spectrum to compare with that of an unknown sample. Changes may then be made and another synthetic prepared, closer to the unknown in spectral pattern.

With solid rock samples this is not possible. Grain sizes and orientation play important parts in the relative peak intensities of the constituent minerals. To explore these parameters powdered mounts were prepared in lucite blocks and polished. (see Sec. C., p. 9)

The results (shown in Fig. 56) are not too encouraging. Basically the problem rests in the lowered area of reflection surface available in a powder mount where the lucite matrix has to hold each grain in place. But the method has a certain amount of promise in that different rocks can be recognized by their powder mounts, and this may serve as a method to match their mineralogical and modal analyses quantitatively.

INFRARED EMISSION ANALYSIS OF MINERALS AND ROCKS

The foregoing discussions have been based upon an analysis of reflection and absorption infrared spectra. The same type of analysis is applicable to emission spectra for here the spectral data appear as minima superimposed upon the familiar Planck-Wien radiative curve. Spectral position defines the minerals; spectral shape and complexity may be used to determine the mineral content of the rock.

Infrared emission has been previously investigated by only a few experimenters. Some data on the "emissive power" of minerals may even be taken from the early pioneering work of Coblentz[7] (1 to 8 microns), and more recently from the studies of Fredrickson[39] (2 to 5 microns), and Bell et. al.[16,17] (1 to 20 microns), who have studied the thermal emission of terrain for several years.

The work of Bell's group will be of importance to any future emission studies. Working with mobile spectrophotometers, they were able to observe the major spectral peak for the sulfate group in the infrared emission from gypsum sand at White Sands, N.M., and the peak for the silica functional group in the emission from quartz sand at Cocoa Beach, Florida. Although their data show only the major peak for each mineral,* this study shows that compositional data may be read from the thermal emission of sand, at ambient temperatures of only about 40°C. This is also an important contribution to the problem of obtaining adequate spectral data on the emission curves of powdered materials, for while neither sample has the particle size believed to characterize lunar "dust" (0.1-mm diameter and below), the feasibility of the method has been proven under field operating conditions.

* A reason for the lower degree of spectral resolution in Bell's data, may reside in the spectral resolution of his equipment, which was only 25 cm^{-1}. This highlights a major specification which arises from our work, that spectral resolution of 5 cm^{-1} or less in the wavelength range of 1000 to 400 cm^{-1} (10 to 25 microns), is an essential prerequisite to obtaining spectral information from emission measurements of rocks.

Our early theoretical studies of thermally emitted infrared radiation from rocks at lunar ambient temperatures are briefly described in Appendix C. It will suffice to say that once a catalogue of absorption spectra for minerals has been amassed, the characteristics of the emitted infrared radiation from these surfaces can be evaluated. The incident energy of a particular wave number that falls on a surface is transmitted, absorbed, reflected spectrally, or reflected diffusely (scattered) by the surface. Transmission measurements made at normal incidence through a thin layer of the sample are useful for giving the general shape of the absorption curve; but they are dependent upon thickness. Spectral reflection measurements, on the other hand, on polished surfaces (where scatter is almost zero) of infrared opaque materials (where transmission is negligible) give data which are both qualitative and quantitative. Applying Kirchhoff's law ($\alpha = 1 - \rho$) and thermal equilibrium conditions ($\alpha = \epsilon$), where α = absorptivity, ρ = reflectivity, and ϵ = emissivity, one can calculate the spectral emissivity of the surface at any given temperature. This is most readily accomplished by the use of a computer, with the printout on an X-Y plotter. Such results for a quartz X-cut oscillator plate appear in Fig. 57.

FEASIBILITY OF INFRARED SPECTROPHOTOMETRY FOR COMPOSITIONAL ANALYSIS UNDER LUNAR CONDITIONS

A. Operations on the Lunar Surface

There is nothing intrinsically different between the operation of infrared equipment on the lunar surface and on earth. In fact the lack of an atmosphere would be a decided advantage, obviating the necessity of exactly balancing double-beam instruments. The sun could be used as a "trouble-free" source of intensive infrared radiation for absorption or reflection measurements, being kept in view by sun-seeking mirrors during the two-week period of sunlight.

1. Unmanned Operation

It is probable that only reflection and emission measurements could be made with an unmanned operation on the lunar surface, as the KBr pelleting process would be too difficult to automate. Specular reflection analysis would be best performed on small surfaces, polished on solid rocks, but thermal emission measurements could be made either on solid rock, or on crushed drill-cuttings. These cuttings will also be automatically analyzed by other instruments aboard the spacecraft. The optimum size of the cuttings could be controlled by screens if particle size is proved to be a critical factor.

Roving vehicles would utilize spectral emission analysis in a similar manner to that of orbiting equipment. All analytical data would be digitized and telemetered back to earth, or to a major lunar base.

2. Manned Operation

In a manned lunar laboratory all three analytical methods could be utilized. Samples could be analyzed automatically by emission analysis, using a small solar-heated furnace with a rotating sample tray, and results could be checked by absorption analysis of KBr pellets from time to time. By simplified curve-matching or any other empirical correlation with previously determined rock spectra, it may be found to be the

easiest analytical tool for use in rock analysis.

Data could be recorded in either analog or digital form, and interpreted by curve-fitting or by reference to a master file of peak positions and intensities. It would be a simple process to program a computer with an on-line X-Y plotter to reproduce an analog plot of any mineral mixture "synthesized" by computation from the absorbances of its constituent minerals.

3. Summary

Infrared analytical techniques are capable of distinguishing minerals within four major groups:

(a) Minerals of relatively constant chemical composition (e.g., quartz)

(b) Minerals that exhibit marked differences in composition, as between two end-members (e.g., plagioclase feldspars and olivines), or more numerous components (e.g., pyroxenes, and amphiboles). The infrared spectra clearly show small differences in the amounts of major elements but not of trace elements or low-level impurities.

(c) Minerals of constant chemical composition but possessing different structural modifications (e.g., SiO_2 as quartz, coesite, cristobalite, or tridymite; $CaCo_3$ as calcite or aragonite; microcline and orthoclase feldspars)

(d) Minerals which possess both structural modifications and varying compositions (soda-plagioclase with high- and low-temperature forms which may range from An_0 to An_{20} in composition)

The inorganic anion groups have strong, usually simple, absorption spectra. Some of these are listed in Table X and shown in Fig. 58. A strong absorption within one of these bands implies that a given functional

Table X

FREQUENCIES OF THE PRINCIPAL ANION ABSORPTIONS

Group	Absorption Peak Frequencies (cm^{-1})
CO_3--	1450 - 1410 880 - 800
NO_2-	1400 - 1300 840 - 800
NO_3-	1410 - 1340 860 - 800
PO_4---	1100 - 950
SO_4--	1130 - 1080 680 - 610
All silicates	1100 - 900

anion group (e.g., CO_3--) is present; either the wave number of this strong absorption peak or that of smaller peaks elsewhere in the spectrum will indicate to which metal cation the group is bonded (such as to calcium as $CaCO_3$ or to magnesium as $MgCO_3$). Intermediate values for the principal absorptions may be considered diagnostic of solid solutions (crystalline solutions). Details for the carbonate groups appear in Table XI.

It is quite feasible already for a manned lunar laboratory to use these analytical techniques for rock analysis. With more experience it should be possible to automate thermal emission measurements for unmanned operation on a Surveyor-type vehicle. Before complete assurance can be given, it is required to know more fully the effect of surface roughness, porosity, and particle size, upon the thermal emission of rocks. Computer programming for mineralogical analysis direct from spectral data remains as the final step in compositional analysis.

Table XI

CARBONATE GROUP ABSORPTION FREQUENCIES SHOWING VARIATION WITH BONDED METAL

Mineral	Frequencies (cm^{-1})		
Calcite sub-group			
Calcite $CaCO_3$	1435	873	712
Rhodochrosite $MnCO_3$	1433	867	727
Siderite $FeCO_3$	1422	866	737
Magnesite $MgCO_3$	1450	887	748
Dolomite sub-group			
Ankerite $Ca,Fe(CO_3)_2$	1450	877	726
Dolomite $Ca,Mg(CO_3)_2$	1435	881	730
Aragonite sub-group			
Cerussite $PbCO_3$	1440	841	677
Witherite $BaCO_3$	1445	860	693
Strontianite $SrCO_3$	1470	860	707
Aragonite $CaCO_3$	1450	860	712

B. Operations on a Vehicle Orbiting above the Lunar Surface

Only analysis of the thermally emitted radiation is available for use on a vehicle orbiting above the lunar surface. The parameters of grating scan-rate, orbital speed, field of view, orbital height (and stability), and the lunar surface temperature, which changes with each orbit, from hot to cold, are much more important and present problems of great magnitude. Minimum and preferred values for these factors have been selected as follows,[15] to yield as high a signal-to-noise ratio as is possible with present-day, uncooled detectors.

Wavelength Range: 8 to 25 microns (1250 to 400 cm^{-1})

Spectral Resolution: 80 cm^{-1}, minimum (interferometer)

5 cm^{-1}, preferred (grating)

Field of View at a distance of 100 miles:	100-miles diameter, minimum 10-miles diameter preferred
Signal-to-Noise Ratio:	10, minimum 100, preferred
Intensity Reproducibility:	1% to 2%
Type of Detector:	Ambient temperature thermistor, minimum Cu-doped Ge elemental detector (cooled), preferred
Power Requirement:	3 to 5 watts
Weight:	2 to 5 pounds

APPENDIX

BACKGROUND FOR THERMAL EMISSIVITY STUDIES*

A. Relationship of Thermal Emissivity, Absorptivity, and Dependence of Emissivity upon Wavelength and Temperature *

Because of compositional characteristics inherent in minerals, the absorptivity and hence, emissivity, of these materials is a function of the wavelength of the radiant energy. The radiant energy, (λ, T) from the lunar surface is equal to

$$\mathcal{R}(\lambda, T) = \epsilon_b \epsilon(\lambda) W(\lambda, T) \qquad (1)$$

where ϵ_b is the efficiency of emission, a measure of the departure from "blackbody" towards "graybody" character,

$\epsilon(\lambda)$ is the emissivity of the surface which is dependent on wave length, and

$W(\lambda, T)$ is the energy of a blackbody at wavelength, λ, and temperature, T.

The term ϵ_b is very nearly unity in most instances, particularly if the surface is a finely divided powder. The term $\epsilon(\lambda)$ is the important term for it is dependent upon the composition of the emitting surface and varies widely as a function of wavelength. At thermal equilibrium the product of $\epsilon_b \epsilon(\lambda)$ is equal to the absorbed energy, $\alpha(\lambda)$.

To establish the composition of the lunar crust, $\epsilon_b \epsilon(\lambda)$ must be determined experimentally; then interpretation by correlation with previously amassed catalogs of $\alpha_o(\lambda)$ for minerals must be made. Qualitative analysis is achieved readily from the general shape of the $\epsilon_b \epsilon(\lambda)$ versus λ curve. For quantitative work the term ϵ_b must be determined so that it can be eliminated from subsequent calculation; this is readily accomplished at a wavelength where $\epsilon(\lambda) = 1.00$.

---

* Sections contributed by E. A. Burns, co-worker on this project.

The catalog of $\alpha_o(\lambda)$ can be obtained in the laboratory in a variety of ways. Absolute emission measurements give values of $\epsilon_b\alpha_o(\lambda)W(\lambda, T)$ and after detailed calculation, $\alpha_o(\lambda)$ is obtained directly. Because a great deal of care must be exercised in temperature control and because energy losses in the optical system must be known to permit accurate calculation of $\alpha_o(\lambda)$, these values are more easily obtained by indirect means. The incident energy (I_o) of a particular wavelength (λ) that falls on a substrate is either transmitted (I_t), absorbed (I_α), reflected spectrally (I_ρ), or reflected diffusely (scattered) (I_s) by the substrate. That is

$$I_o = I_t + I_\alpha + I_\rho + I_s \tag{2}$$

or

$$1 = t_o(\lambda) + \alpha_o(\lambda) + \rho_o(\lambda) + s_o(\lambda) \tag{3}$$

Transmission measurements normal through thin layers of sample [$\rho_o(\lambda)$ and $s_o(\lambda) = 0$] are useful for giving the general shape of the $\alpha_o(\lambda)$ curve; however they are dependent on the thickness of sample and hence are not useful for quantitative analysis of lunar surfaces. Spectral reflection measurements, on the other hand, on polished surfaces [$t_o(\lambda)$ and $s_o(\lambda) = 0$] give data for $\alpha_o(\lambda)$ which are usable for both qualitative and quantitative evaluation.

In calculations of the changes in the radiant energy of quartz compared with a blackbody at the same temperature, $\epsilon(\lambda)$ was obtained from reflection studies, i.e., $[1-\rho_o(\lambda)]$, and then the term $\epsilon(\lambda)W(\lambda, T)$ was evaluated. Over the temperature range 250°K to 500°K the shape of $\epsilon(\lambda)W(\lambda, T)$ and the wavelength of maximum energy vary markedly with the temperature of quartz. In fact, if the temperature of quartz were to be determined using equipment designed to give only the wavelength of maximum energy, considerable error in this measurement would exist in this temperature range. Data indicate that a maximum error of 65°K could result. Temperature determination by radiometric measurements

will also be in error when the emissivity is a function of wavelength. In this method the temperature is calculated from the following equation,

$$T = \left[\frac{\mathcal{R}}{\sigma \epsilon_{avg}}\right]^{\frac{1}{4}} \tag{4}$$

where σ is the Stefan-Boltzmann's constant.

A prerequisite for the applicability of this method is that ϵ_{avg} is independent of temperature; however, because of its dependence on wavelength, it is also a function of temperature. The average emissivity over the wavelength interval 3 to 25 microns is defined as

$$\epsilon_{avg} = \frac{\int_3^{25} \epsilon(\lambda) W(\lambda, T) d\lambda}{\int_3^{25} W(\lambda, T) d\lambda} \tag{5}$$

for any temperature T. Values of ϵ_{avg} for quartz in this wavelength interval are listed in Table C.1.

Table C.1

AVERAGE EMISSIVITY AS A FUNCTION OF TEMPERATURE FOR QUARTZ

Temperature (^{o}K)	ϵ_{avg}
250	0.748
300	0.763
350	0.768
400	0.778
450	0.801
500	0.819

From this table it is seen that the change in emissivity as a function of temperature range is of the order of 0.04%/^{o}K, or $\frac{1}{\epsilon}\frac{d\epsilon}{dt} \approx 0.0004$.

The relative error of absolute radiometry can be evaluated by taking differentials of Eq. (4).

$$\frac{d\mathcal{R}}{\mathcal{R}} = \frac{d\epsilon}{\epsilon} + \frac{4dT}{T} \qquad (6)$$

A calculated temperature change of 1.25%(4.4°K at 350°K) results from a radiant energy change of 5%. However, this radiant energy change could be entirely accounted for instead by a 5% change in the emissivity. From the data of Table C.1 we find that $\frac{d\epsilon}{\epsilon}$ values as high as 5% are unlikely; hence temperature changes of the same material as observed by radiometric methods are valid. On the other hand, absolute values of the temperature can be significantly in error.

Because of the predominance of the strong Si-O vibrational band near 10 microns for most rock-forming minerals, it is reasonable to conclude that a situation similar, though perhaps not as dramatic, as that described for quartz would exist for lunar surfaces. This statement is diametrically opposed to the theories expounded by Pettit and Nicholson;[40] after some detailed calculations based on an assumed magnitude of stellar radiation they concluded that the moon was a blackbody in the wavelength range 8 to 14 microns. The classical works of Coblenz,[6,7] however, as well as the recent studies of Bell et al.,[16,17] present a strong contradiction of the Pettit-Nicholson theories. It is impossible to confirm or deny either theory for the emissivity of the moon even with the use of modern infrared equipment, while situated on the earth, because of spectral interference at 9.2 microns from ozone in the earth's atmosphere.

B. Interpretation of Temperature Differences

Standard methods used for the estimation of the temperature of a radiating source are inadequate unless the relationship of the emissivity (ϵ) of the source as a function of wavelength (λ) is established. Calculations of the temperature of the moon based upon location of the wavelength of maximum energy can be in error by as much as 65°K, and the error for temperature differences using radiometric techniques can be of the order of 10°K.

Incorporation of the measured values of $\epsilon(\lambda)$, (obtained from reflectance data) for four samples of granite, obsidian, dunite, and chondritic meteorite, into the 350°K blackbody energy curves permits calculation of the emittance curves for these rock samples at a typical lunar ambient temperature (Fig. C.1).[40,41] From these we note that changes in composition can yield changes in $d\epsilon/\epsilon$ of 10%. This 10% relative change in the emissivity between granite and the chondritic meteorite is relatable to a change of 2-1/2% in the temperature, or to an error of about 9°K at 350°K [see Eq. (6)].

Use of this spectral data applied to emission measurements can readily account for the temperature differences observed by Shorthill and Saari.[42] They noted local changes of 5°K which can be explained by compositional changes. Explanations for the observed maximum temperature changes of 30°K are much less certain, and are likely to be a composite of temperature change and compositional change. It is clear that if the variations in emissivity as a function of composition are evaluated, then the differences in lunar surface temperatures, as already observed from the earth, may be resolved.

Because the lunar surface temperature is estimated to vary between 115°K and 374°K, it is particularly ill-advised to determine temperature from the wavelength of maximum energy or by integrated radiometric methods; however, if the radiant energy spectrum were obtained, a blackbody curve could be constructed from the slope of the $W(\lambda, T)$ curve at short wavelengths [when $\epsilon(\lambda) = 1.00$]. From this careful approximation, good estimates of the temperature could be made.

ACKNOWLEDGMENTS

The samples were collected, and then purified, and the KBr disc prepared in the Geochemical Laboratory, by R. Seetharam under the direction of Dr. R. J. P. Lyon. Spectrographic analyses were performed under the direction of Dr. E. A. Burns, Manager of the Analytical Laboratory, Propulsion Sciences Division, who also provided invaluable assistance in the many phases of emission spectrophotometry. The data were analyzed and the report prepared by Dr. Lyon.

The many mineralogists who contributed standardized samples of minerals are listed below. Without their assistance a study of this degree of detail could not have been attempted.

Anderson, J.	Titanates
Baker, G.	Australite (tektite)
Beatty, W. B.	Basalt Obsidian Granite
Chao, E. C. T.	Coesite Stishovite
Chinner, G.	Cordierite Muscovite
Coleman, R. G.	Pyroxenes Garnets Micas Lawsonite Zeolites Phosphates Carbonates
Coombs, D. S.	Wairakite
DeCarli, P.	Shock-loaded minerals
Dickinson, W. R.	Gabbro
Edwards, A. B.	Muscovite
Erd, R.	Zeolites Phosphates Pyroxenes
Fairbairn, H. W.	Mica
Floyd, P.	Obsidian
Foster, M. D.	Micas Chlorites
Frederiksson, R.	Chondrite
Fryklund, V.	Garnet Mica
Grines, D.	Shock-loaded limestone
Gulbrandsen, R. A.	Phosphates
Hannah, R.	Al-Hydrates
Heinrich, E. W.	Micas
Hemley, J.	Micas Synthetic minerals
Hess, H. H.	Pyroxenes
Howie, R. A.	Pyroxenes
Hutton, C. O.	Pyroxenes Micas
Jackson, E. D.	Feldspars Pyroxenes Olivines Gabbro Dunite

Kunze, G. W.	Clay
Lee, D.	Garnets
Lipman, P.	Hornblende
Loomis, A. A.	Chondrites
Lyons, S. C.	Kaolinite
Mein, W. J.	Anauxite
Milton, D.	Stishovite
	Limestone
	Sandstone
	Coesite
	Pyroxene
Mountsier, S. R.	Talc
Olsen, R.	Zeolites
Pabst, A	Anauxite
Parks, G.	Perlites
	Opal
	Phosphate
	Chrysocolla
Roberts, R.	Turquoise
Sands, L. B.	Clays
Schieltz, N. C.	Celadonite
Schlocker, J.	Micas
Sedlacek, R.	Rutile
Shell, H. R.	Micas
Short, N.	Granite
Speed, R. C.	Gabbro
	Granite
	Serpentine
	Anorthosite
	Quartzite
	Tuff, Bishop
	Rhyolite
	Dunite
	Basalt
Stephens, J.	Kaolinite
Stevens, R.	Lepidolites
Stringham, B.	Clays
Taylor, W.	Zeolites
Theobald, P.	Biotites
Threadgold, I.	Mica
Tuddenham, W. M.	Olivines
Vernon, R.	Hornblende
	Mica
	Cummingtonite
Weir, A.	Beidellites
Whelan, J.	Clay
	Phosphates
Wilshire, H.	Pyroxenes
	Zeolites
Wones, D.	Synthetic feldspar
Yates, R	Hornblende

Stanford Research Institute
Menlo Park, California
September 1962

REFERENCES

1. Hunt, J. M., Wisherd, P., and Bonham, L. C., Infrared Absorption Spectra of Minerals and other Inorganic Compounds, Anal. Chem. 22, 1478-1497 (1950)

2. Hunt, J. M. and Turner, D. S., Determination of Mineral Constituents of Rocks by Infrared Spectroscopy, Anal. Chem. 25, 1169-1174 (1953)

3. Tuddenham, W. M. and Lyon, R. J. P., Relation of Infrared Spectra and Chemical Analysis for some Chlorites and Related Minerals, Anal. Chem. 31, 377-380 (1959)

4. Tuddenham, W. M. and Lyon, R. J. P., Infrared Techniques in the Identification and Measurement of Minerals, Anal. Chem. 32, 1630-41 (1960)

5. Lyon, R. J. P., Tuddenham, W. M., and Thompson, C. S., Quantitative Mineralogy in 30 Minutes, Econ. Geol. 54, 1047-1055 (1959)

6. Coblentz, W. W., Investigation of Infrared Spectra, Pub. 65, Carnegie Institute of Washington, 1906

7. Coblentz, W. W., Selected Radiation from Various Solids, II, Nat. Bur. Standards (US) Bull, 6, 301 (1910)

8. Pfund, A. H., The Identification of Gems, J. Opt. Soc. Amer., 35, 611-614 (1945)

9. McMahon, H. O., Thermal Radiation Characteristics of Some Glasses, Jour. Am. Ceram. Soc., 34, 91-6 (1950)

10. Simon, J. and McMahon, H. O., Study of the Structure of Quartz, Cristobalite, and Vitreous Silica by Reflection in Infrared, Jour. Chem. Phys. 21, 23-30 (1953)

11. Gardon, R., The Emissivity of Transparent Materials, J. Am. Ceram. Soc. 39, 278-285 (1956)

12. Keller, W. D., Spotts, J. H., and Biggs, D. L., Infrared Spectra of some Rock-Forming Minerals, Am. Jour. Sci. 250, 453-471 (1952)

13. Launer, P. J., Regularities in the Infrared Absorption Spectra of Silicate Minerals, Am. Min. 37, 774-784 (1952)

14. Burns, E. A., and Lyon, R. J. P., Errors in the Measurement of the Temperature of Radiating Lunar Materials, paper to be presented at the First Annual Pacific Meeting of Applied Spectroscopy and Analytical Chemistry, (Oct. 19, 1962)

15. Lyon, R. J. P., and Burns, E. A., Temperature and Compositional Mapping of the Lunar Surface from an Orbiting Vehicle, SRI Proposal PRU 62-251 to NASA, June 22,(1962)

16. Bell, E. E. and Eisner, I. L., Infrared Radiation from the White Sands at White Sands National Monument, New Mexico, Jour. Opt. Soc. Am., 46, 303-4 (1956)

17. Bell, E. E., Eisner, I. L. Young, J. B., Abolins, A. and Oetjen, R. A., Infrared Techniques and Measurements, Ohio State Research Foundation, Final Engineering Report, Contract 33(616)3312, p.105 (ASTIA - AD 151221),(1957)

18. Miller, F. A. and Wilkins, C. H., Infrared Spectra and Characteristic Frequencies of Inorganic Ions, Anal. Chem. 24, 1253-94 (1952)

19. Uhlrich, W. F., Applications of Specular Infrared Reflectance, The Analyzer (Beckman Inc. House Journal), July, 14-16,(1961)

20. Hannah, R., Perkin-Elmer Corporation, Norwalk, Conn., Private communication.

21. Duyckaerts, G., The Infrared Analysis of Solid Substances, Analyst, 84, 201-214 (1959)

22. Lyon, R. J. P. and Burns, E. A., Analysis of Rocks by Reflected Infrared Radiation,(Manuscript submitted to Economic Geology Magazine, August, 1962)

23. Laves, F. and Hafner, St., Order/Disorder and Infrared Absorption I; (aluminum, silicon)--Distribution in feldspars, Zeitschr. Kristallographie, 108, 52-63 (1956)

24. Hafner, St. and Laves, F., Order/Disorder and Infrared Absorption II: Variation of the Position and Intensity of some Absorptions of Feldspars; The structure of orthoclase and adularia, Zeitschr. Kristalographie, 109, 204-225 (1957)

25. Lyon, R. J. P. and Tuddenham, W. M., Determination of Tetrahedral Aluminum in Mica by Infrared Absorption, Nature, 185, 374-5 (1960)

26. Stübican, V. and Roy, R., Infrared Spectra of Layer-Structure Silicates, J. Amer. Ceram. Soc., 44, 625-627 (1961)

27. Stübican, V. and Roy, R., Isomorphous Substitution and Infrared Spectra of the Layer-Lattice Silicates, Am. Min. 46, 32-51 (1961)

28. Lyon, R. J. P., Evaluation of Infrared Spectrophotometry for Compositional Analysis of Lunar and Planetary Soils, Stanford Research Institute, Project No. SU-3943, Interim Report No. 1, NASA contract NASr-49(04),(1962)

29. Berry, L. G. and Mason, B., Mineralogy-Concepts, Description and Determinations, W. H. Freeman and Co., Press, San Francisco, pp. 630, (1959)

30. Duke, D. A., Infrared Investigation of the Crystal Chemistry of Olivine and Humite Minerals, Ph.D. Thesis University of Utah, (1962)

31. Vernon, R. H., Co-existing Cummingtonite and Hornblende in an Amphibolite from Duchess, Queensland, Australia, Am. Min., 47, 360-371 (1962)

32. Bates, T. L., Penn. State University, Personal communication.

33. Tarte, P., and Ringwood, A. E., Infrared Spectrum of the Spinels Ni_2SiO_4, Ni_2GeO_4 and their Solid Solutions, Nature 193, 971-2 (1962)

34. Lyon, R. J. P., Infrared Confirmation of 6-fold Coordination of Silicon in Stishovite (SiO_2): (Manuscript submitted to Nature Magazine, July, 1962)

35. Saksena, B. D., Analysis of the Raman and Infrared Spectra of α-Quartz, Proc. Indian. Acad. Sci., 12A, 92-139 (1940)

36. Saksena, B. D., Infrared Absorption Studies of Some Silicate Structures, Trans. Faraday Soc., 57, 242-255 (1961)

37. Sevchenko, N. A., and Florinskaya, V. A., The Reflection and Transmission Spectra of Various Modifications of Silicon Dioxide in the Wavelength Region 7-24 Microns, (in Russian), Doklady Akad. Nauk USSR, 109, 1115-8 (1956)

38. Matossi, F., and Bronder, O., The Infrared Absorption Spectra of several Silicates, in German, Z. Physik, 111, 1-17 (1938)

39. Frederickson, W. R., and Ginsburg, N., Infrared Spectral Emissivity of Terrain, Dept. of Physics, Syracuse Univ., Interim Report, No. 1, Contract AF 33(616)-5034, p. 49, (ASTIA - AD 132839), (1957)

40. Pettit, E., and Nicholson, S. B., Lunar Radiation and Temperature, Astrophys. Jour., 71, p. 102-137 (1930)

41. Pettit, E., Radiation Measurements on the Eclipsed Moon, Astrophys. Jour., 91, 408 (1940)

42. Shorthill, R. W., and Saari, J. M., Lunar Infrared Temperature during Sept. 4, 5, and 6, 1960, Boeing Aircraft Co., Report under Air Force Contract 18600-1824 (Jan. 30, 1961)

43. Burns, E. A., and Lyon, R. J. P., Errors in the Measurement of the Temperature of Radiating Lunar Bodies, (Manuscript submitted to Nature Magazine, August, 1962)

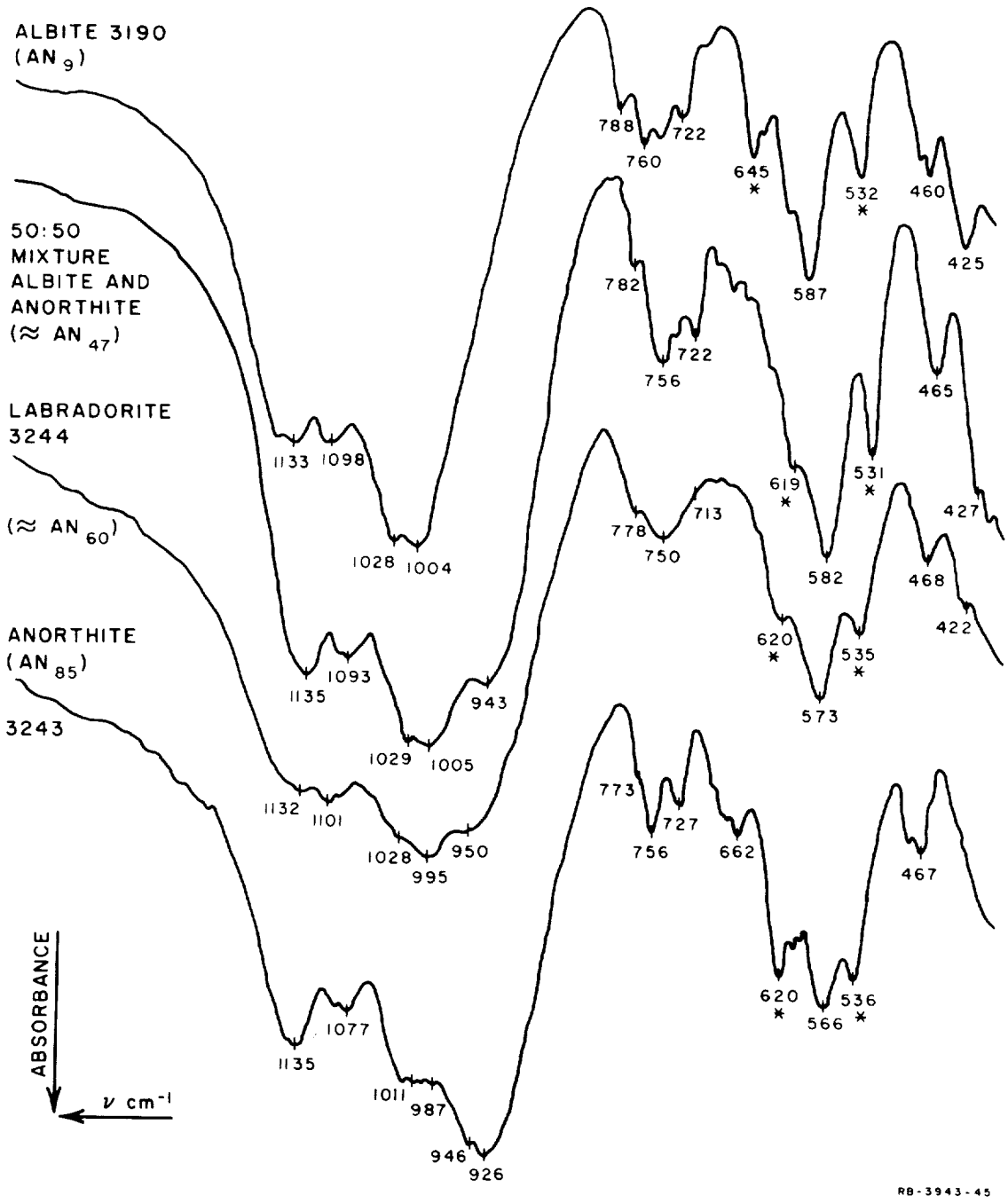

Fig. 1 Absorption spectra for plagioclase mixtures. Note the similarity between the spectra for labradorite and the equal-part mixture of albite and anorthite.

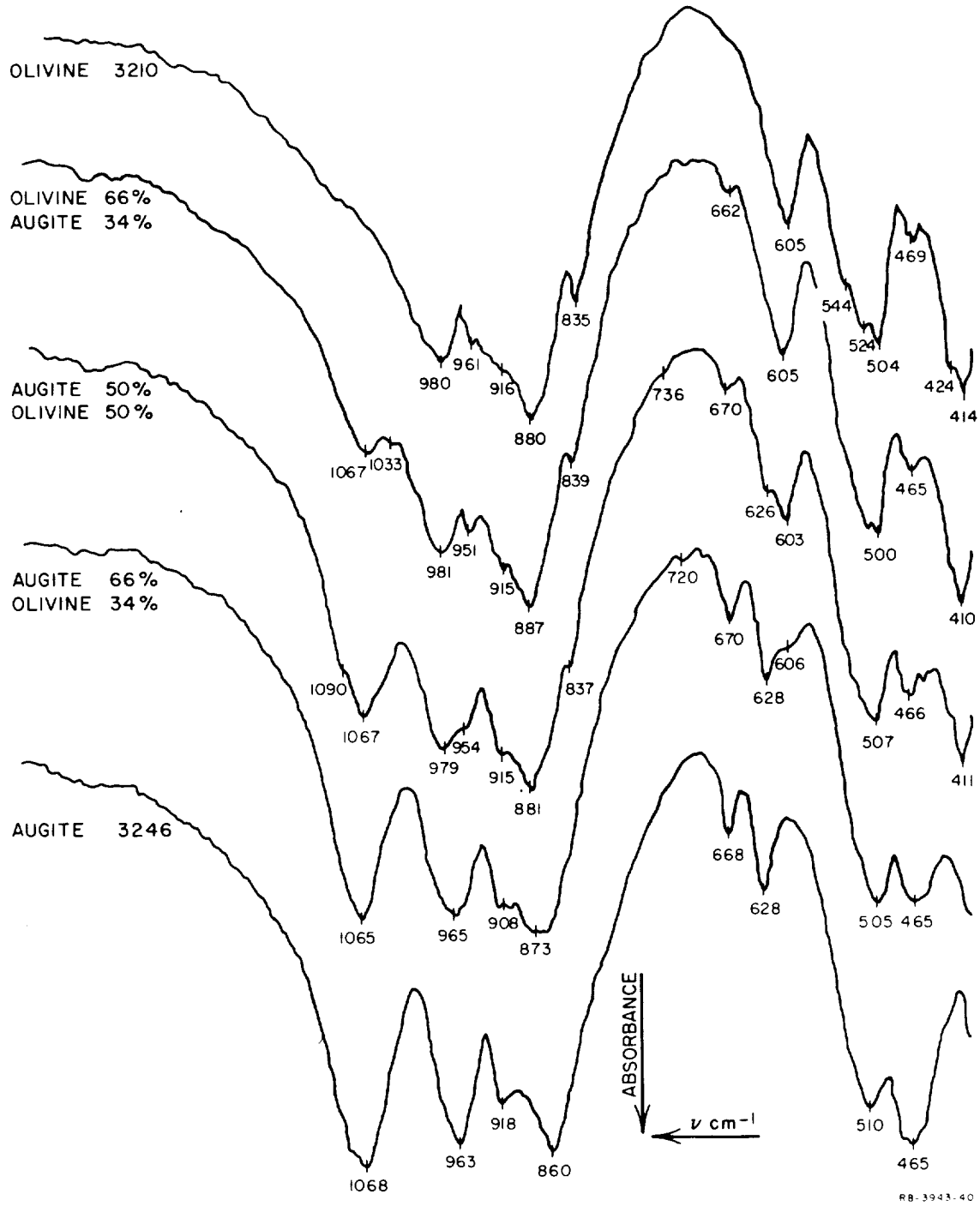

Fig. 2 Absorption spectra for augite and olivine mixtures

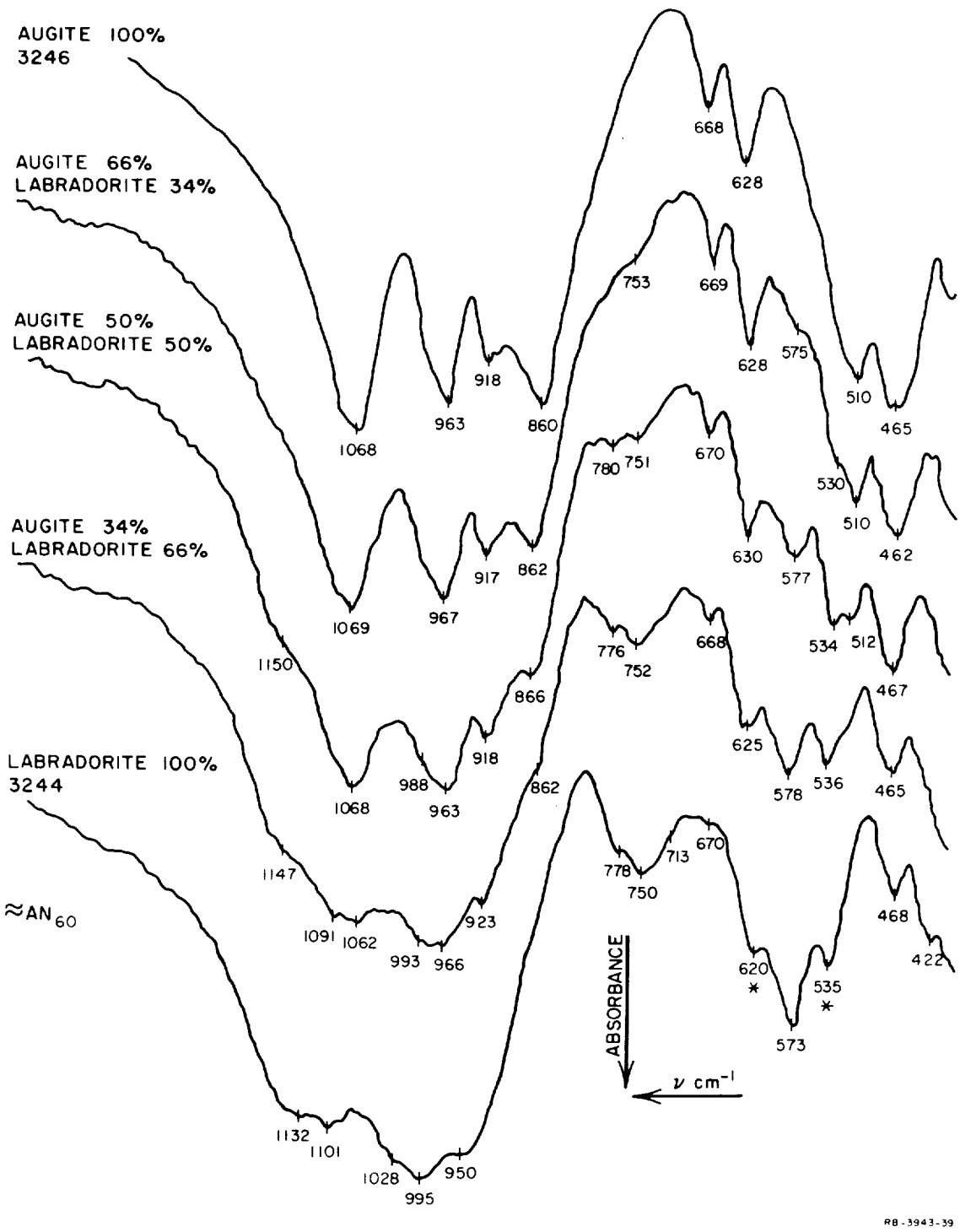

Fig. 3 Absorption spectra for augite and labradorite mixtures

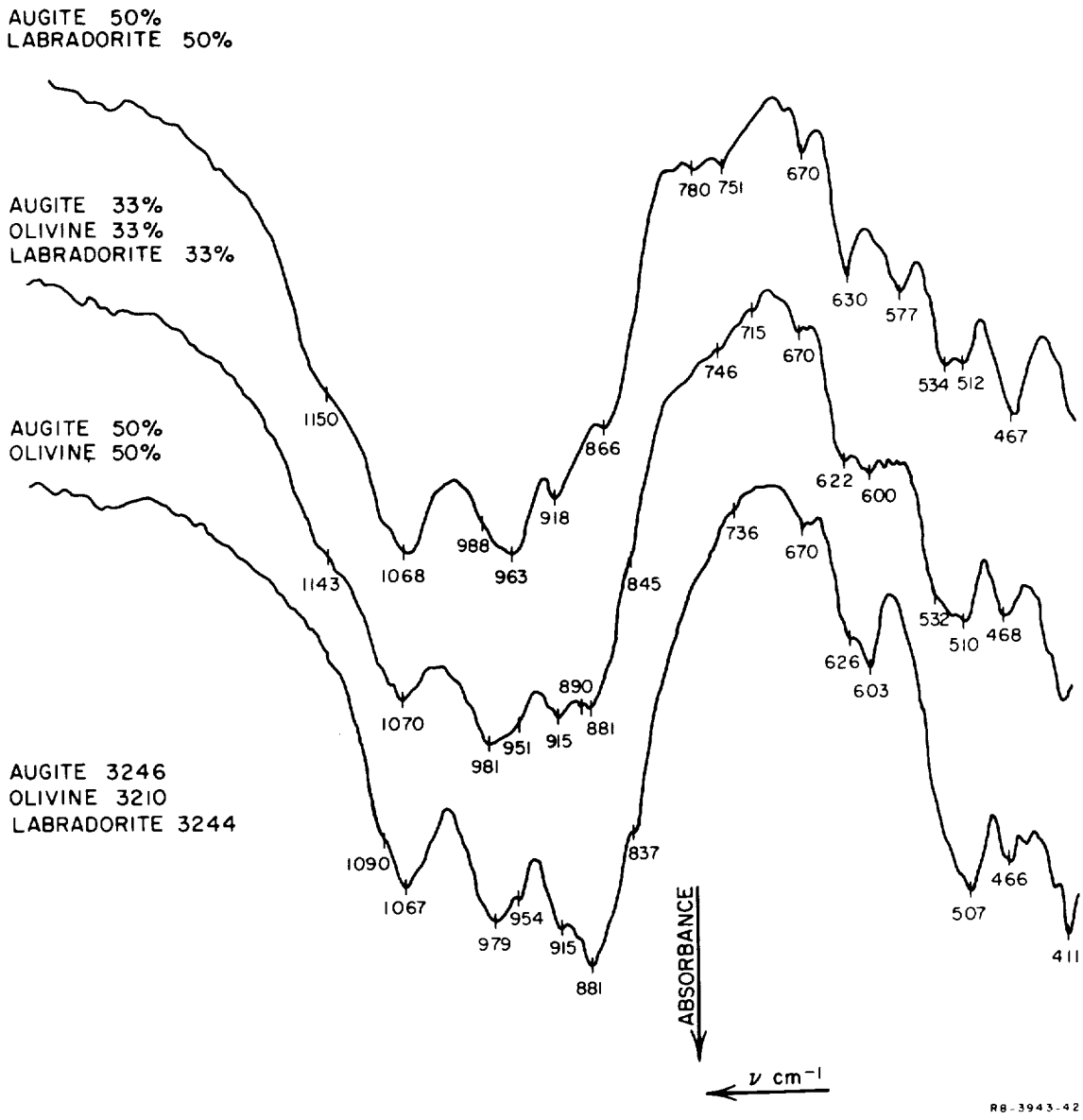

Fig. 4 Absorption spectra for augite, labradorite, and olivine mixtures

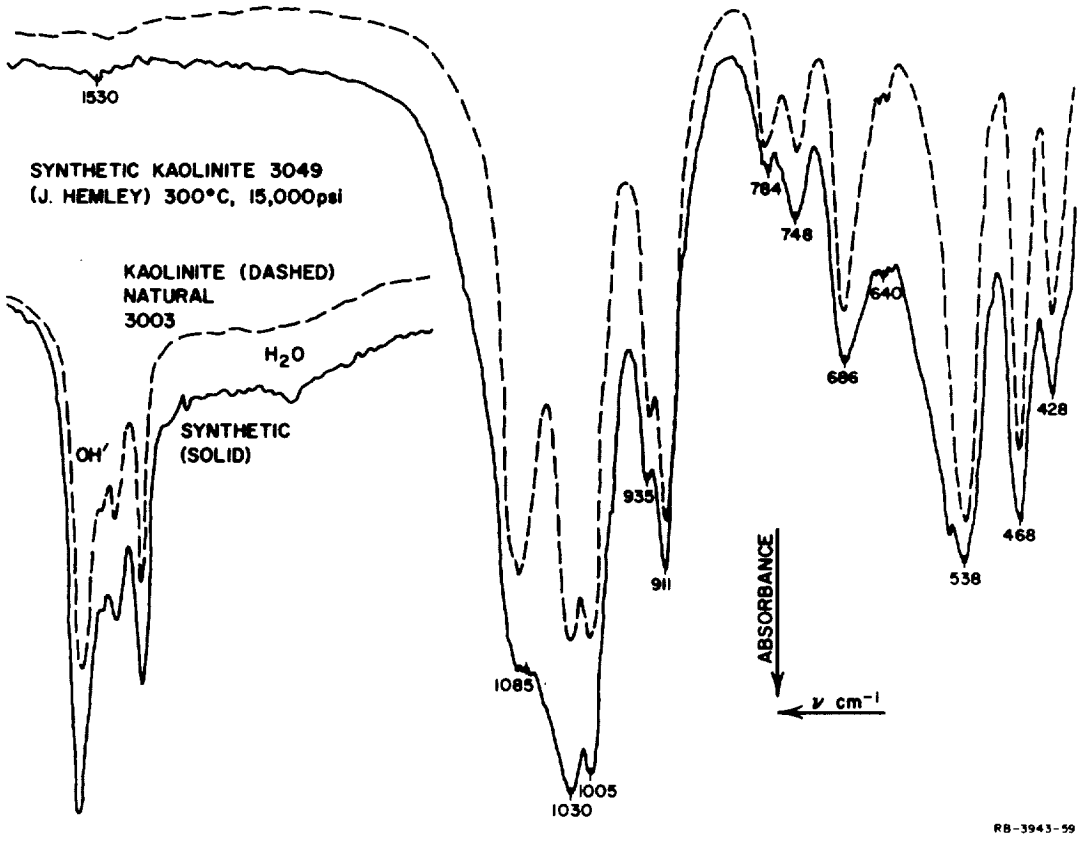

Fig. 5 Absorption spectra for natural and synthetic kaolinite

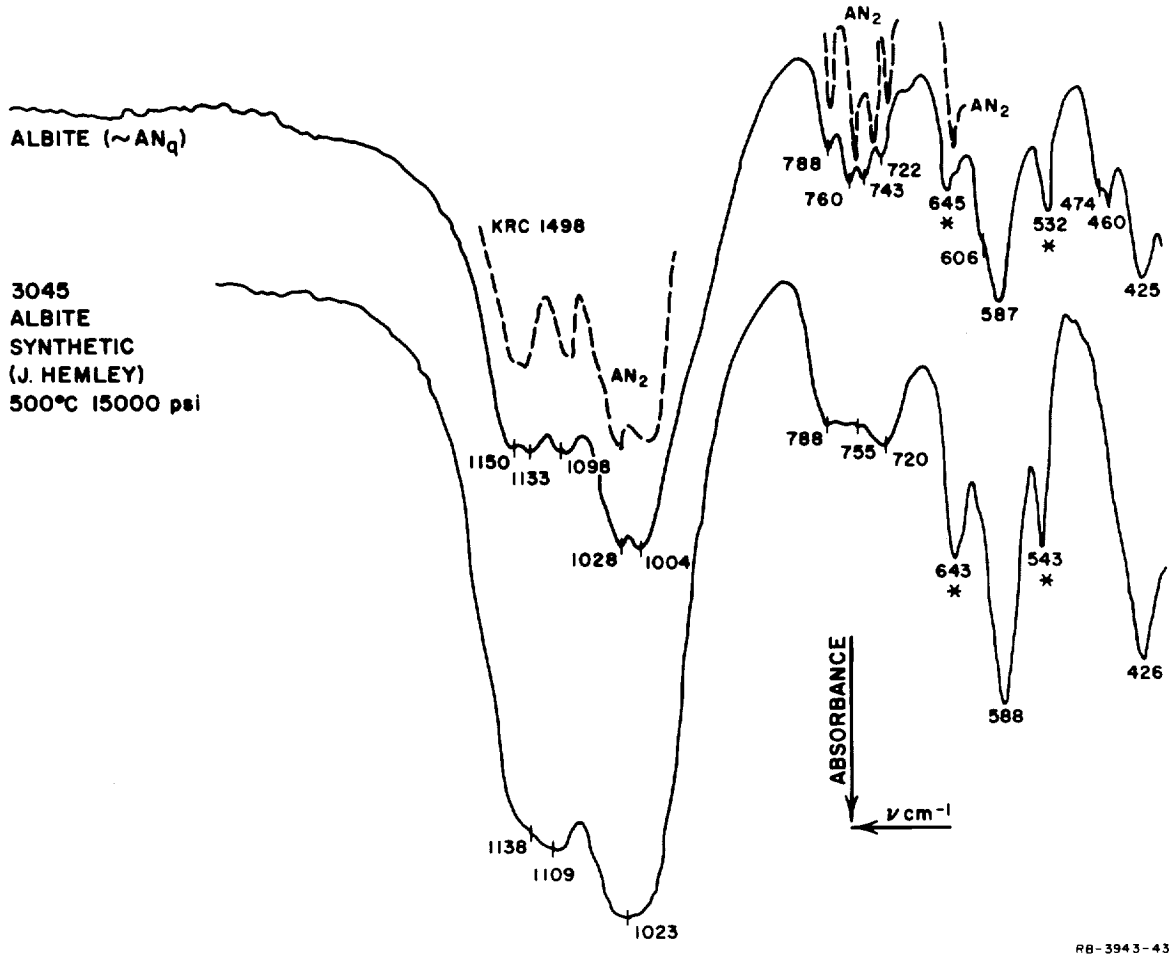

Fig. 6 Absorption spectra for natural and synthetic albite feldspar

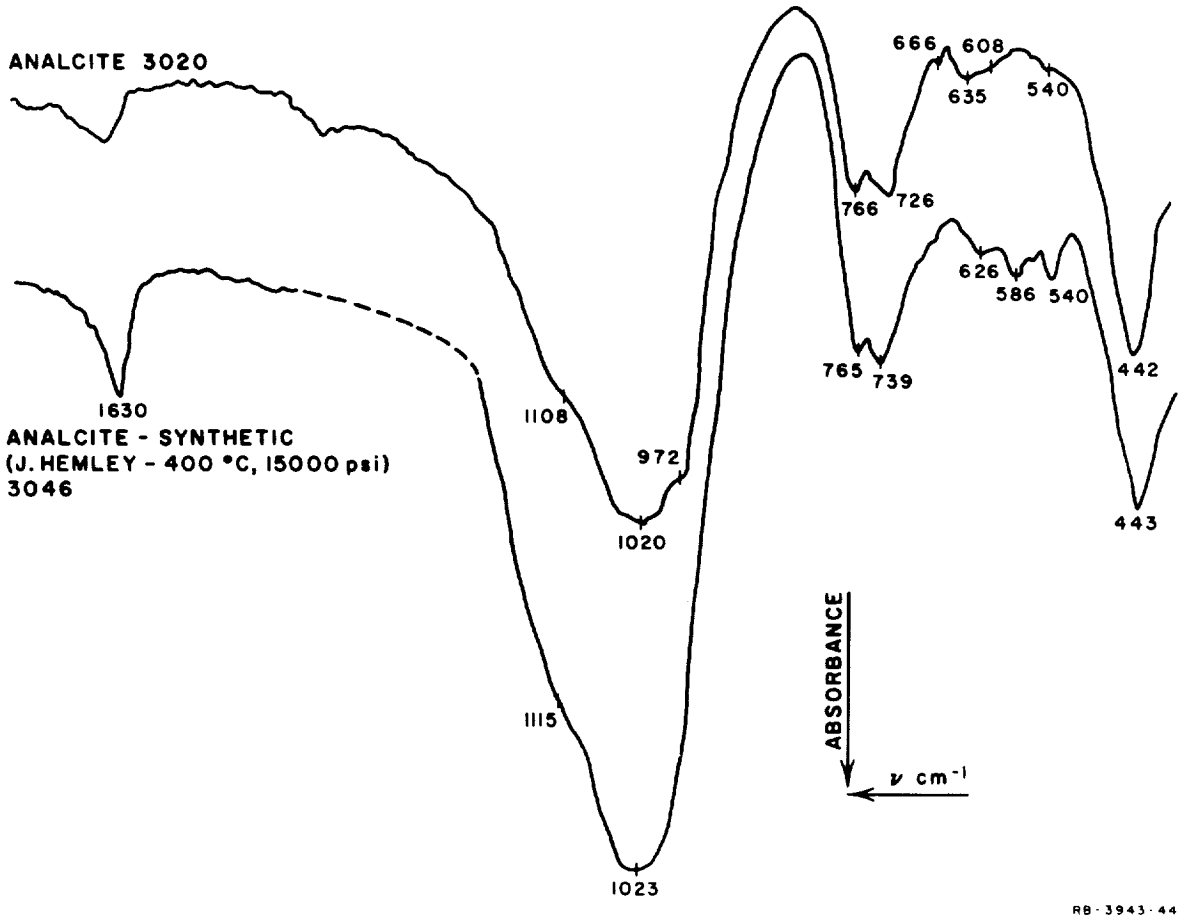

Fig. 7 Absorption spectra for natural and synthetic analcite

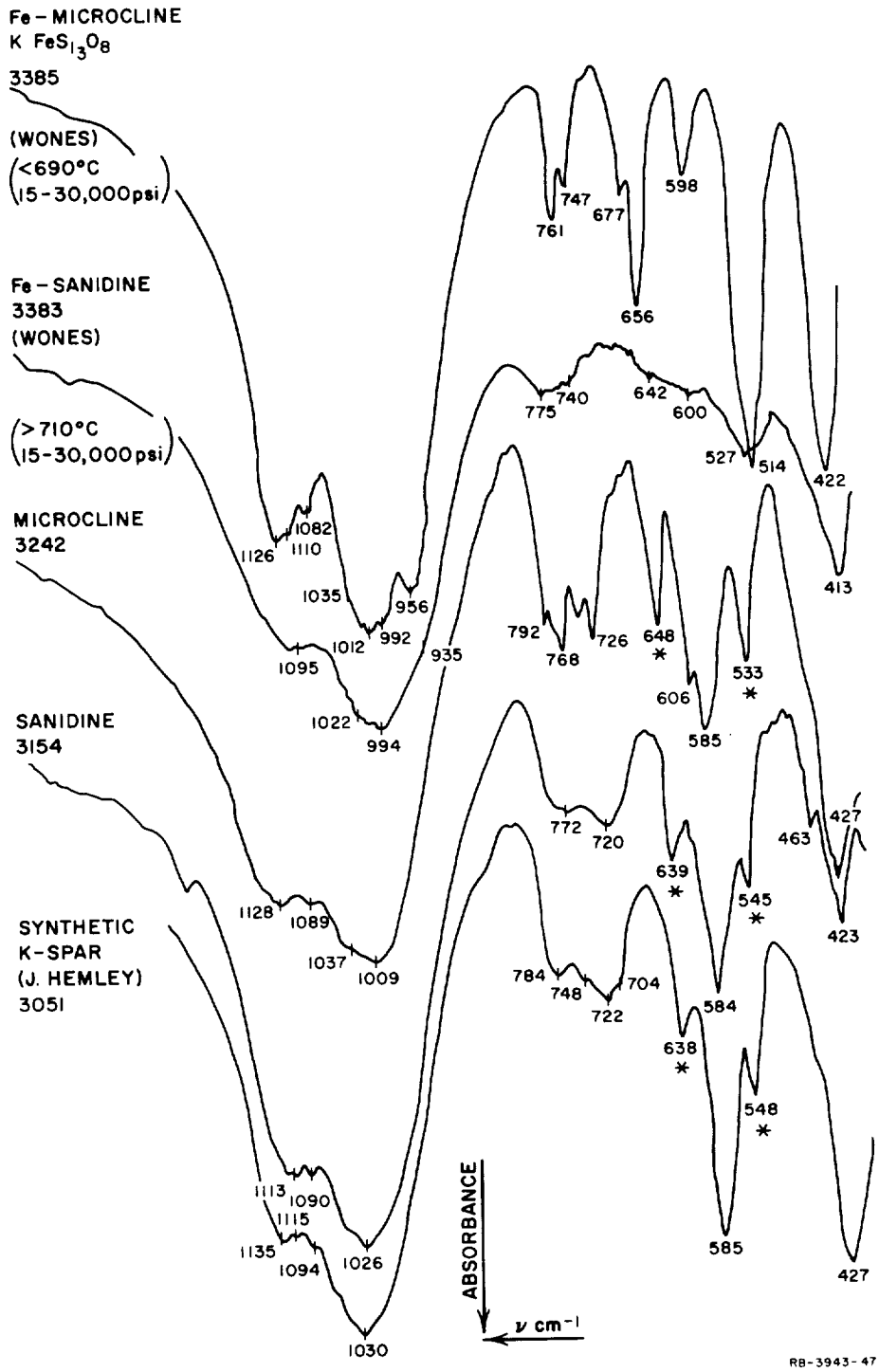

Fig. 8 Absorption spectra for natural and synthetic (iron-bearing) alkali feldspars. Synthetic iron-feldspars are compared with the natural aluminum-feldspars sanidine and microcline. Note the high resolution of the well-ordered form, microcline, as contrasted to the disordered form, sanidine.

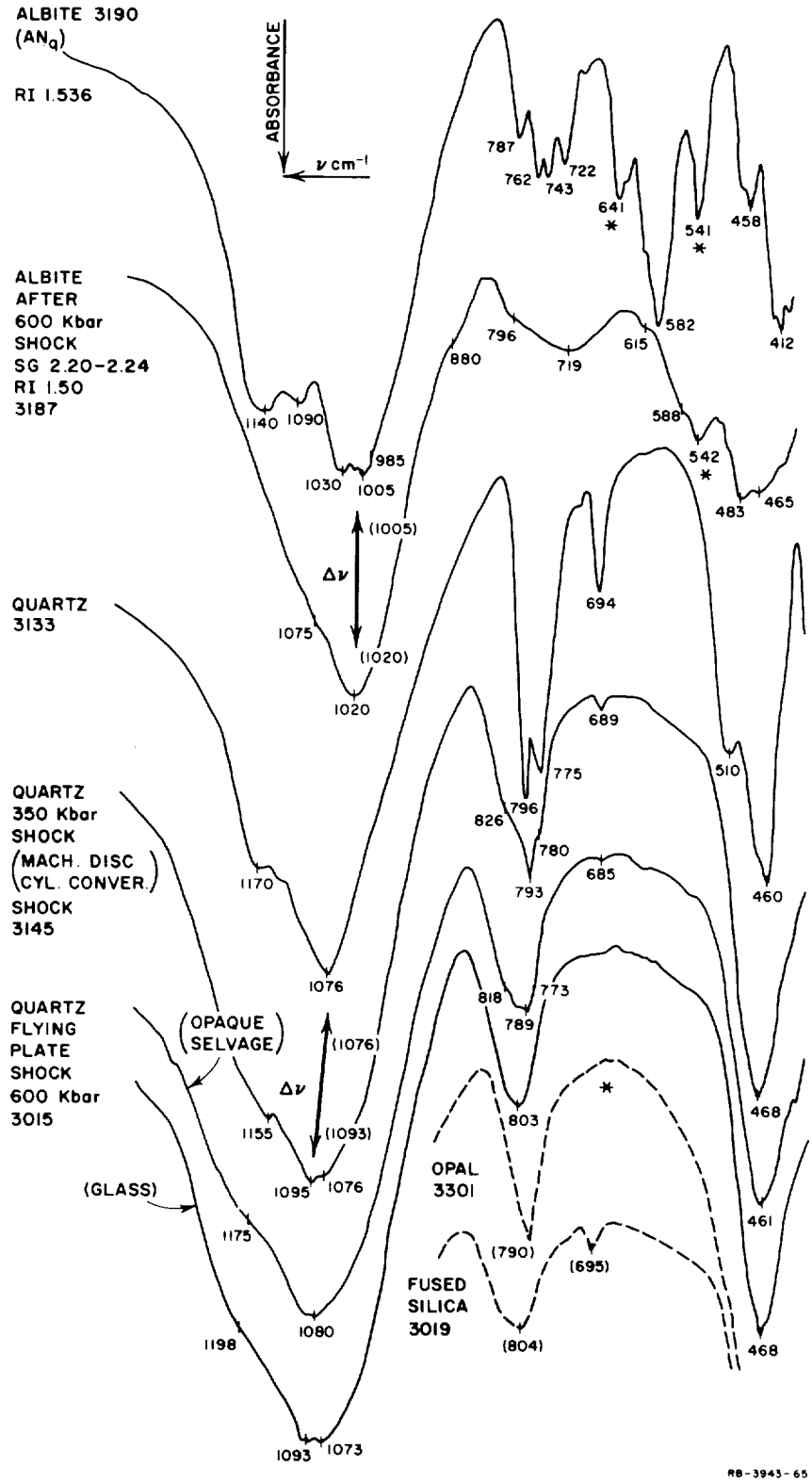

Fig. 9 Absorption spectra of shock-loaded albite feldspar and quartz. The presence of glass results in the loss of detail in their spectra.

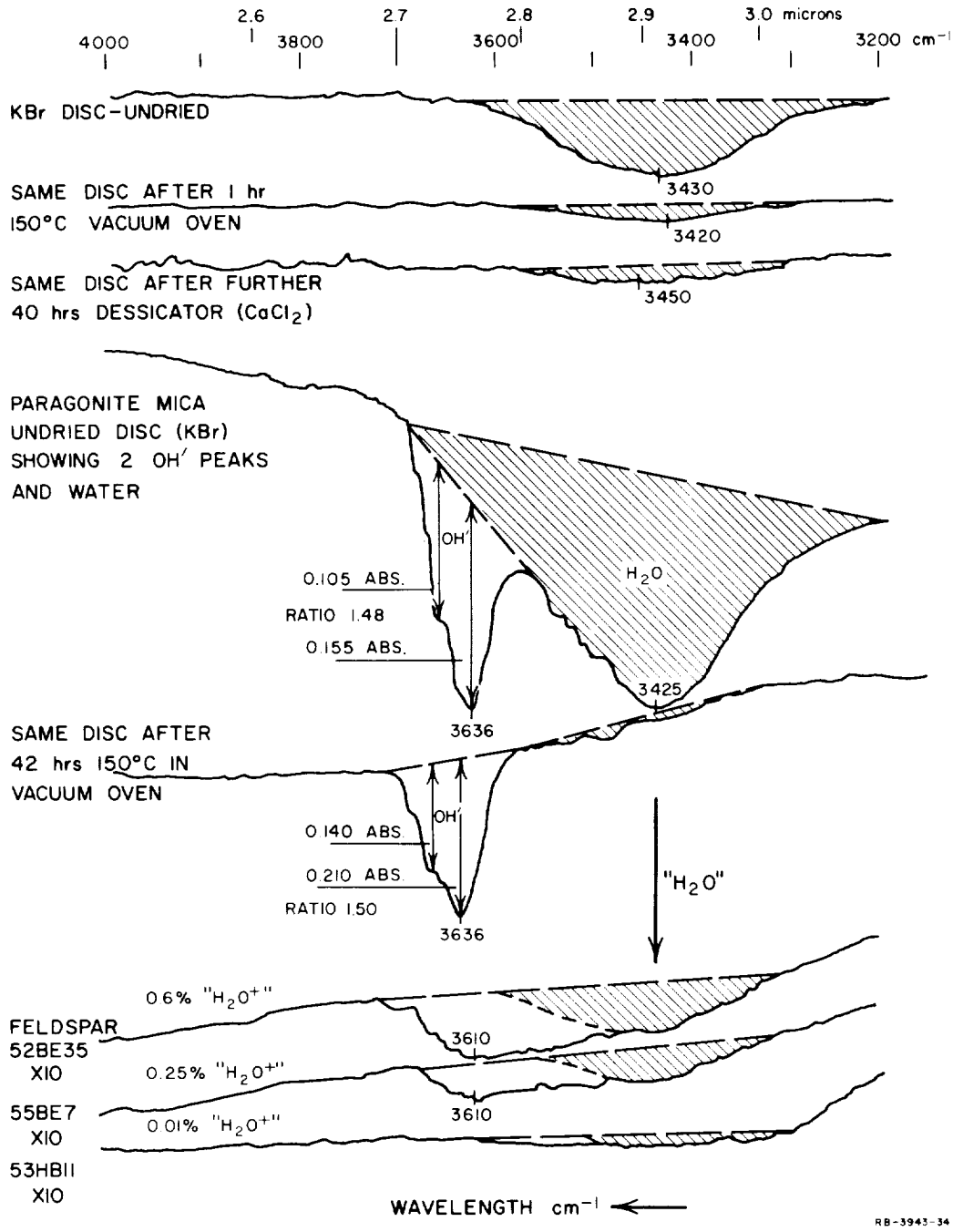

Fig. 10 Absorption spectra showing the "modes" of occurrence of water in minerals and the ability of infrared analysis to differentiate between them. Normal moisture associated with a "wet" sample occurs around 3435 cm^{-1}, but peaks shift to higher wavenumbers with increased strength of bonding in the structure of the crystal. Hydroxyl peaks for muscovite micas are about 3650 cm^{-1}, while that for talc is about 3700 cm^{-1}. The curves are displaced vertically.

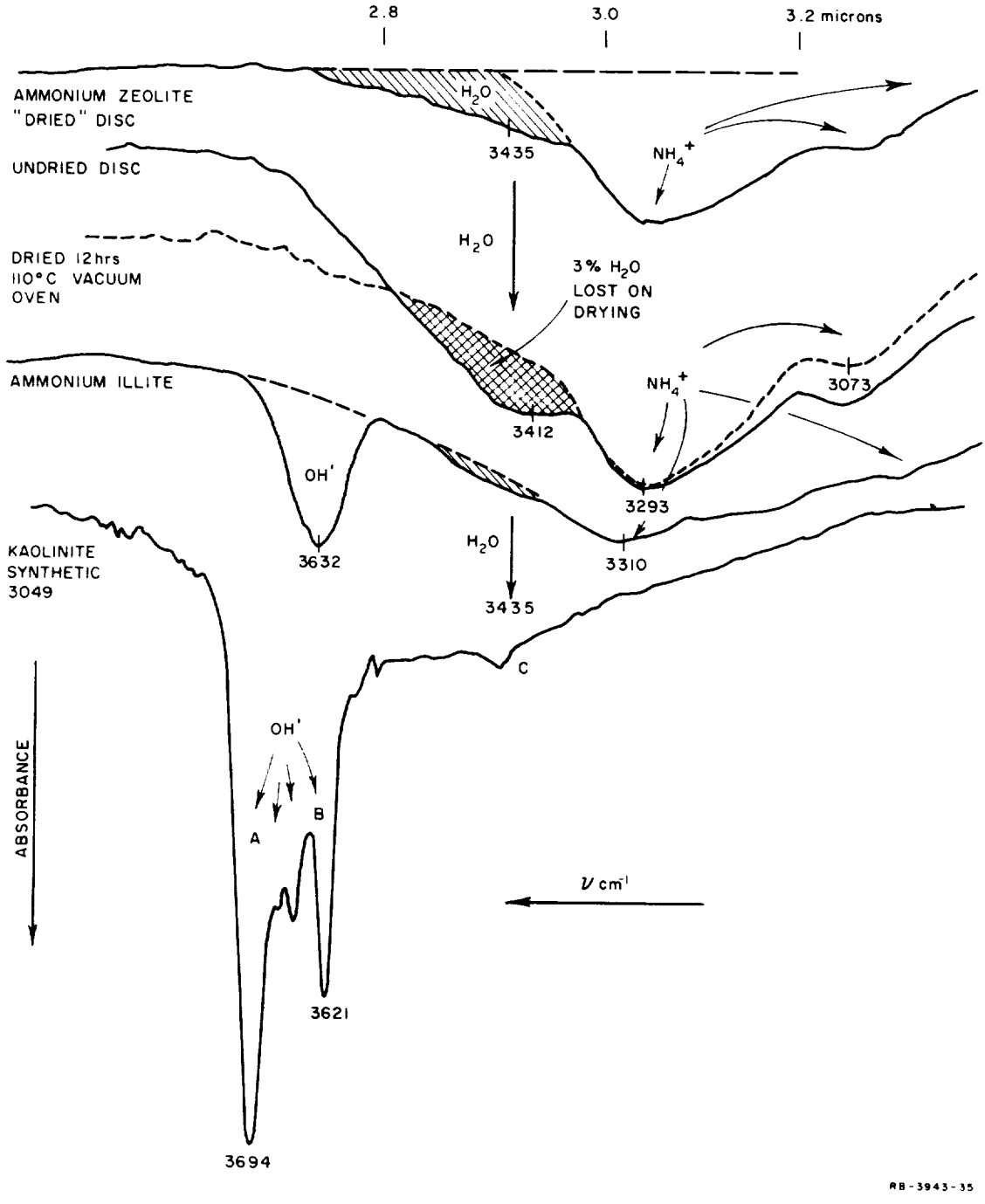

Fig. 11 Absorption spectra for H_2O^-, NH_4^+, and several types of OH'

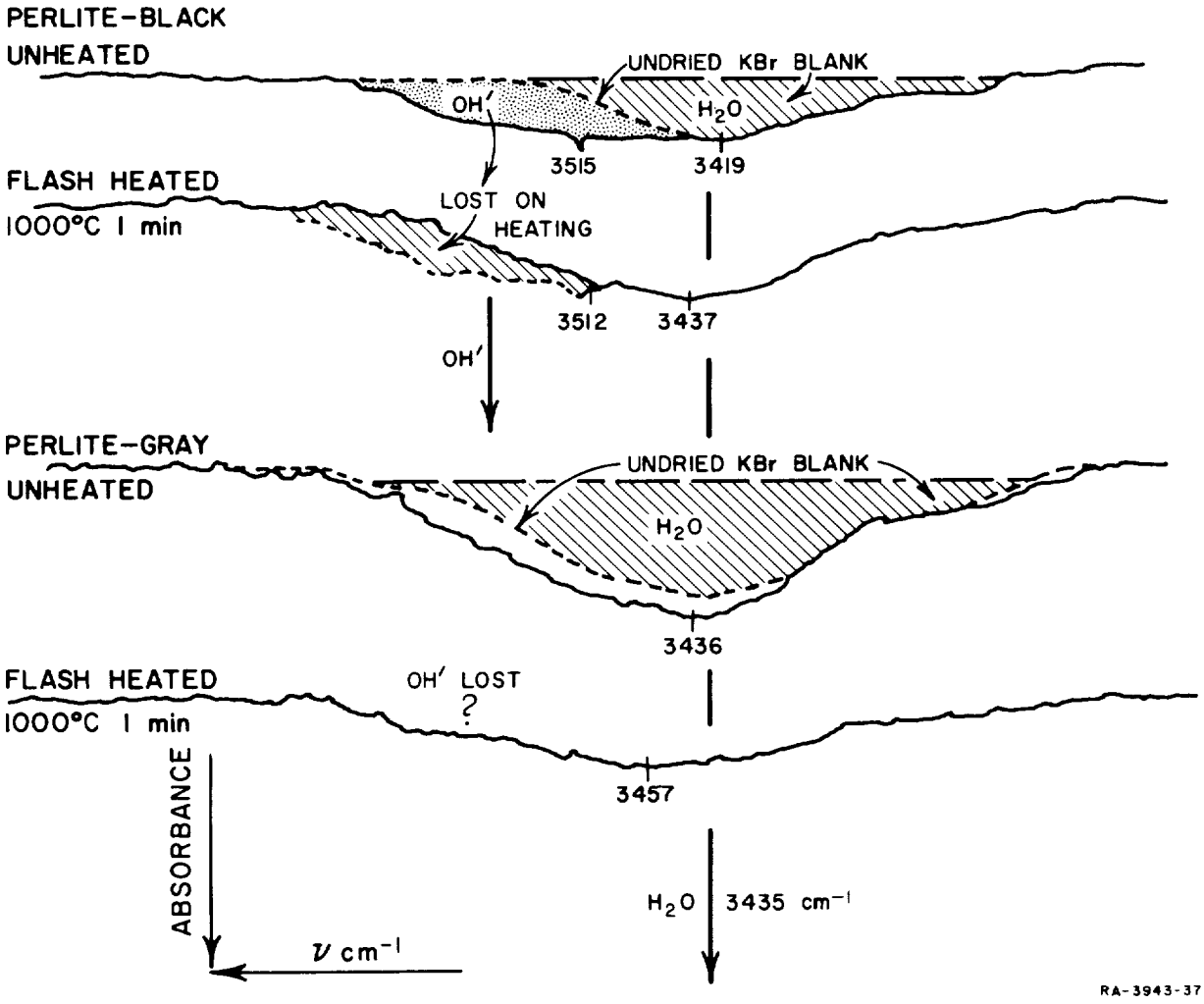

Fig. 12 Absorption spectra showing the possible presence of 1% to 5% water as OH' in black perlite rock. Note that most of the "water" (at 3435 cm^{-1}) can be easily accounted for by the KBr mounting medium. The curves are displaced vertically.

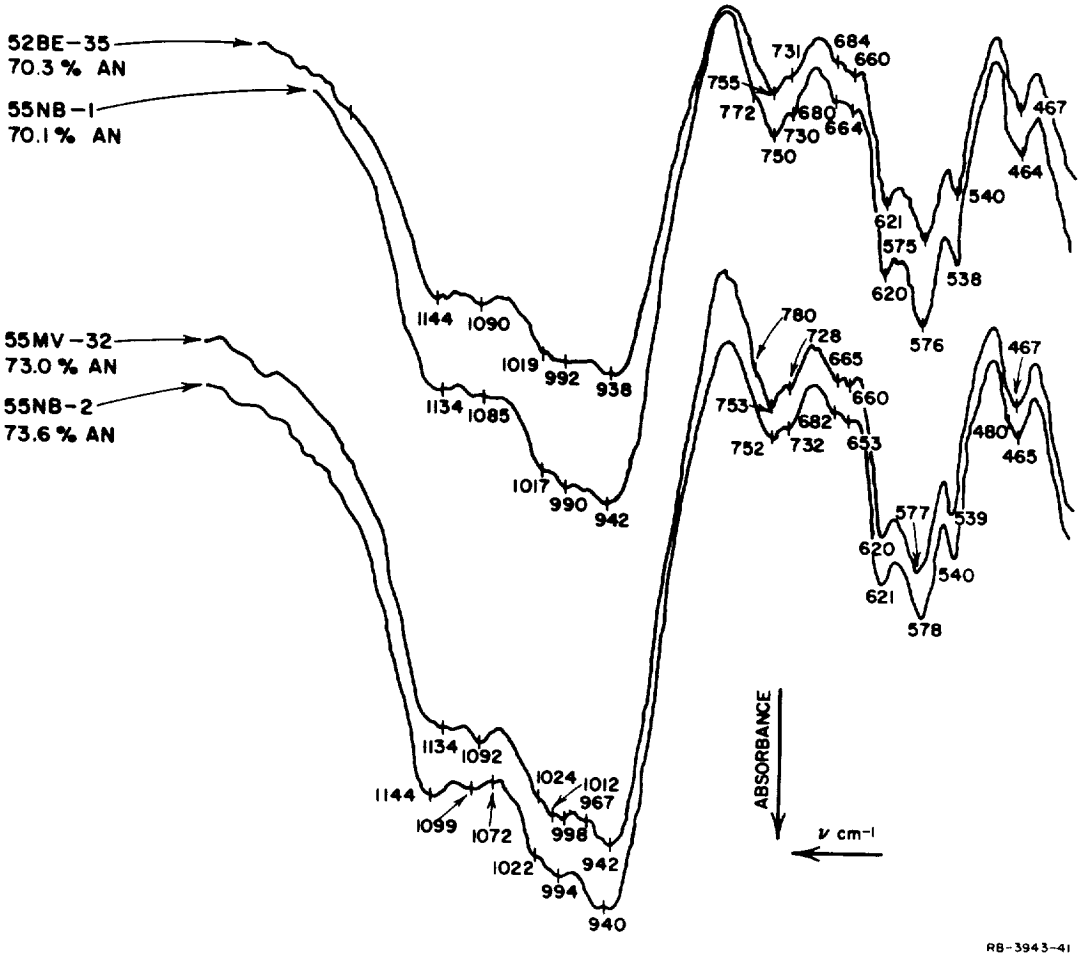

Fig. 13 Absorption spectra of hidden duplicates of plagioclase feldspars. The total variance is shown for all the steps from the initial sampling through the disc preparation to the numerical determination of the peak positions. The curves are displaced vertically.

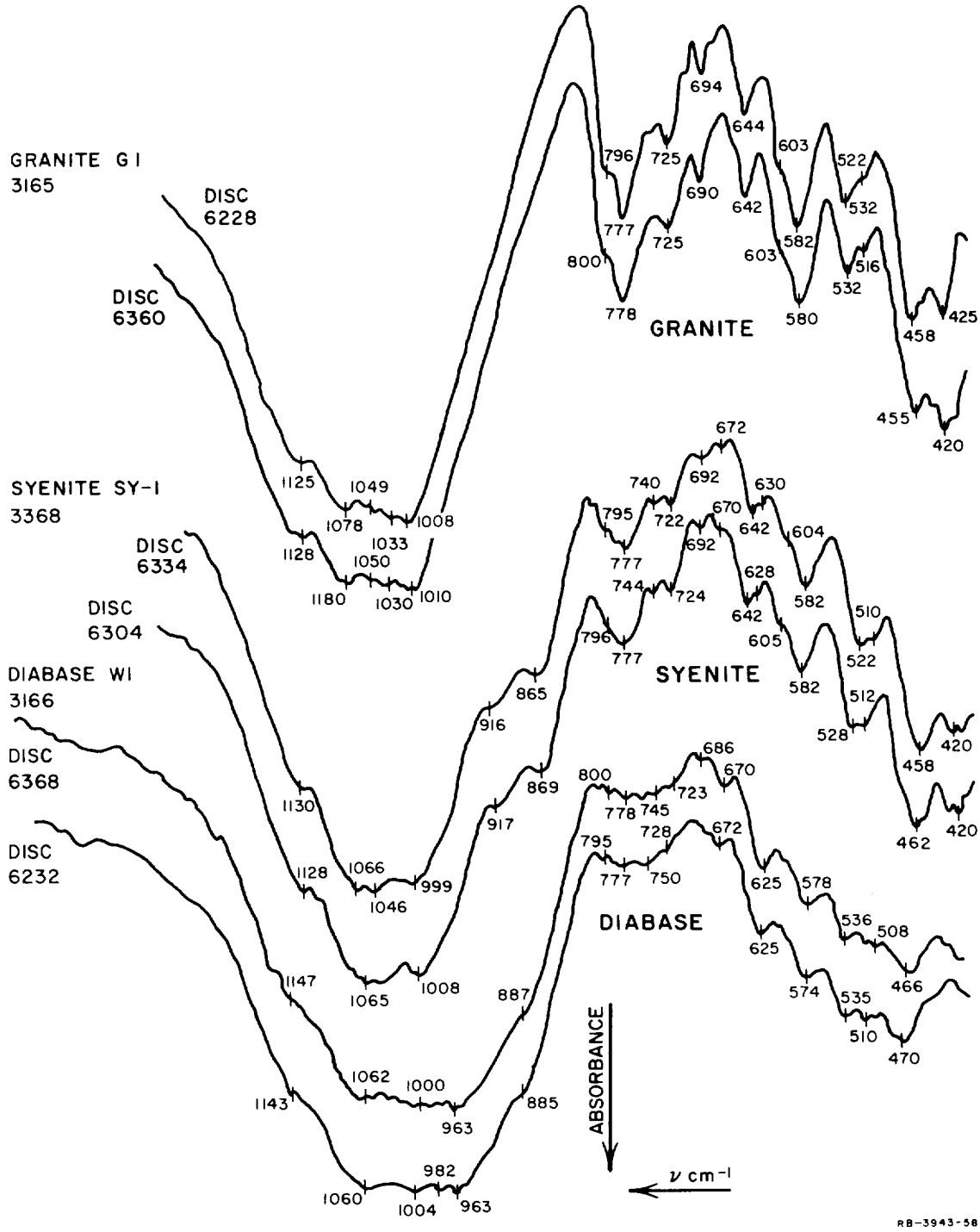

Fig. 14 Absorption spectra for the rock standards used for spectrographic calibration. Duplicate samples were prepared at weekly intervals. This shows the precision of the total process.

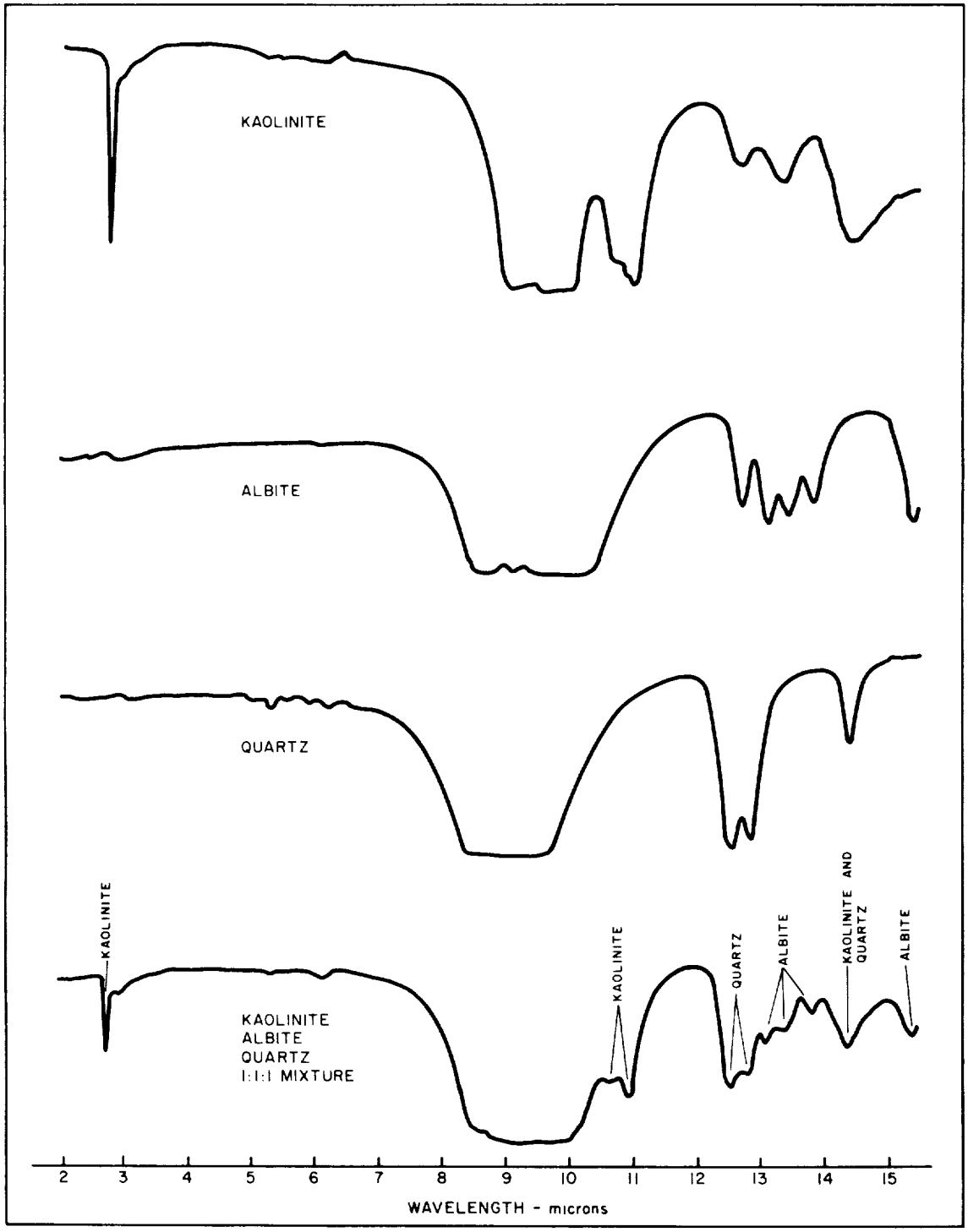

Fig. 15 Absorption spectra of mineral mixtures. The curves are displaced vertically.

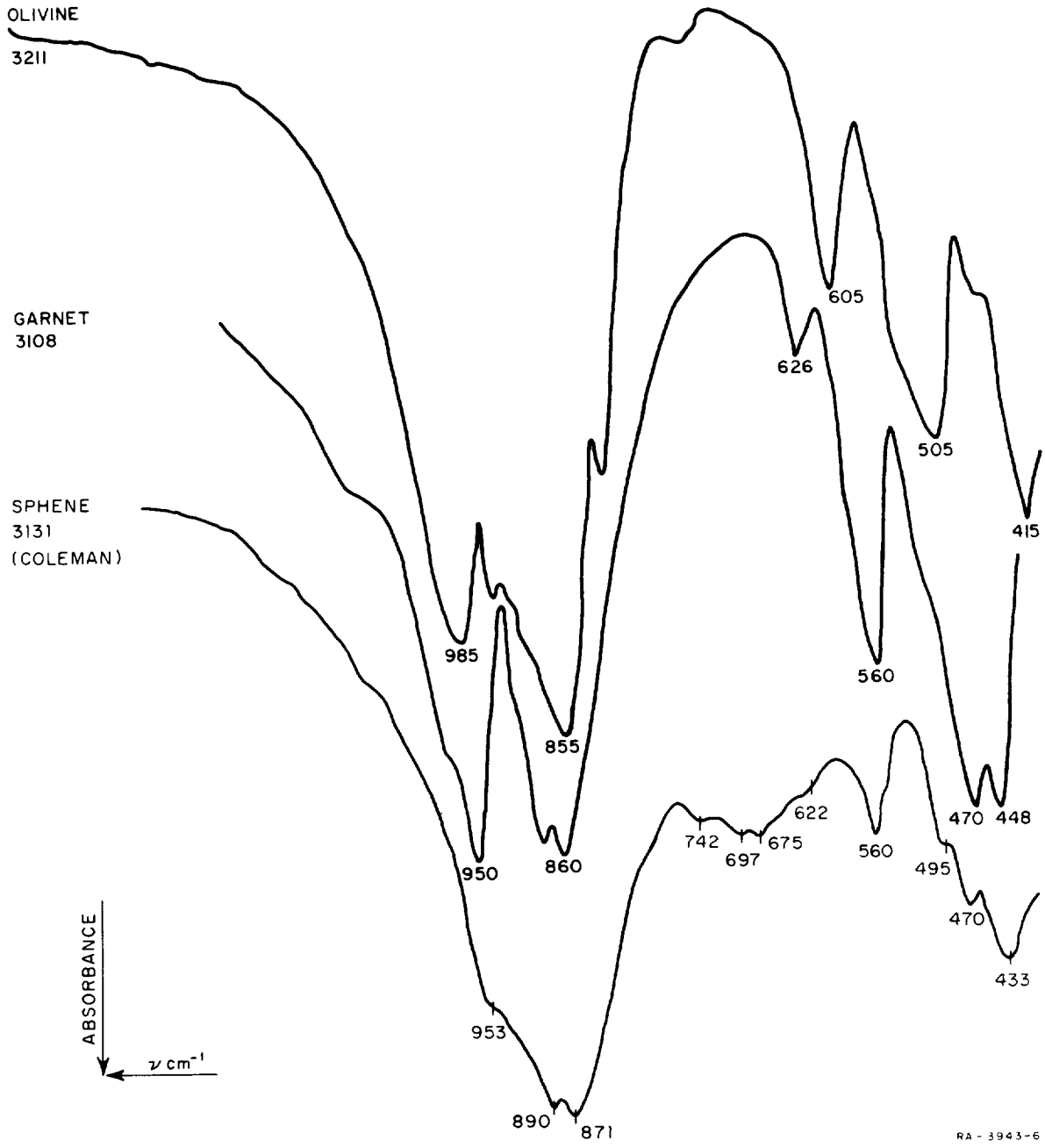

Fig. 16 Absorption spectra for the nesosilicates (independent SiO_4 tetrahedra). Examples shown are the olivine, garnet and sphene groups. The curves are displaced vertically.

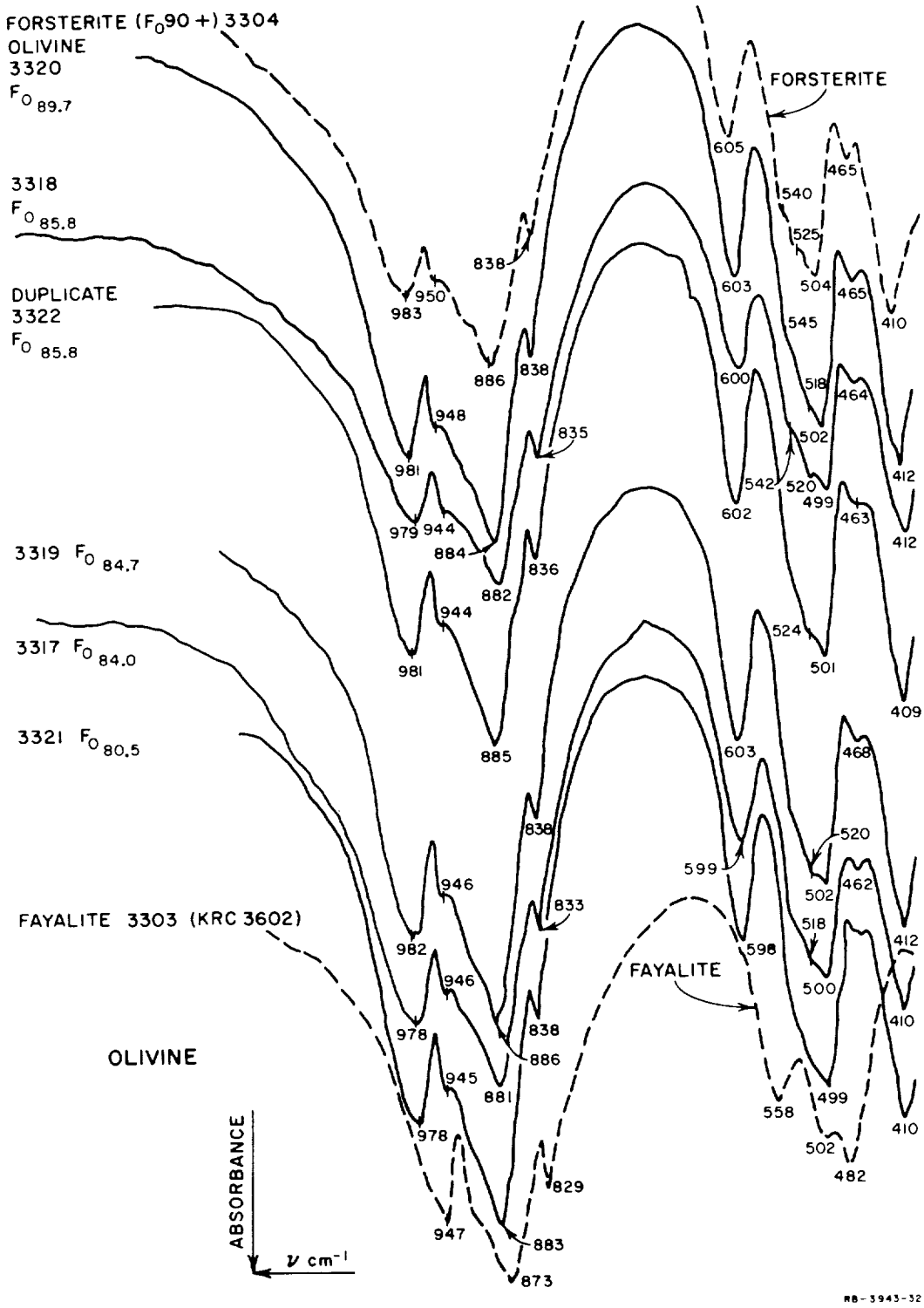

Fig. 17 Detailed absorption spectra of the olivine group near the magnesium-rich end. The curves are displaced vertically.

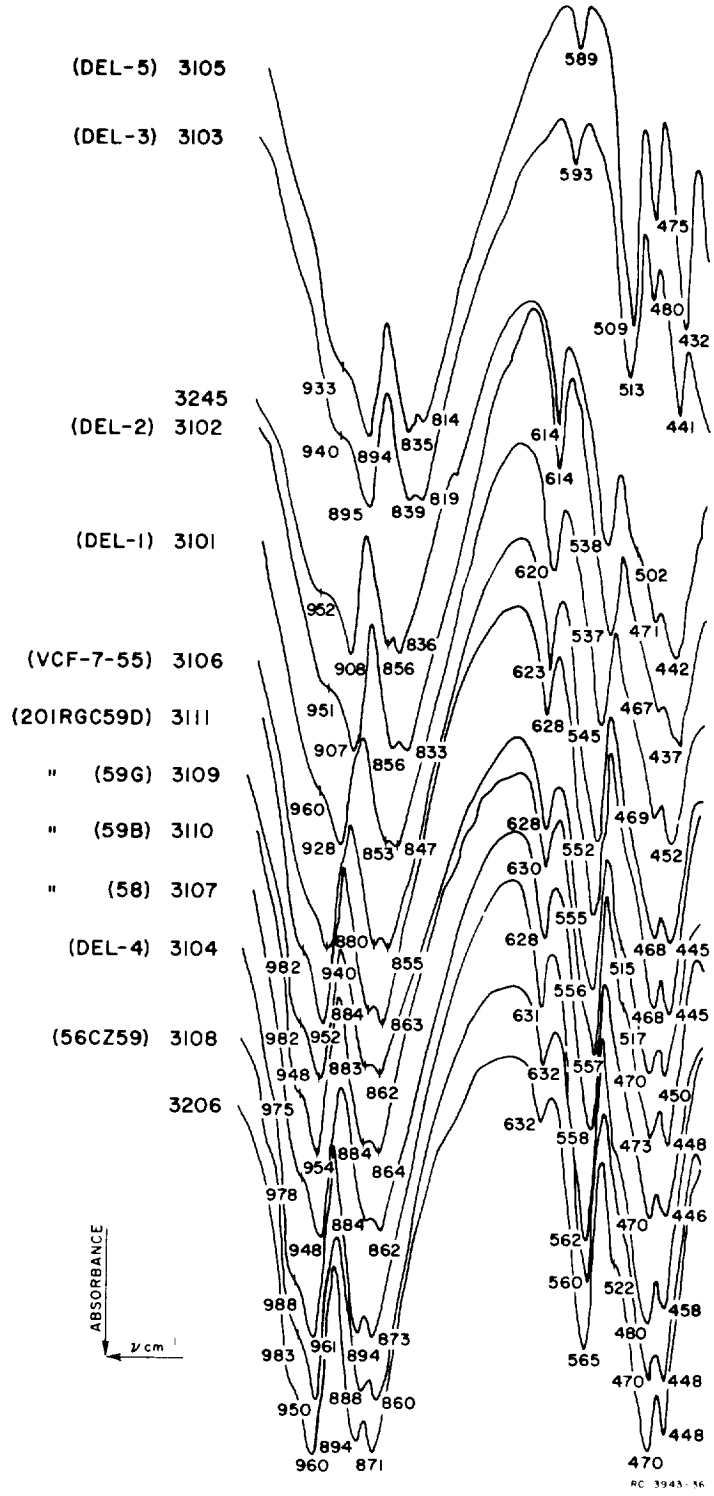

Fig. 18 Detailed absorption spectra of the garnet group. Note the preservation of a basic pattern, but with a progressive peak shift with changing composition. The curves are displaced vertically.

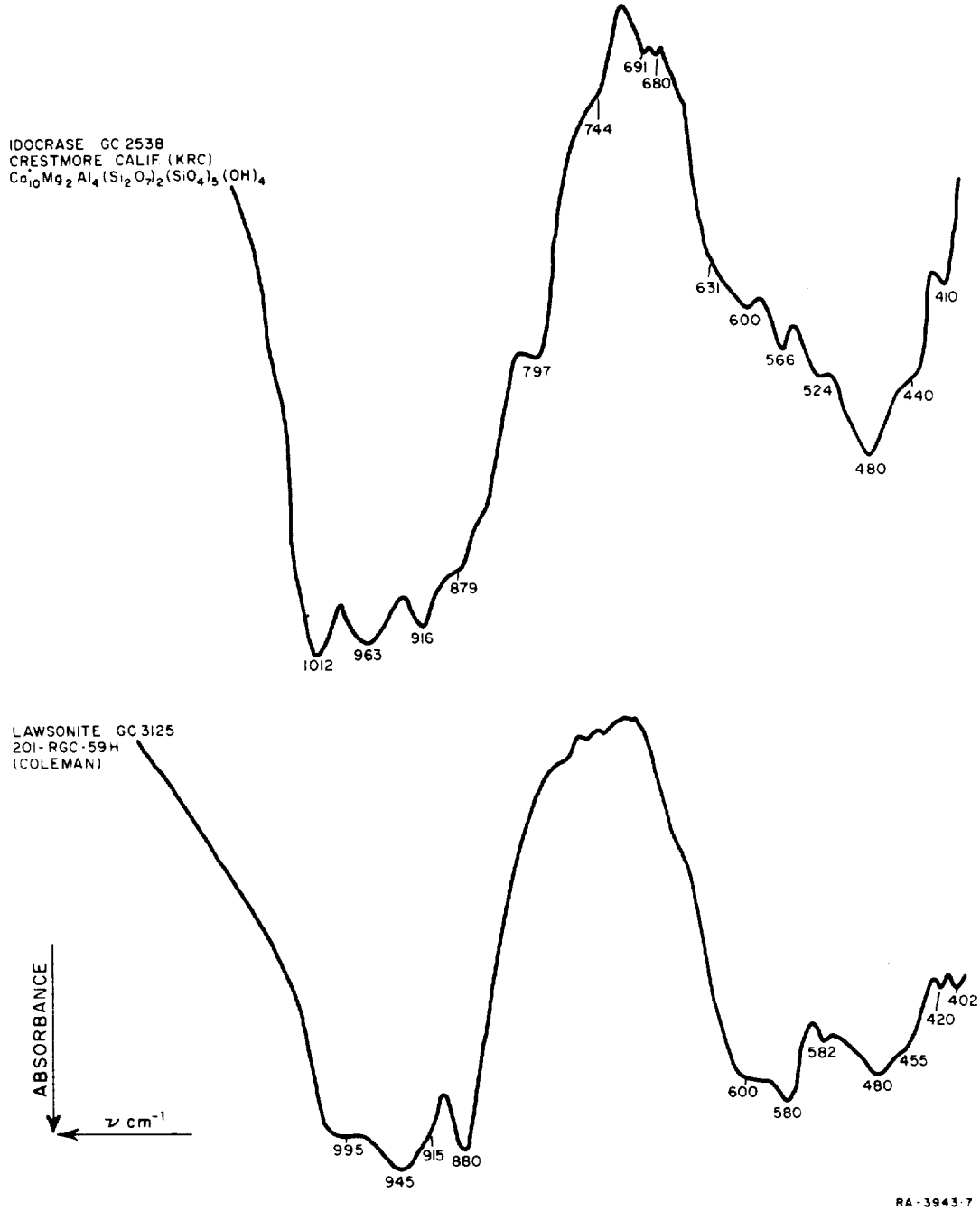

Fig. 19 Absorption spectra of the sorosilicates (two tetrahedra sharing one oxygen, Si_2O_7). Examples shown are idocrase and lawsonite. The curves are displaced vertically.

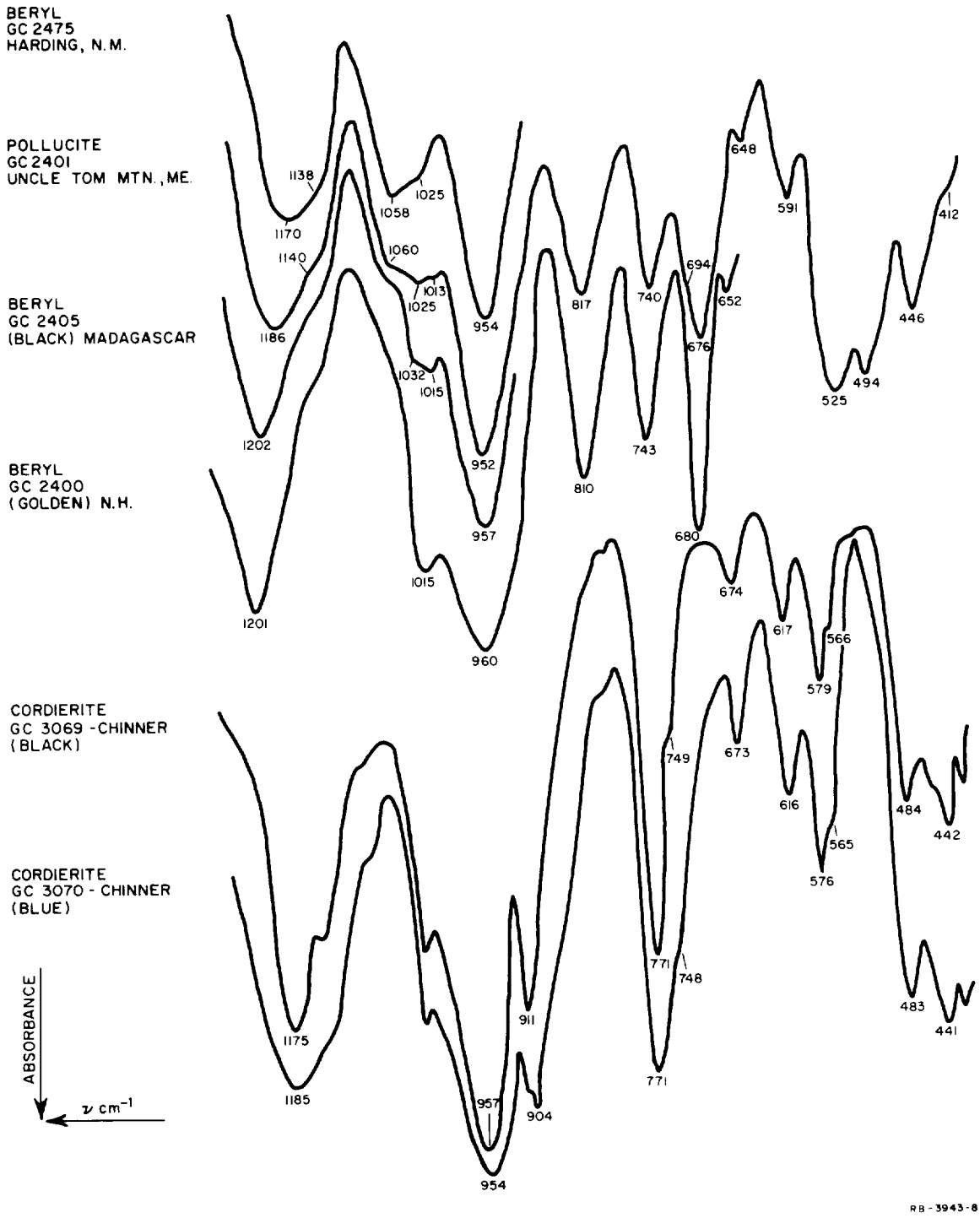

Fig. 20 Absorption spectra for the cyclosilicates (closed rings of tetrahedra sharing oxygens, Si_6O_{18}). Examples shown are beryl and cordierite. The curves are displaced vertically.

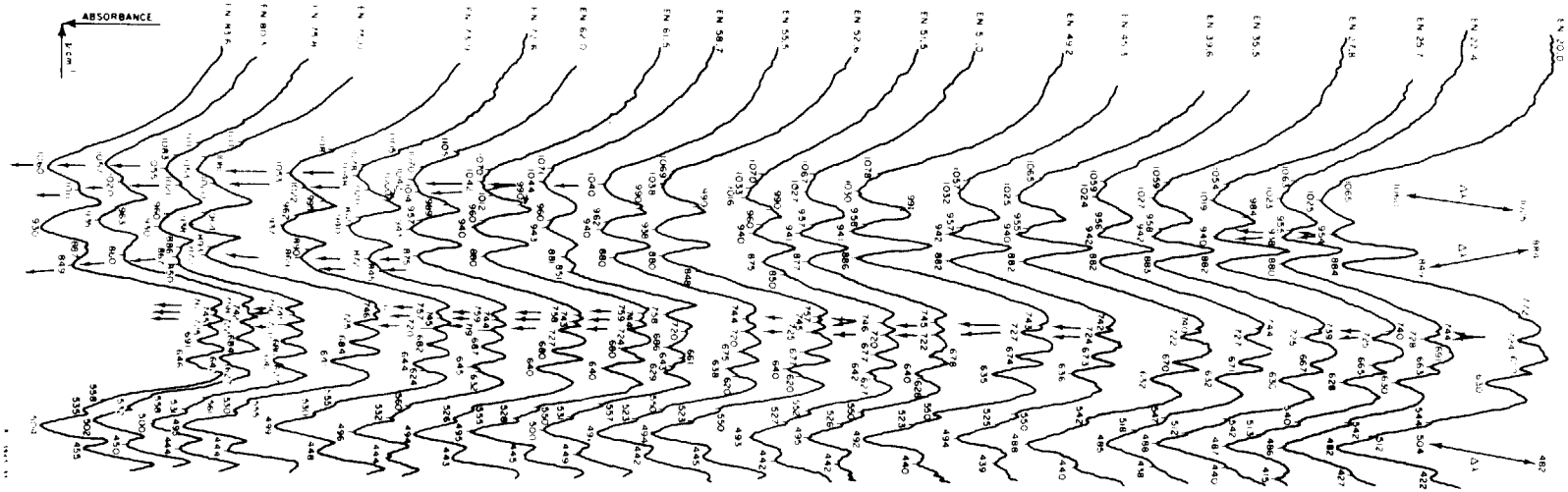

Fig. 21 Detailed absorption spectra for the orthopyroxene inosilicates. Examples shown are the enstatite-hypersthene series, with 21 members shown ranging from En_{20} to En_{84}. Note the preservation of the simple pattern with a progressive shift in peak position with composition change.

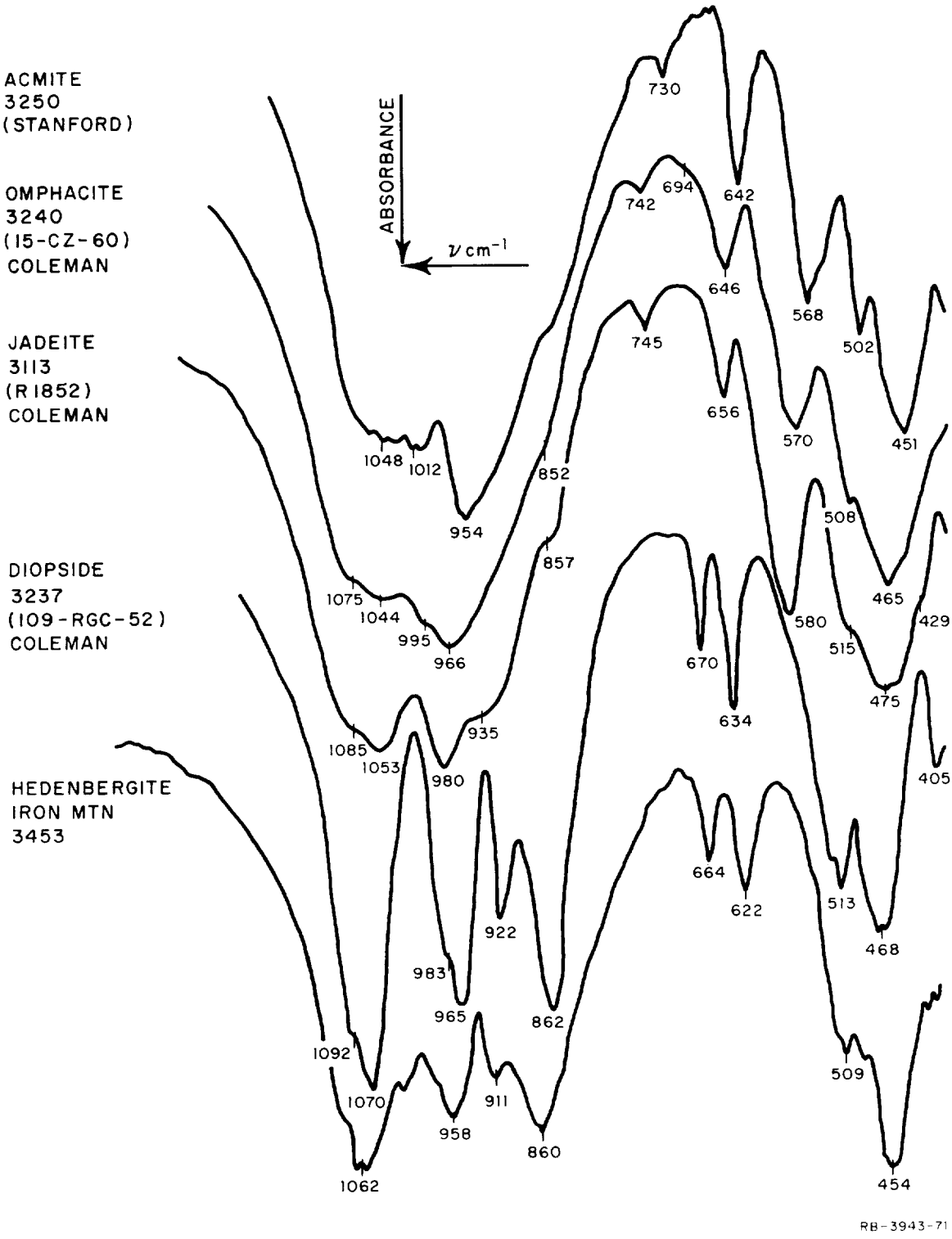

Fig. 22 Absorption spectra for the clinopyroxene inosilicates (single chains of tetrahedra each sharing two oxygens, SiO_3). Examples shown are acmite, omphacite, jadeite, diopside, and hedenbergite. The curves are displaced vertically.

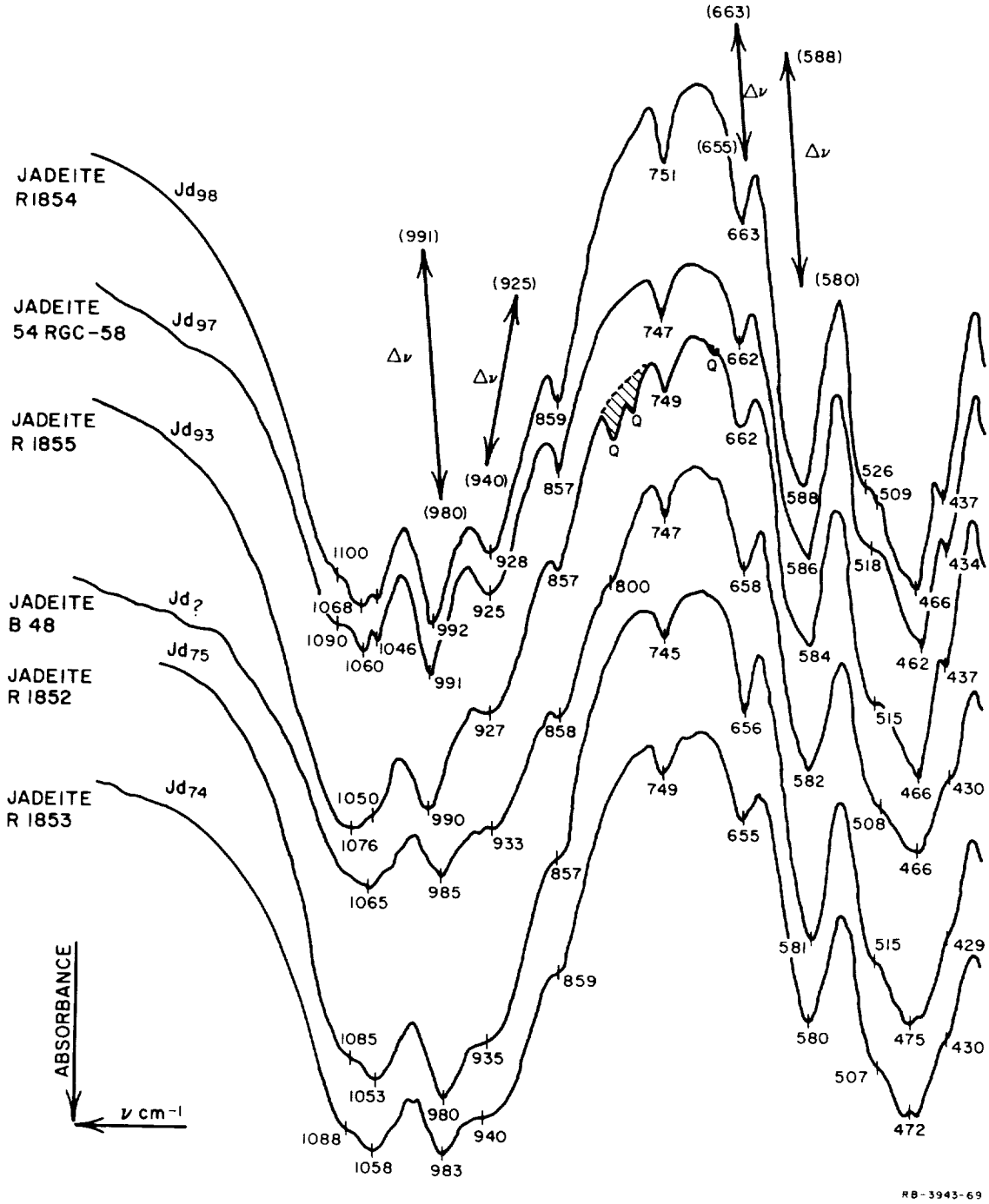

Fig. 23 Absorption spectra for a series of jadeite pyroxenes with increasing amounts of jadeite.

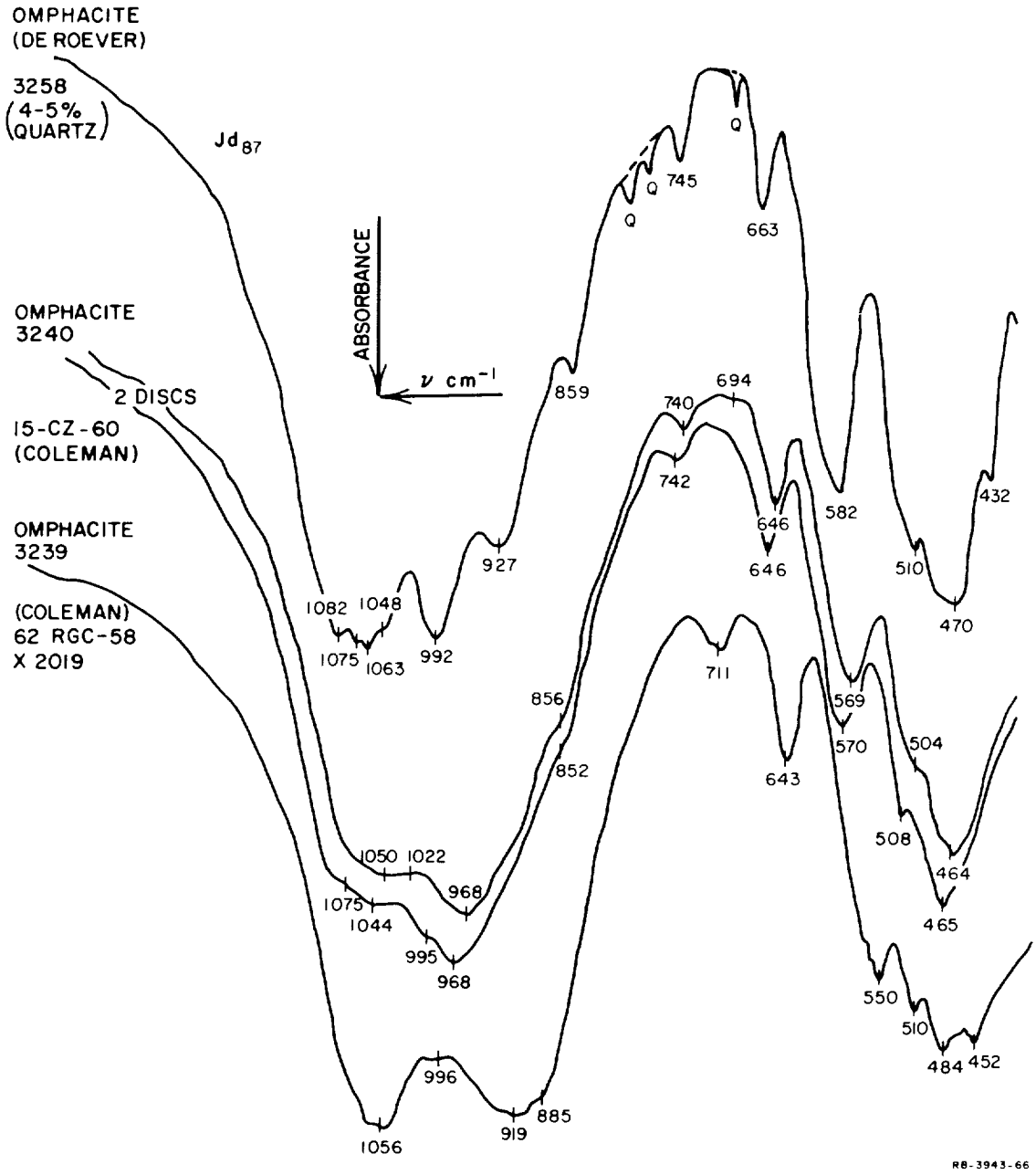

Fig. 24 Absorption spectra of the omphacite pyroxenes showing the variation within the group. Sample 3240 was prepared twice to check the variance of the method.

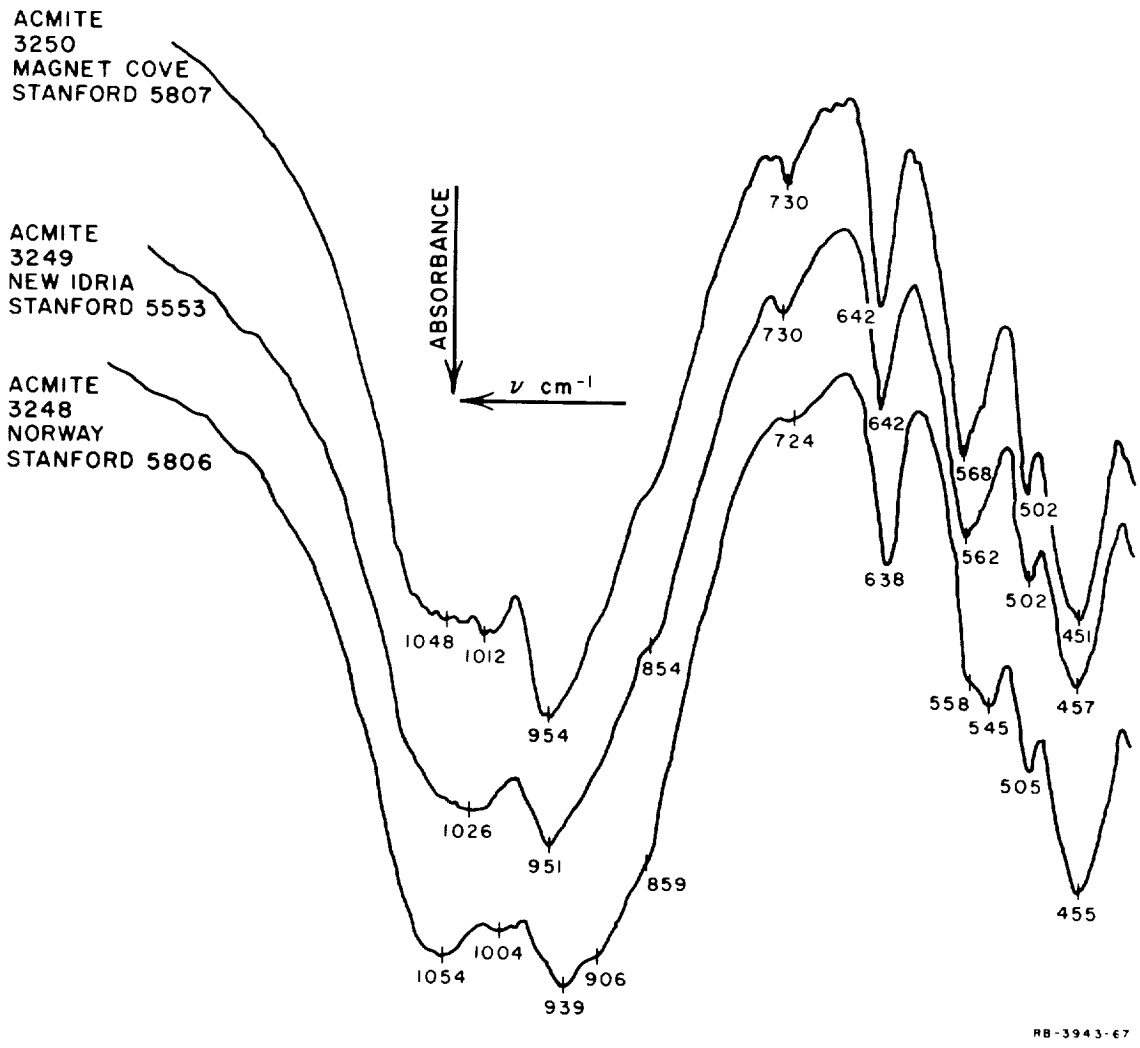

Fig. 25 Absorption spectra for a series of acmite pyroxenes

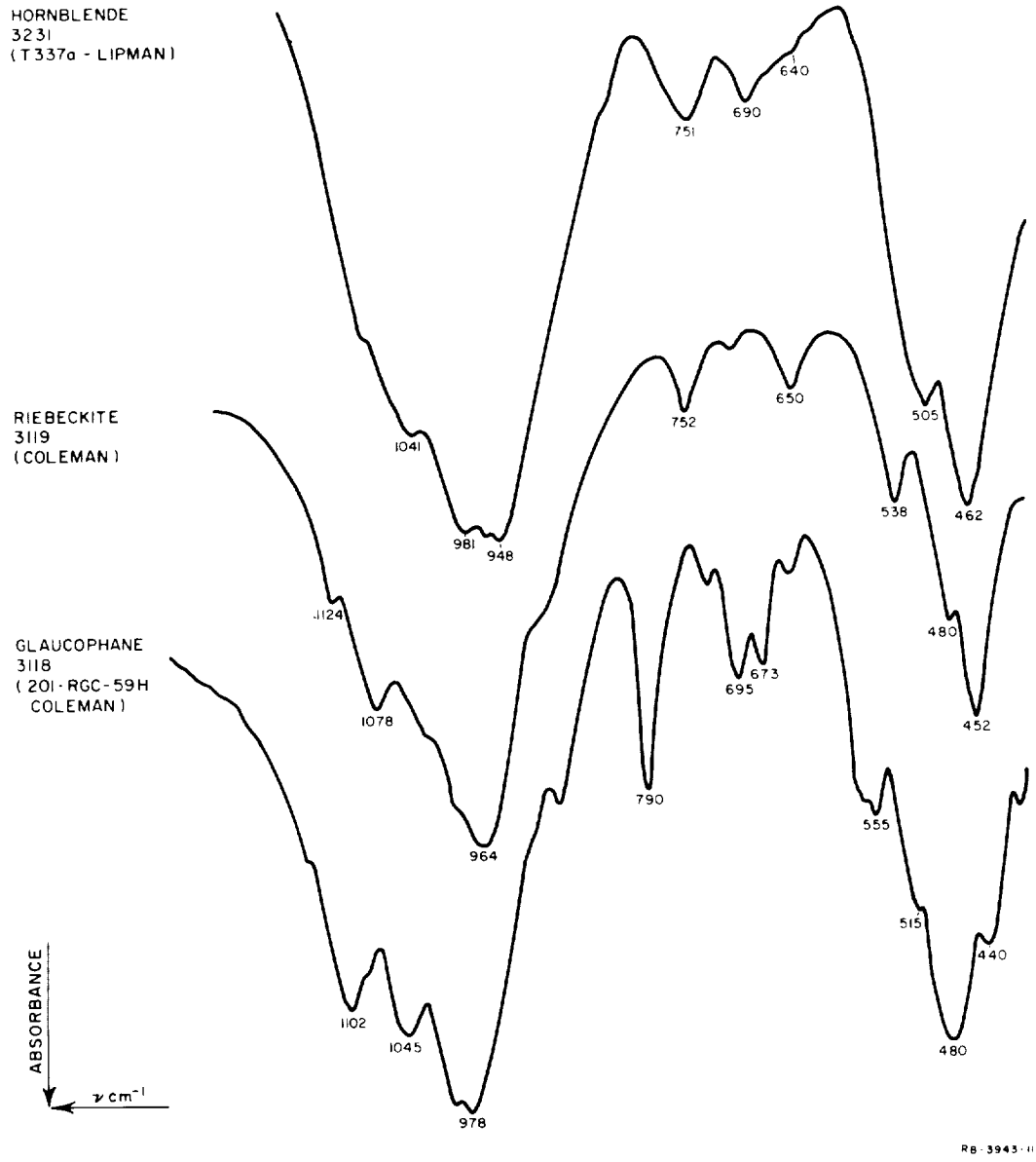

Fig. 26 Absorption spectra for the amphibole inosilicates (continuous double chains of tetrahedra alternately sharing two and three oxygens, Si_4O_{11}). Examples shown are hornblende, riebeckite, and glaucophane. The curves are displaced vertically.

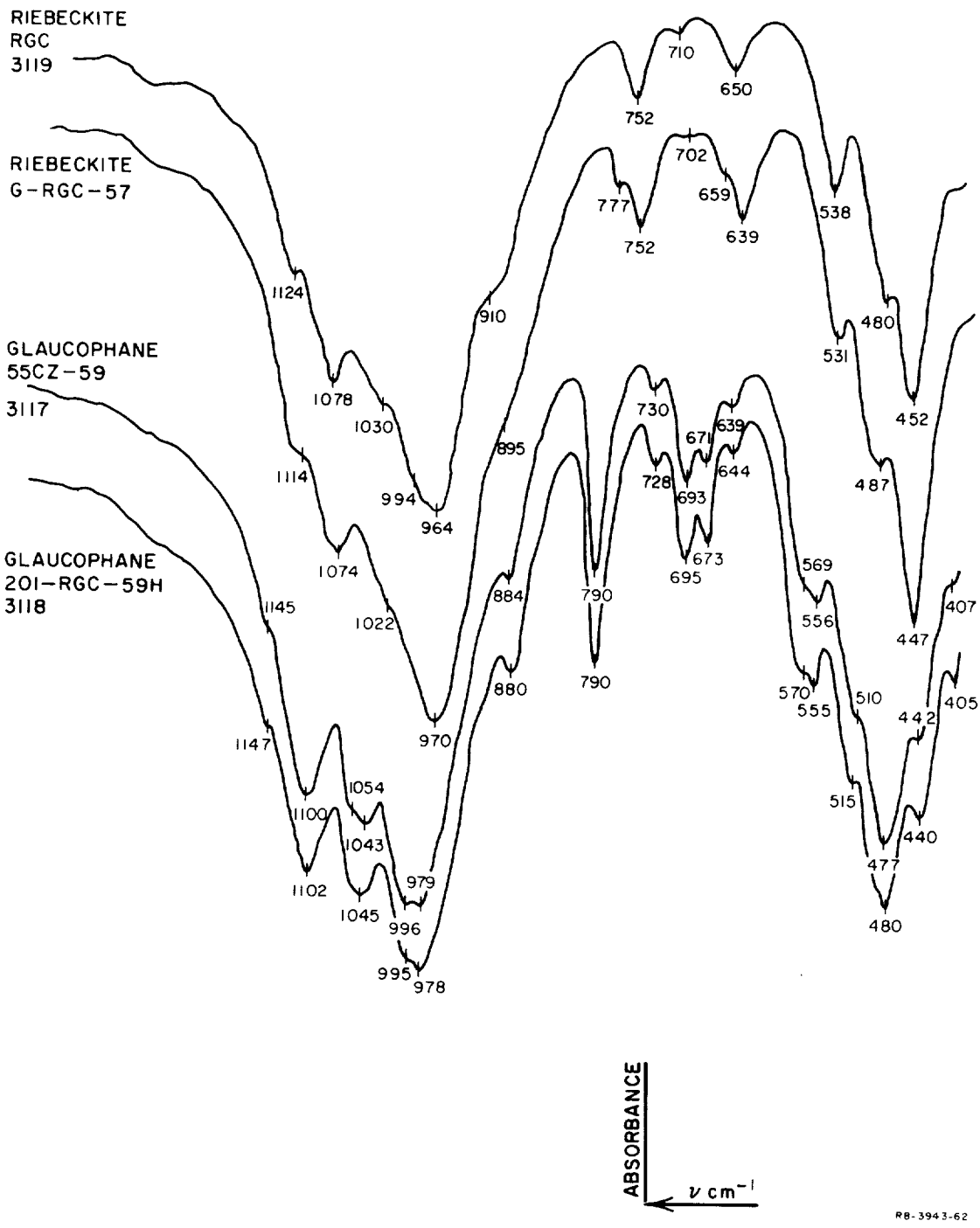

Fig. 27 Absorption spectra for a series of alkali amphiboles -- iron-rich riebeckite and aluminous glaucophane

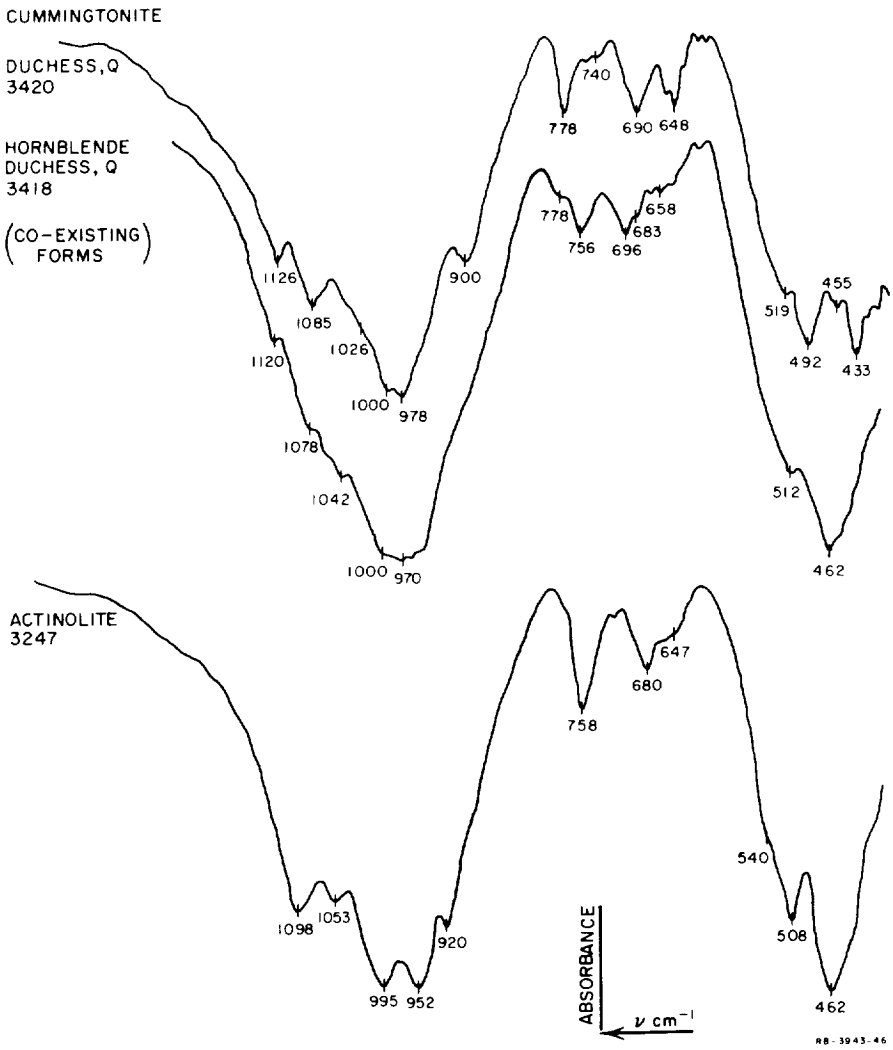

Fig. 28 Absorption spectra for co-existing cummingtonite and hornblende contrasted with actinolite. All are amphiboles.

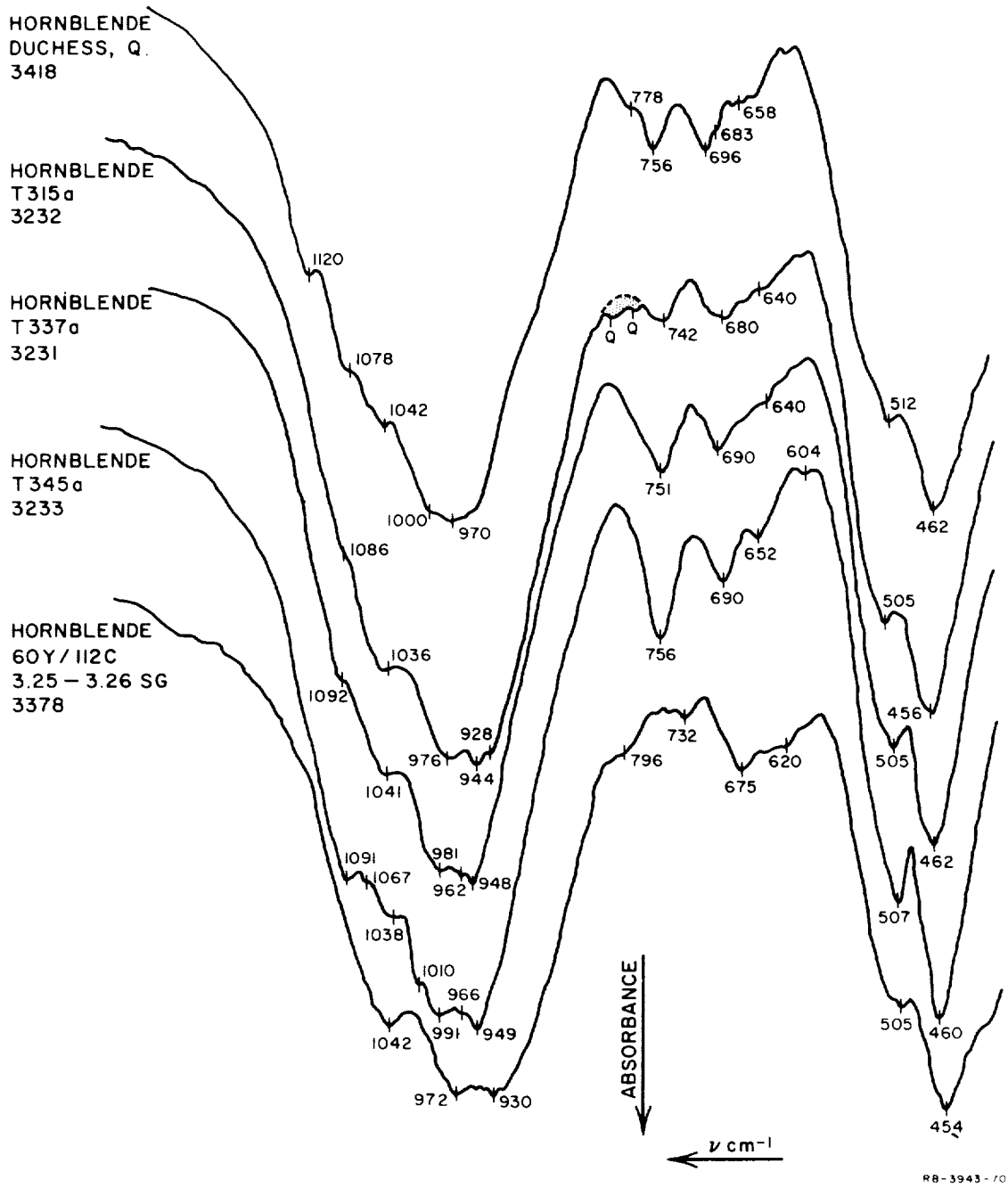

Fig. 29 Absorption spectra for the hornblende group of amphiboles. Sample 3232 contains 2% to 5% quartz as an impurity.

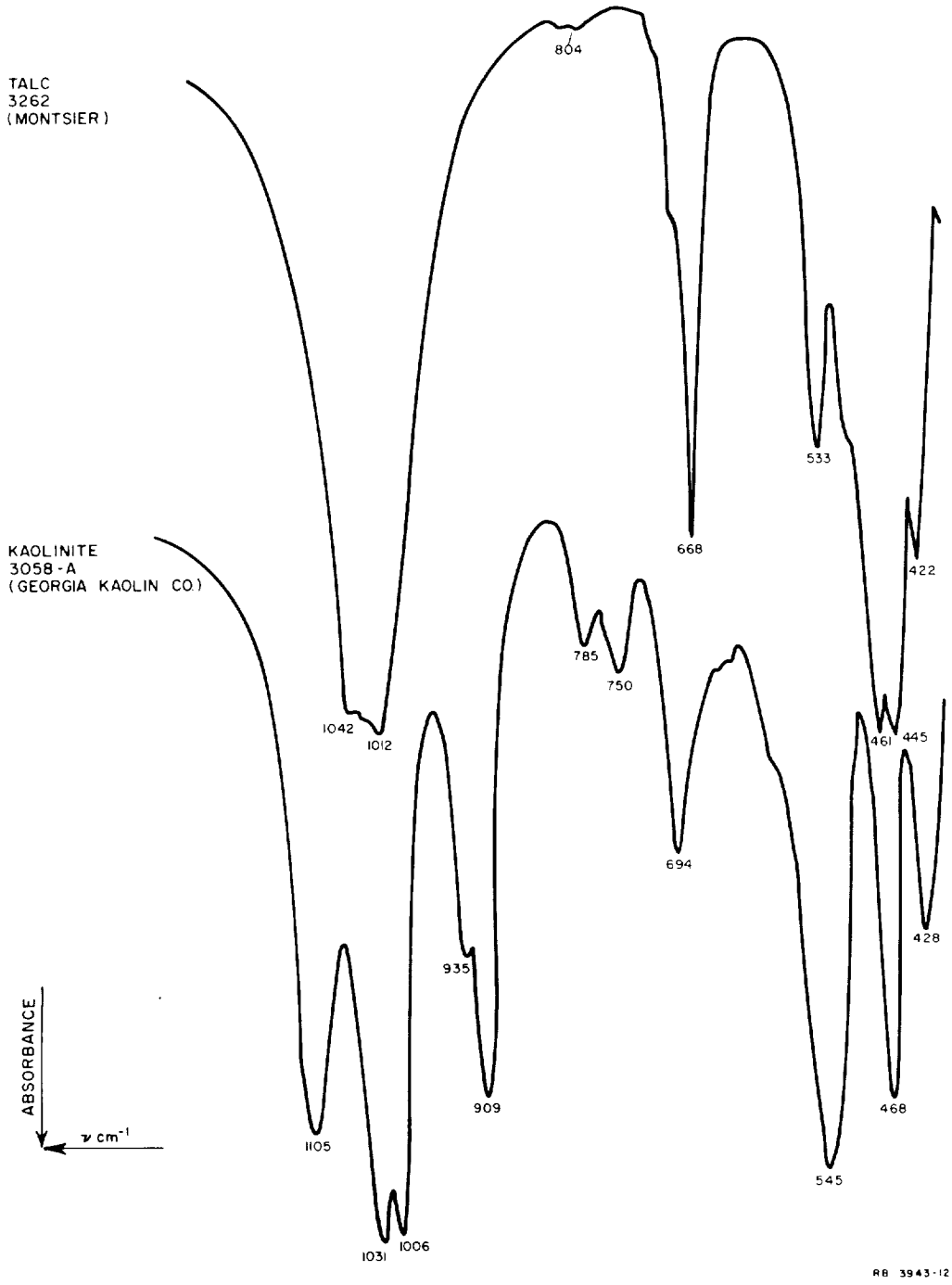

Fig. 30 Absorption spectra for phyllosilicates (continuous sheets of tetrahedra each sharing three oxygens, Si_4O_{10}). Examples shown are talc and kaolinite. The curves are displaced vertically.

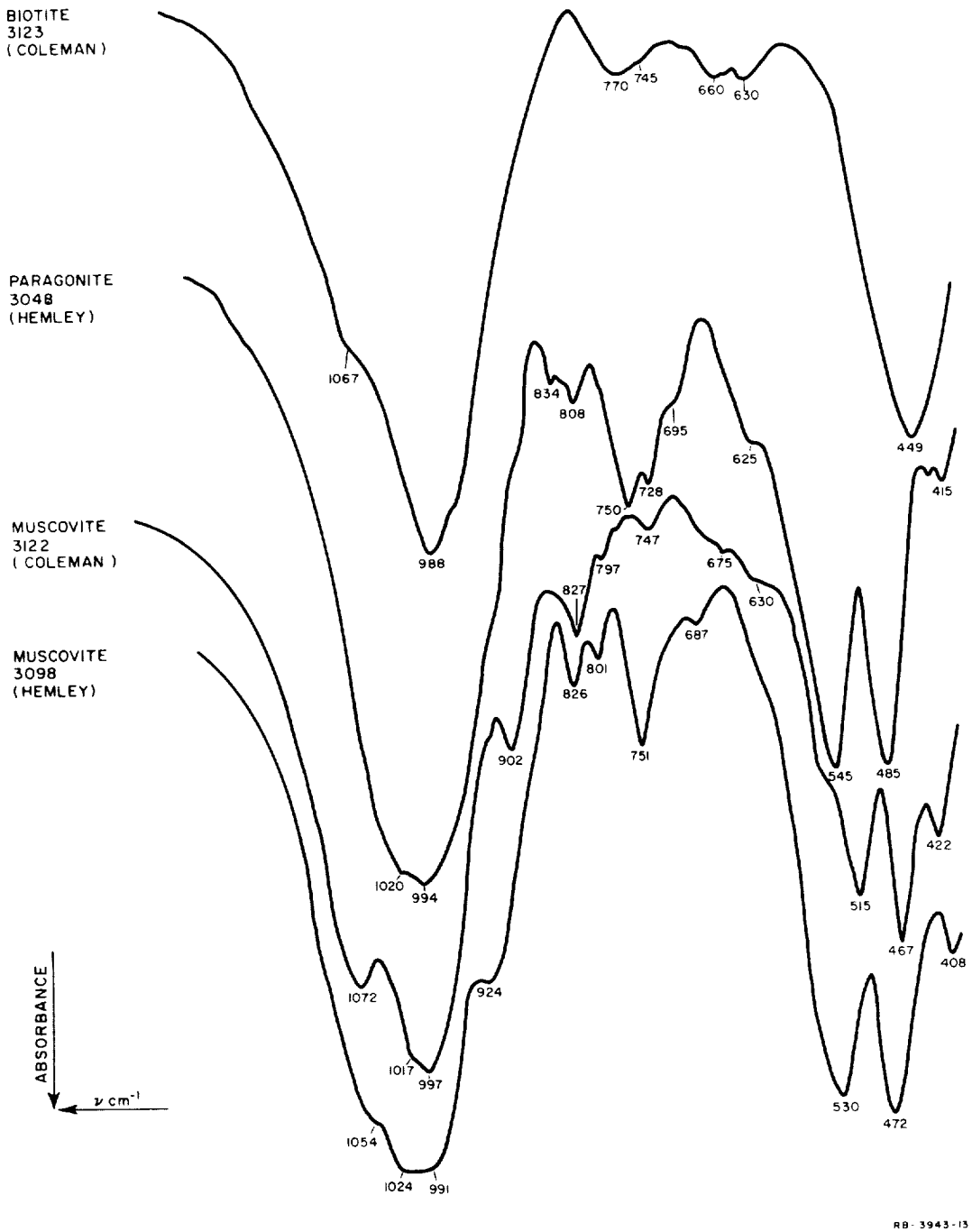

Fig. 31 Absorption spectra for the phyllosilicates biotite, paragonite, and muscovite. Note the effects of substitution in the micas. The curves are displaced vertically.

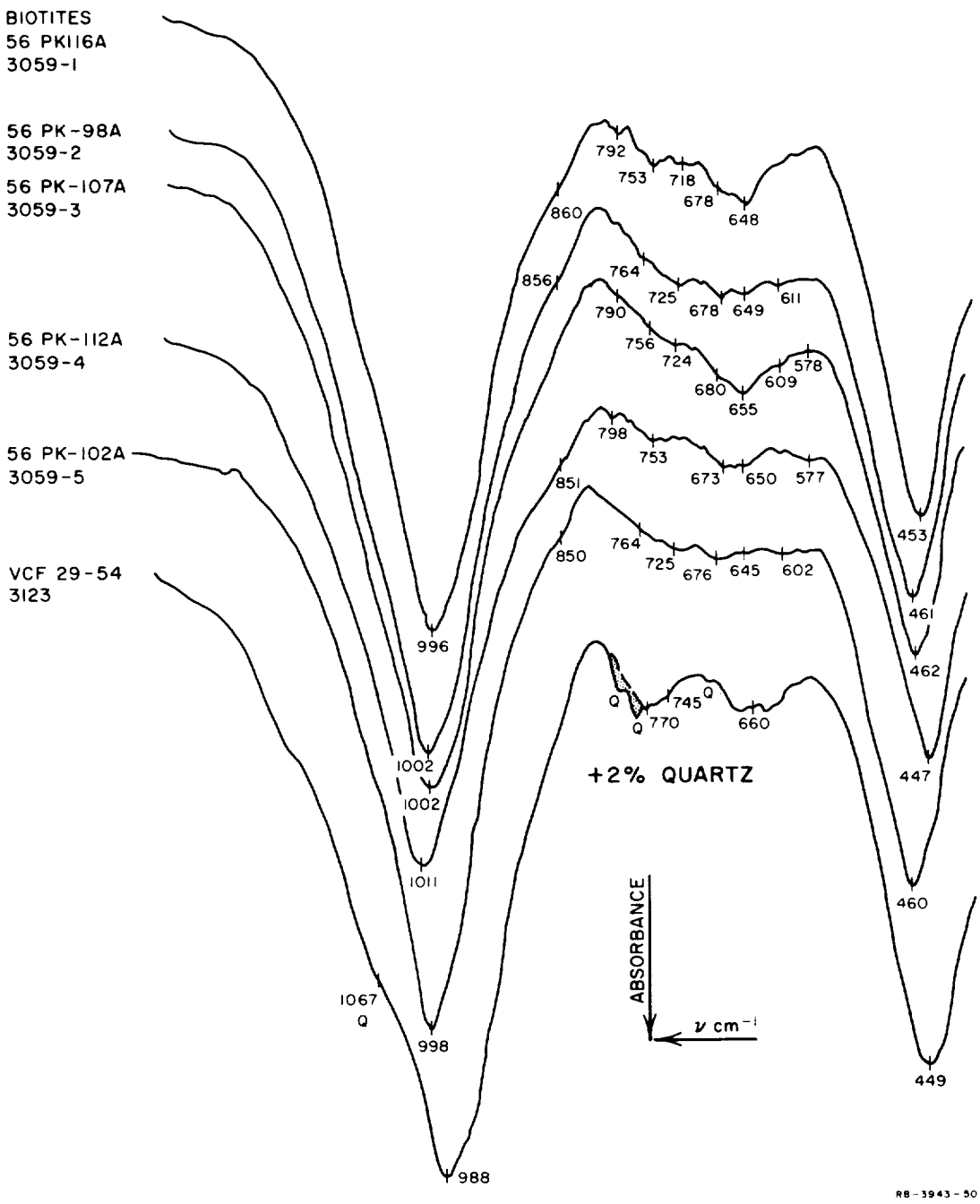

Fig. 32 Absorption spectra for a series of biotite micas

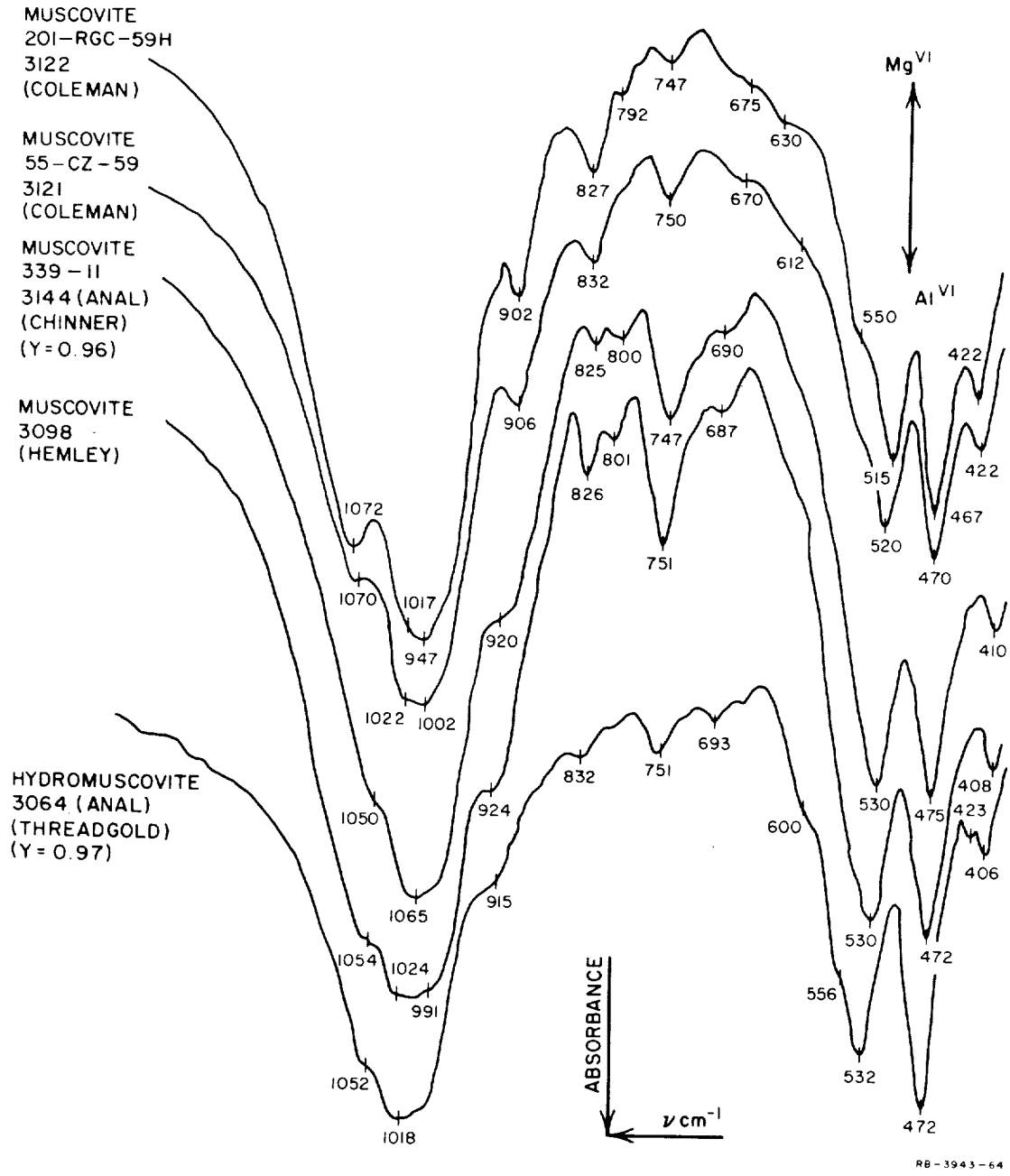

Fig. 33 Absorption spectra for a series of muscovite micas

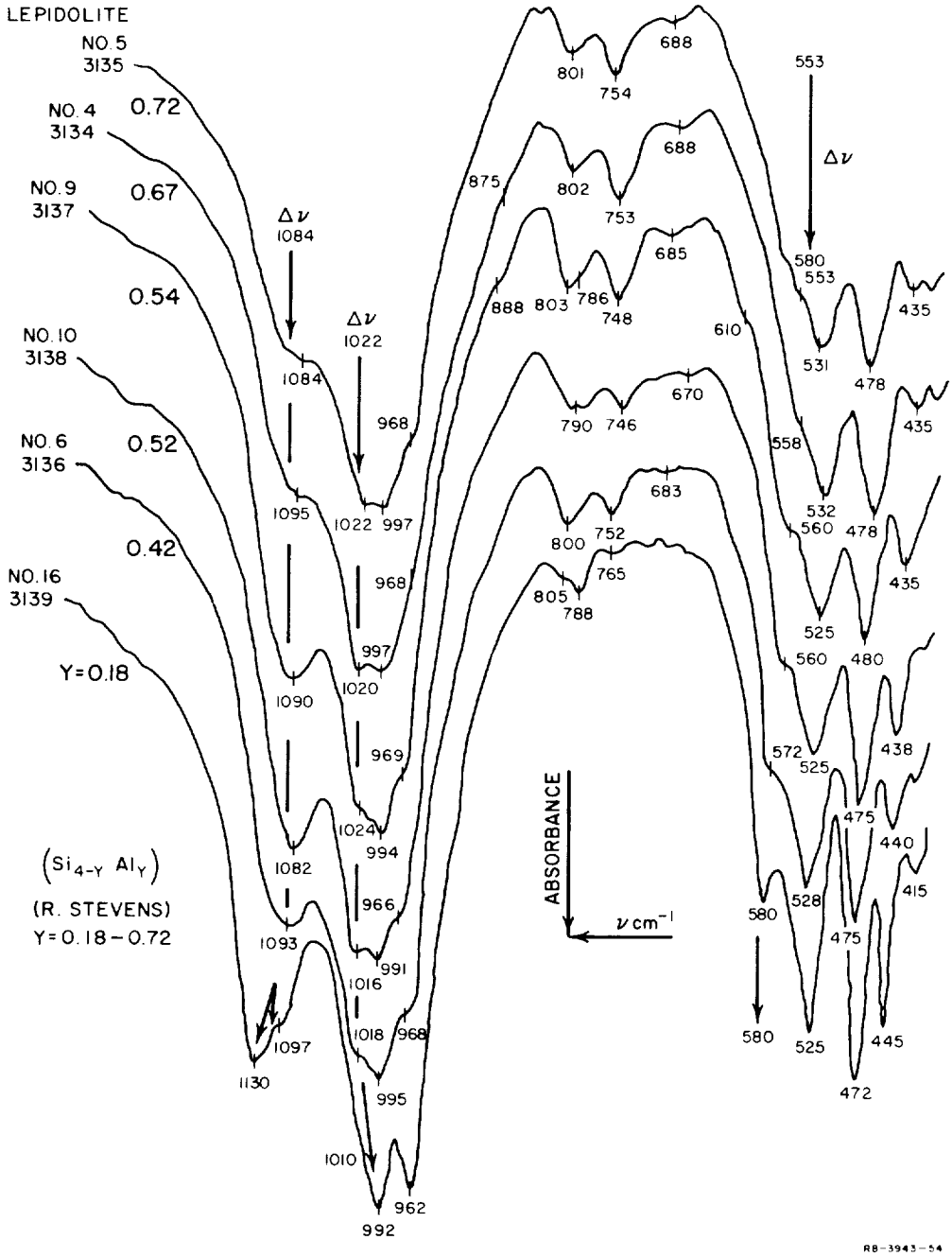

Fig. 34 Absorption spectra for a series of lepidolite micas showing the spectral variation with various amounts of tetrahedral aluminum.

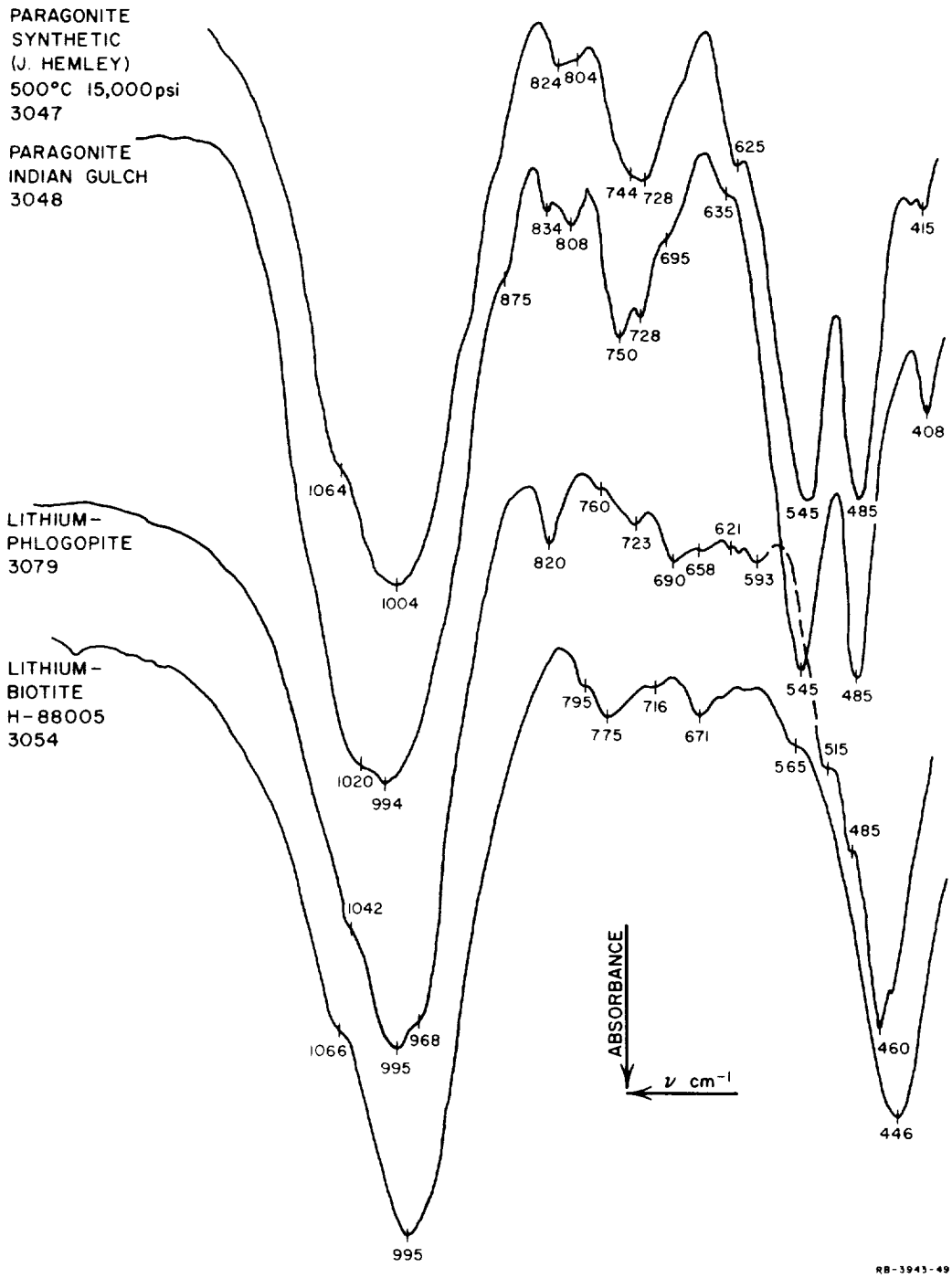

Fig. 35 Absorption spectra for synthetic and natural paragonite with the lithium-bearing micas phlogopite and biotite

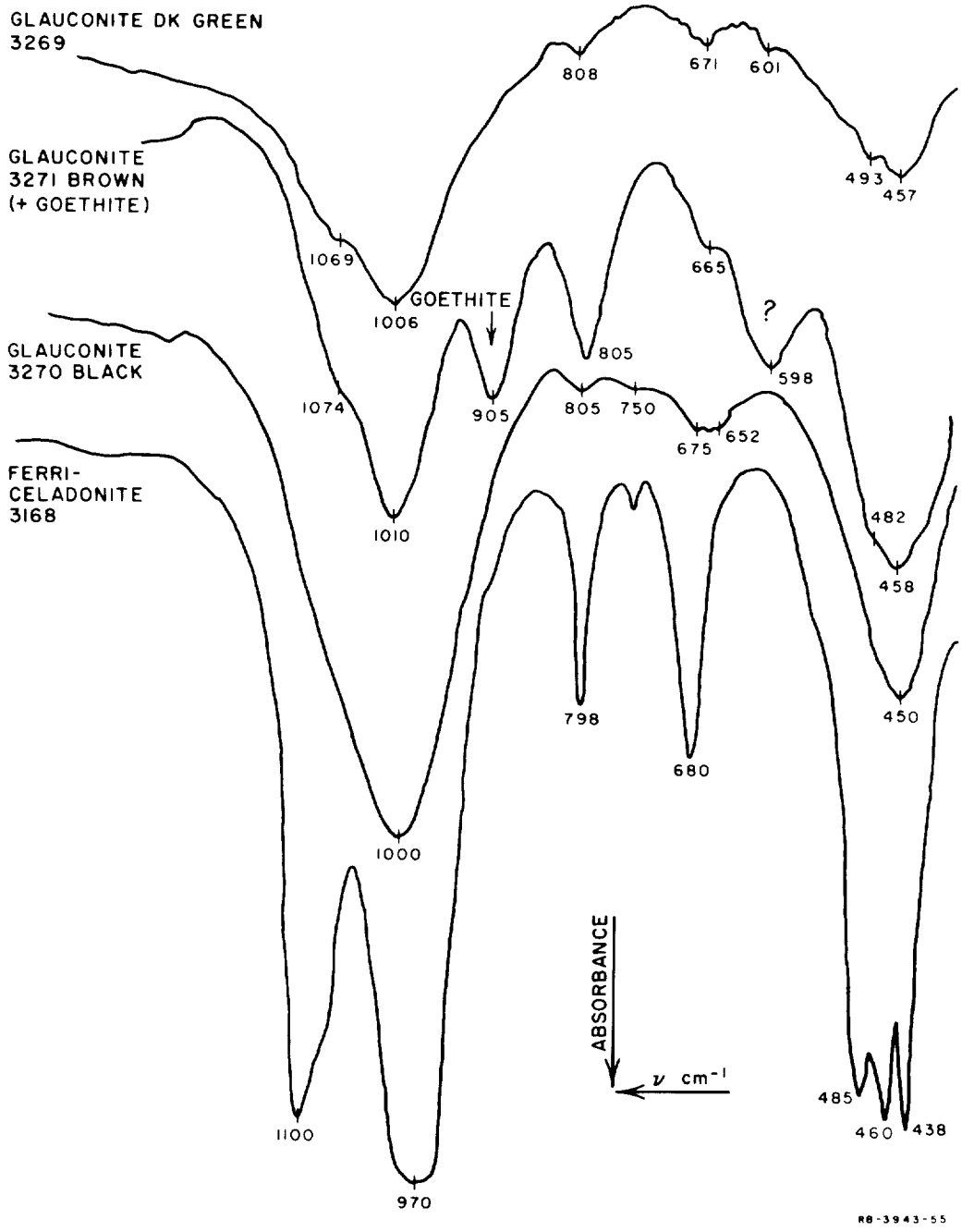

Fig. 36 Absorption spectra for the iron-rich micas glauconite and ferri-celadonite

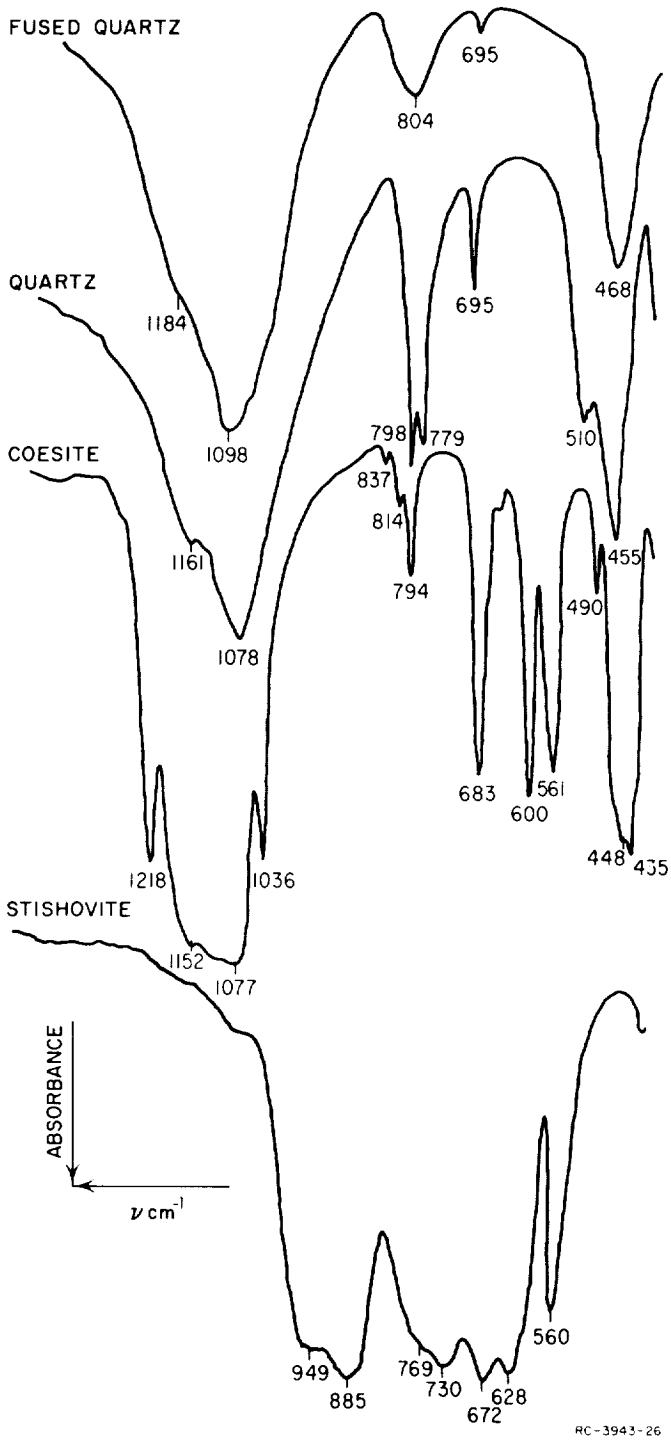

Fig. 37 Absorption spectra for polymorphs of SiO_2--quartz, coesite, stishovite, and fused silica. The curves are displaced vertically.

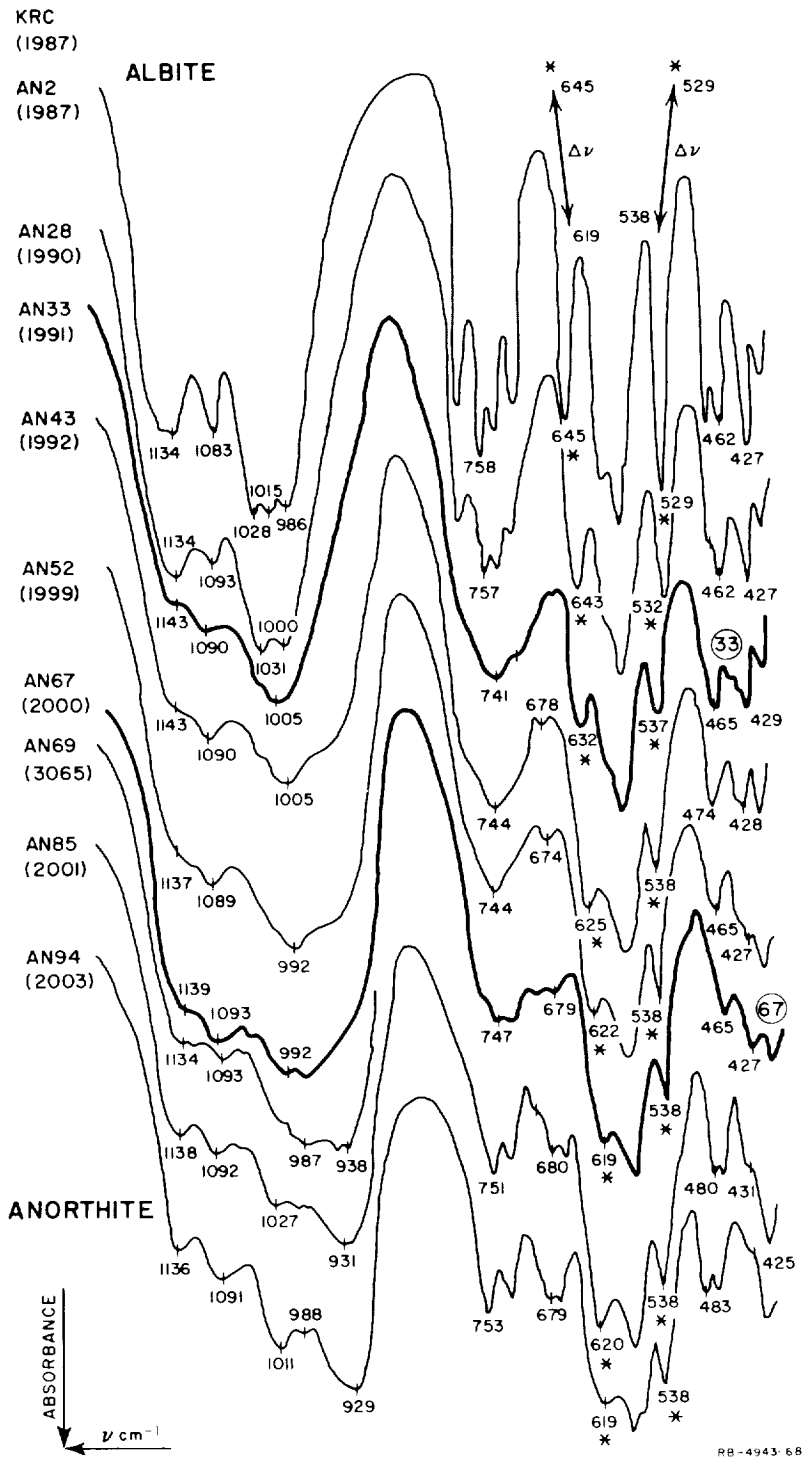

Fig. 38 Absorption spectra for plagioclase feldspar tektosilicates showing the spectral changes with increasing amounts of anorthite (An). Note the marked spectral changes at An_{33} and An_{66}. The curves are displaced vertically.

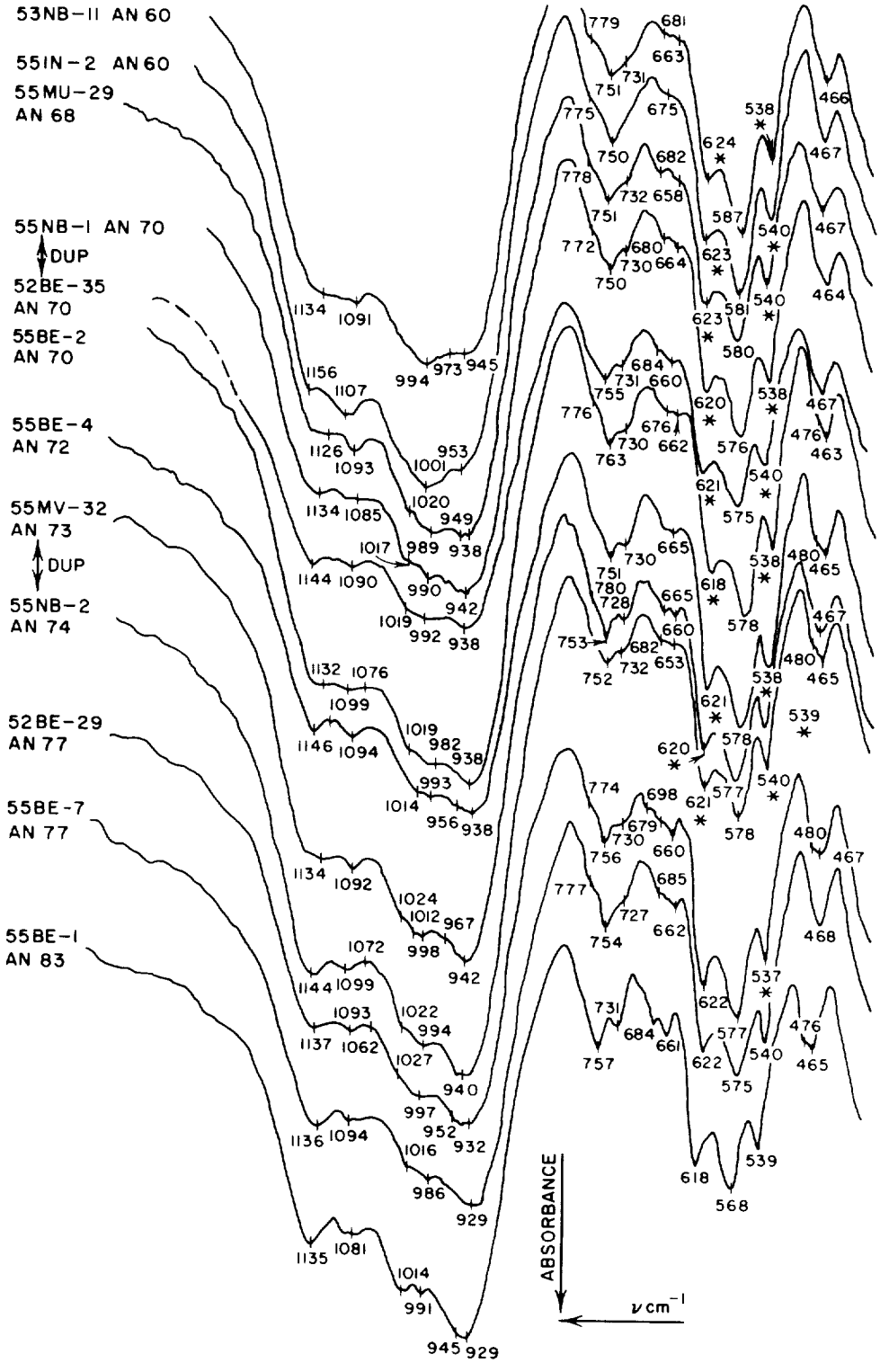

Fig. 39 Absorption spectra for basic plagioclase from An_{60} to An_{83}. Note the change in the importance of the 930 to 940 cm^{-1} peak. The curves are displaced vertically.

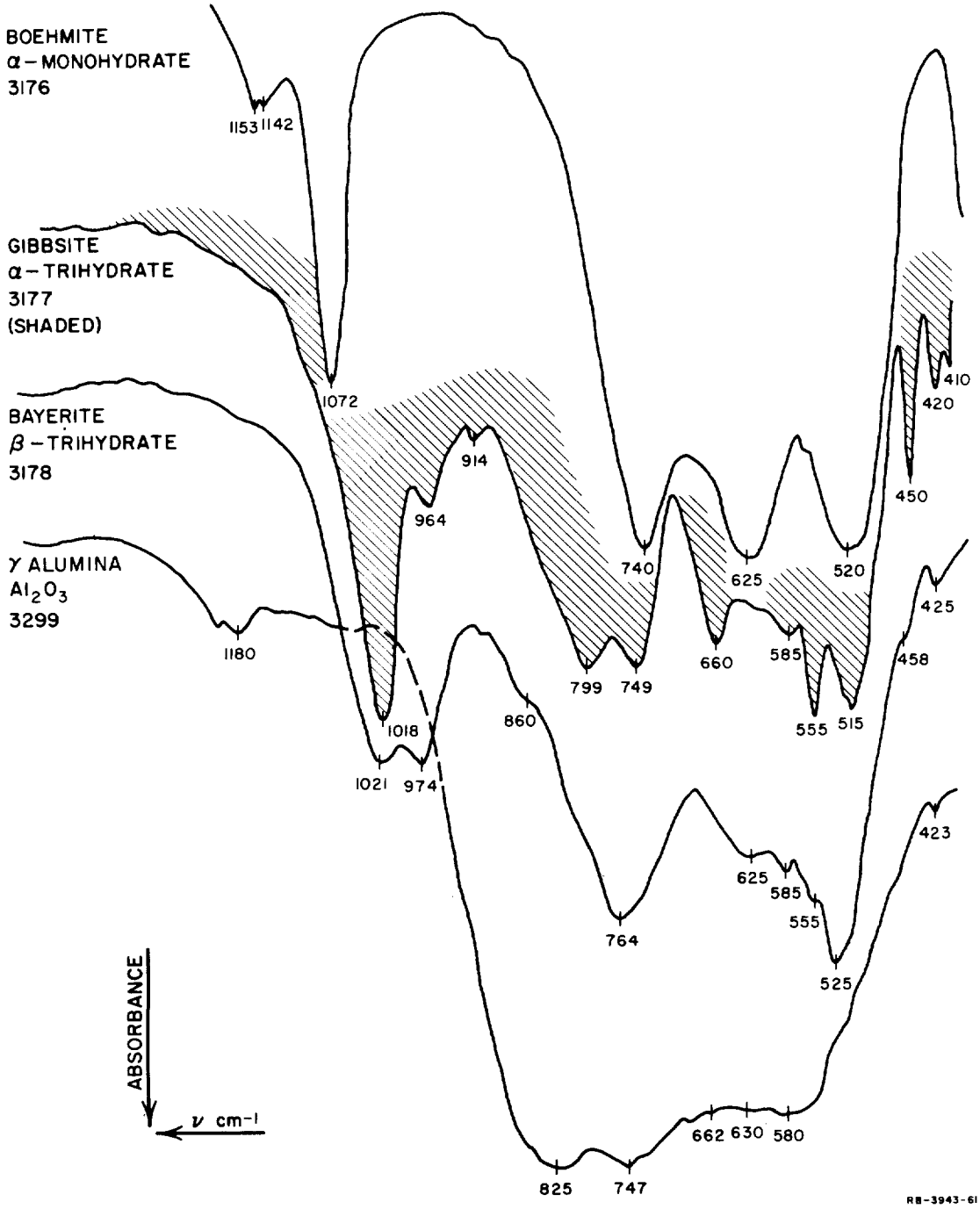

Fig. 40 Absorption spectra for alumina (γ-Al_2O_3) and its hydrates

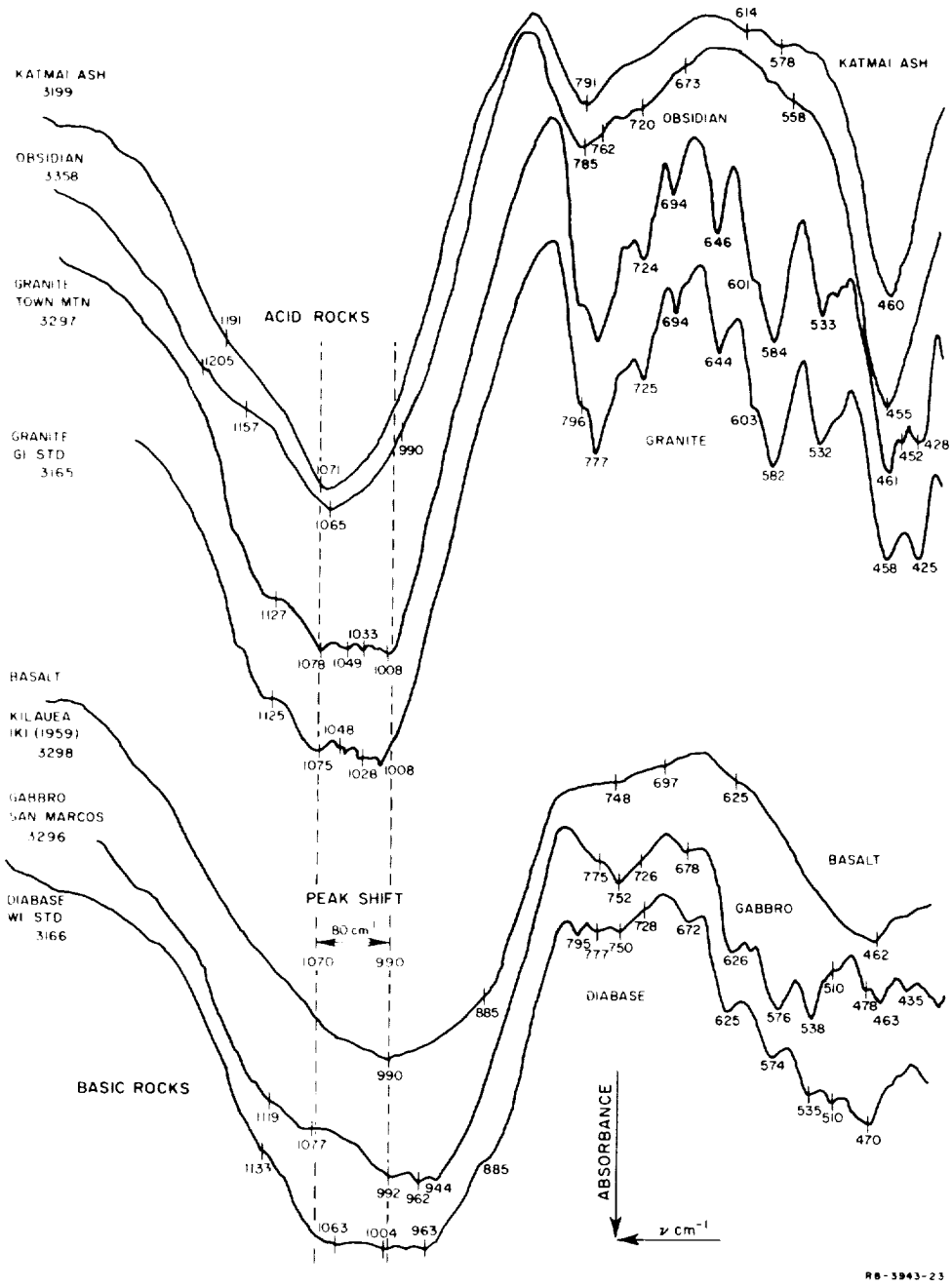

Fig. 41 Comparison of absorption spectra for a group of acid rocks (upper four curves) and a group of basic rocks (lower three curves). Acid samples are from Katmai, Alaska, ash fall; obsidian as noted; granite from Town Mountain, California; and the G-1 standard granite. Basic samples are from the 1959 Kilauea Iki flow, Hawaii; gabbro as noted; and the W-1 standard diabase. The curves are displaced vertically. Note the marked shift in peak position around 990 to 1070 cm^{-1} between the two groups, regardless of the degree of crystallinity of the samples.

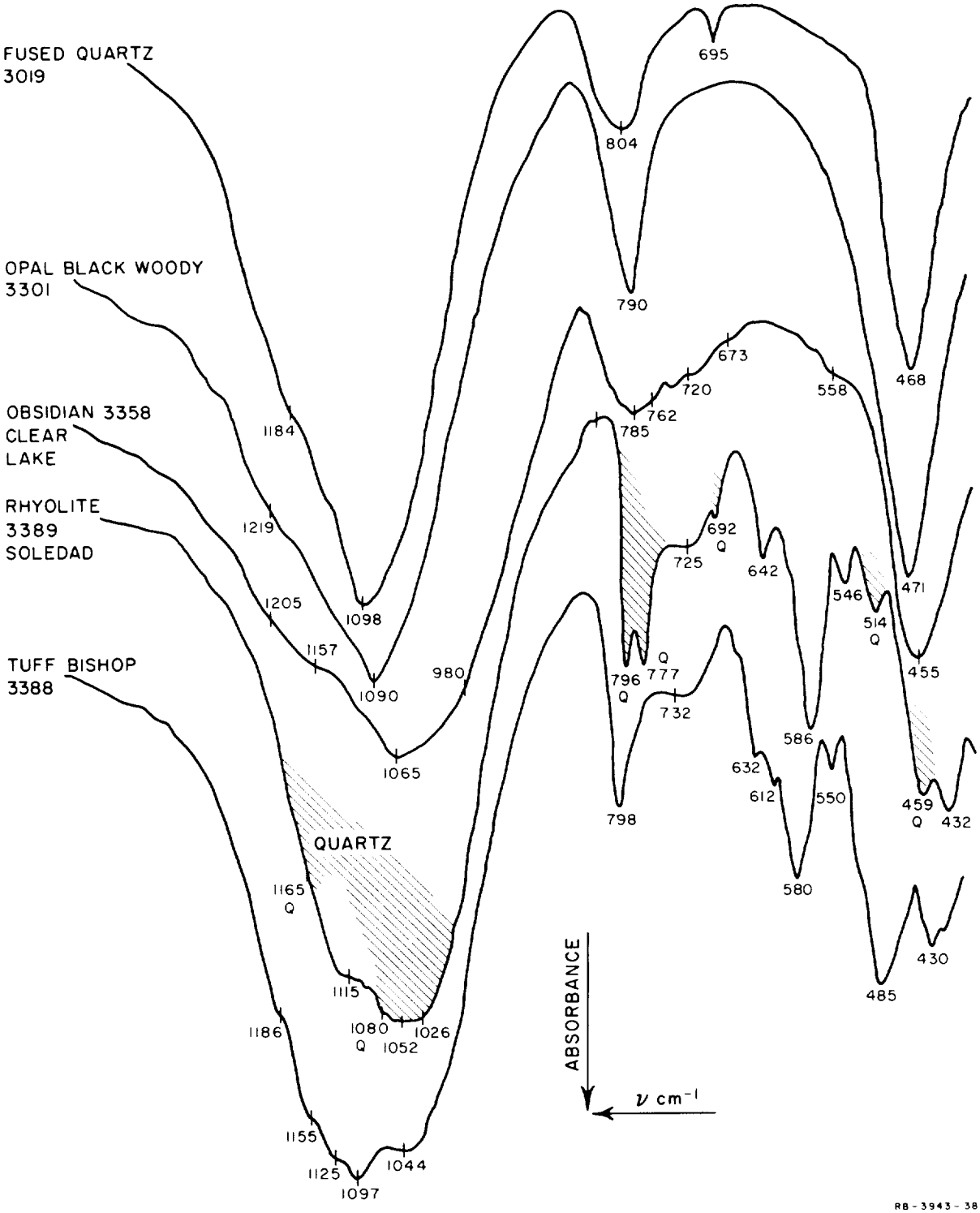

Fig. 42 Absorption spectra for silica-rich rocks compared with those for opal and obsidian. The curves are displaced vertically.

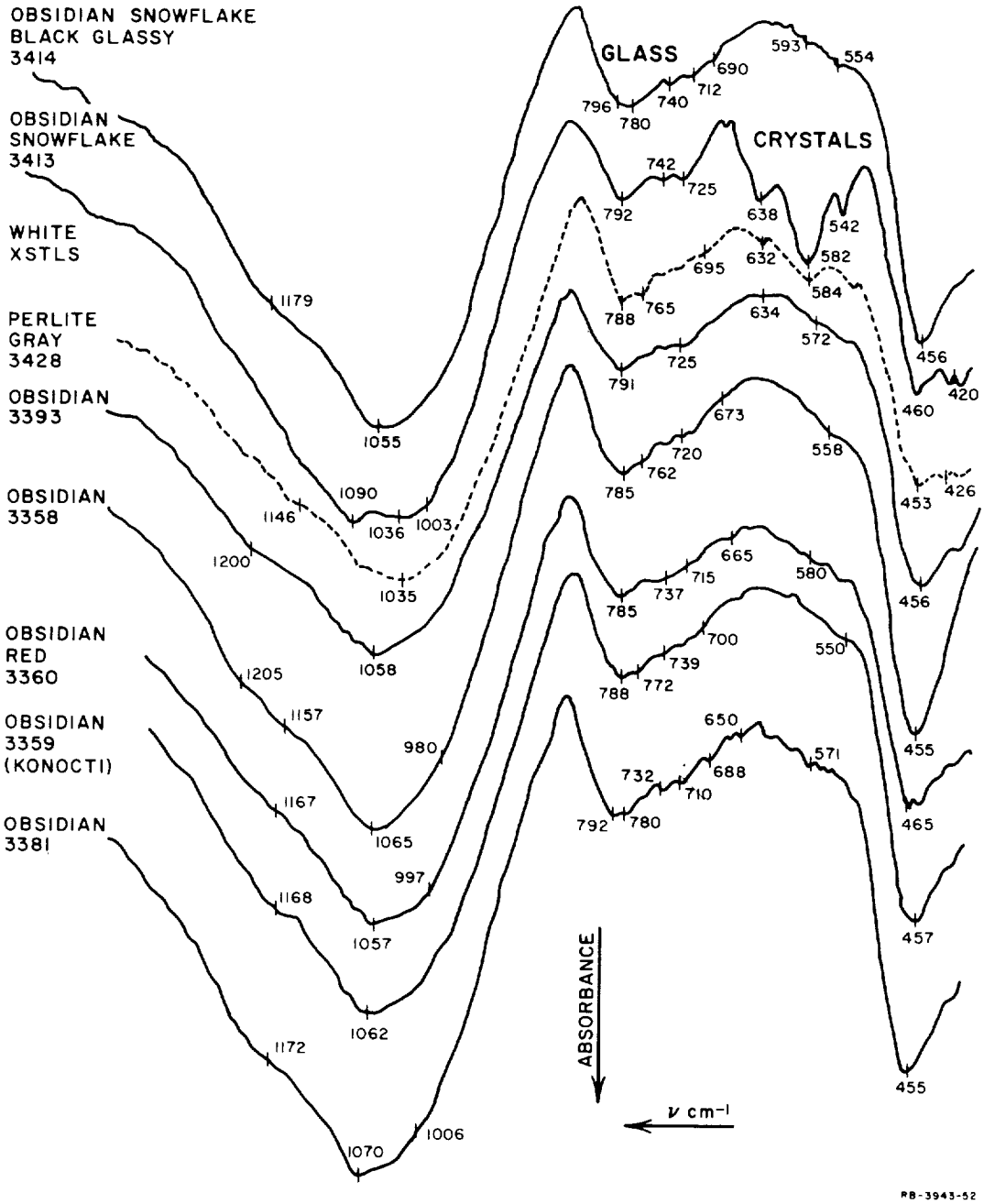

Fig. 43 Comparison of absorption spectra for obsidian samples and perlite. Snowflake obsidian shows both glassy and crystalline (feldspar) phases.

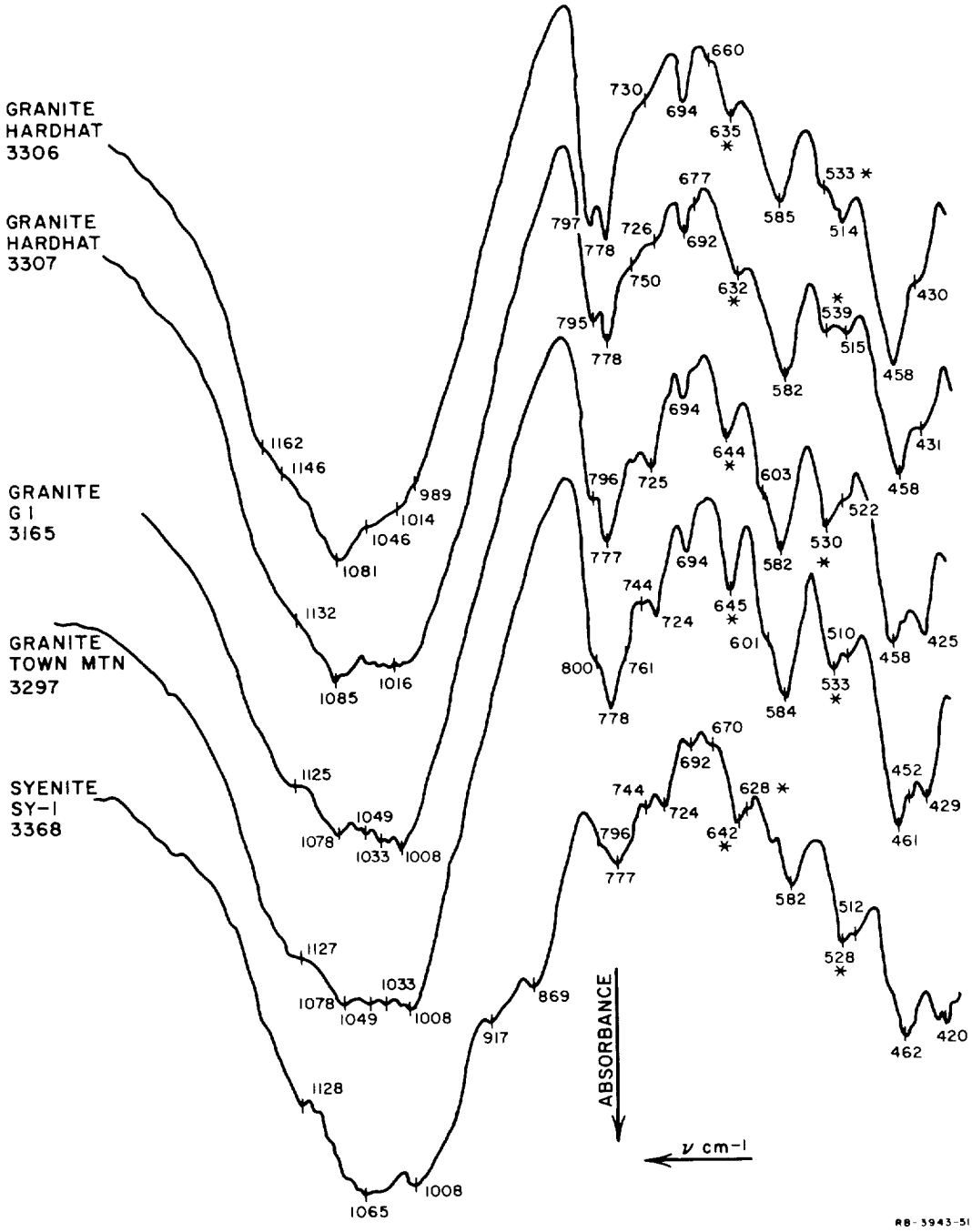

Fig. 44 Absorption spectra for coarse-grained acid rocks -- granite and syenite

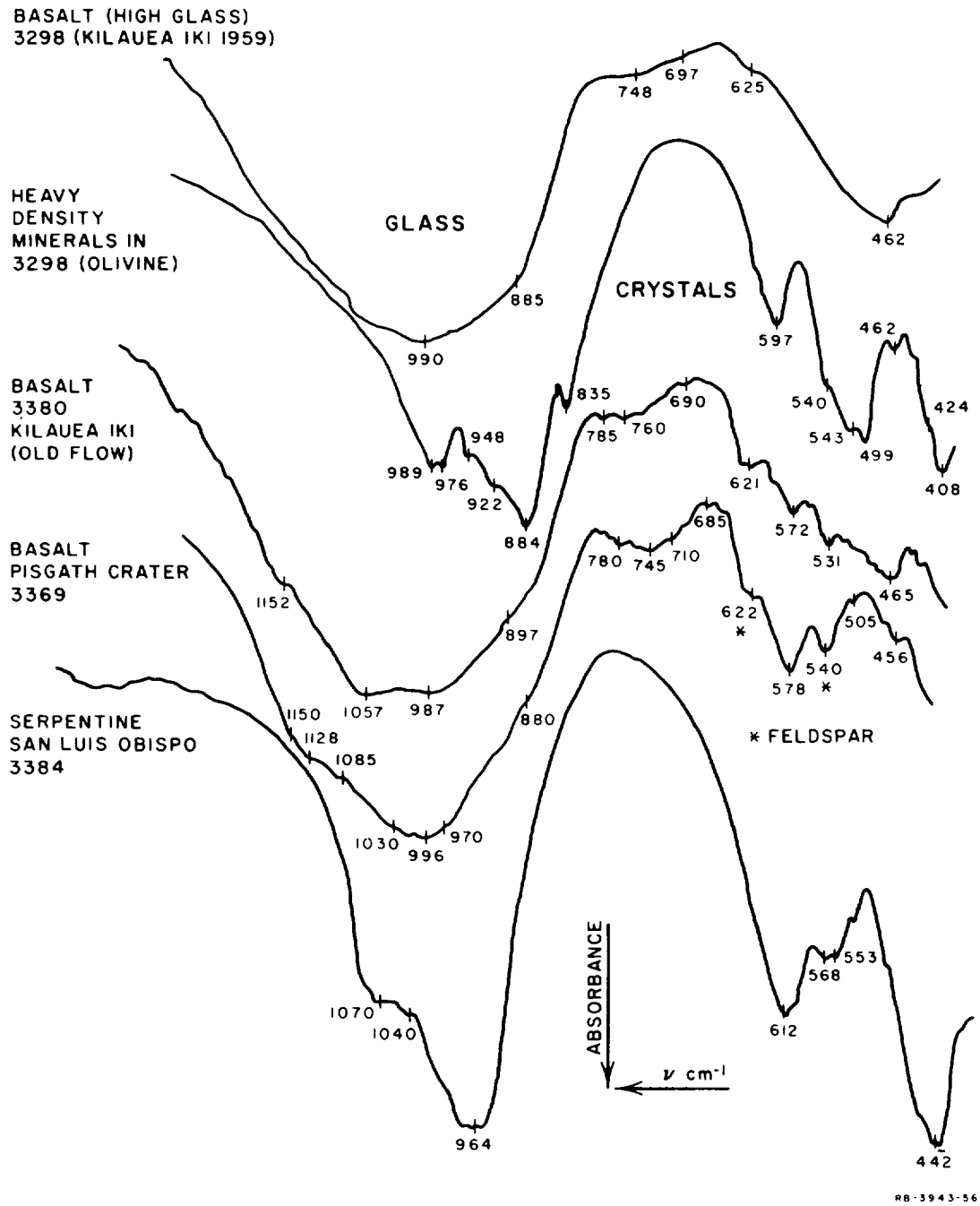

Fig. 45 Absorption spectra for fine-grained basic rocks -- basalts and serpentine

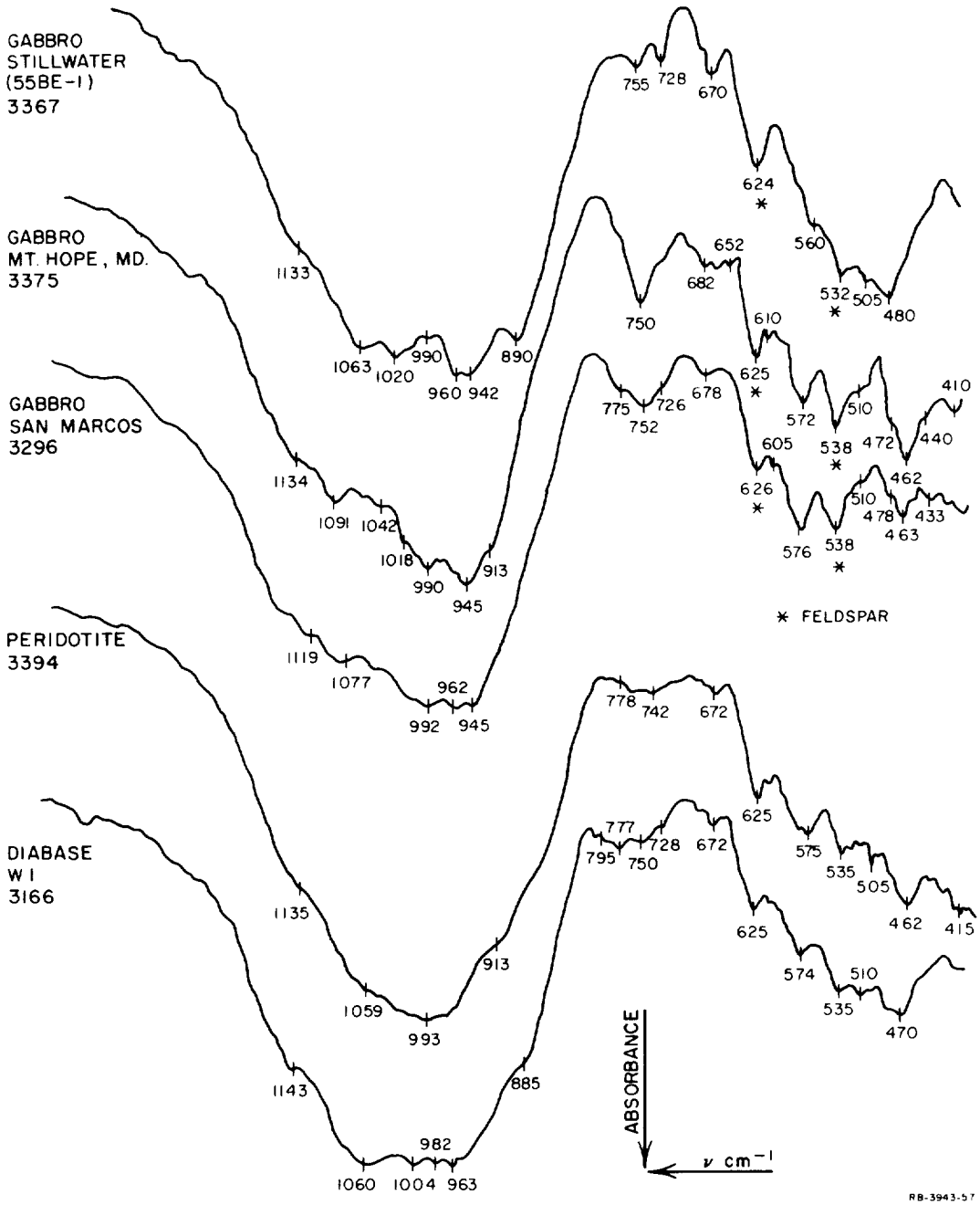

Fig. 46 Absorption spectra for coarse-grained basic rocks -- gabbro and diabase

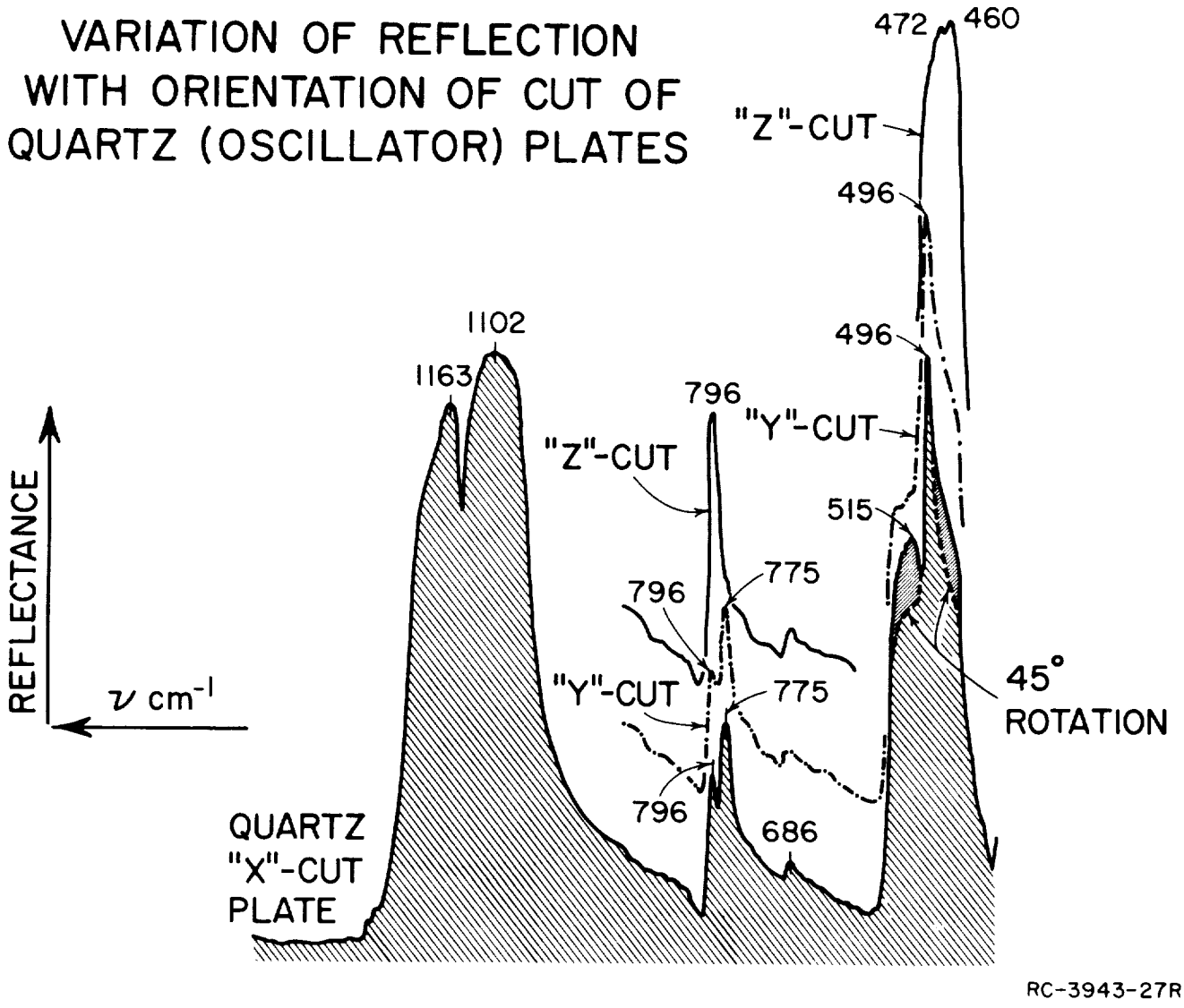

Fig. 47 Variation of specular reflection with orientation of cut of quartz (oscillator) plates. The curves are displaced vertically.

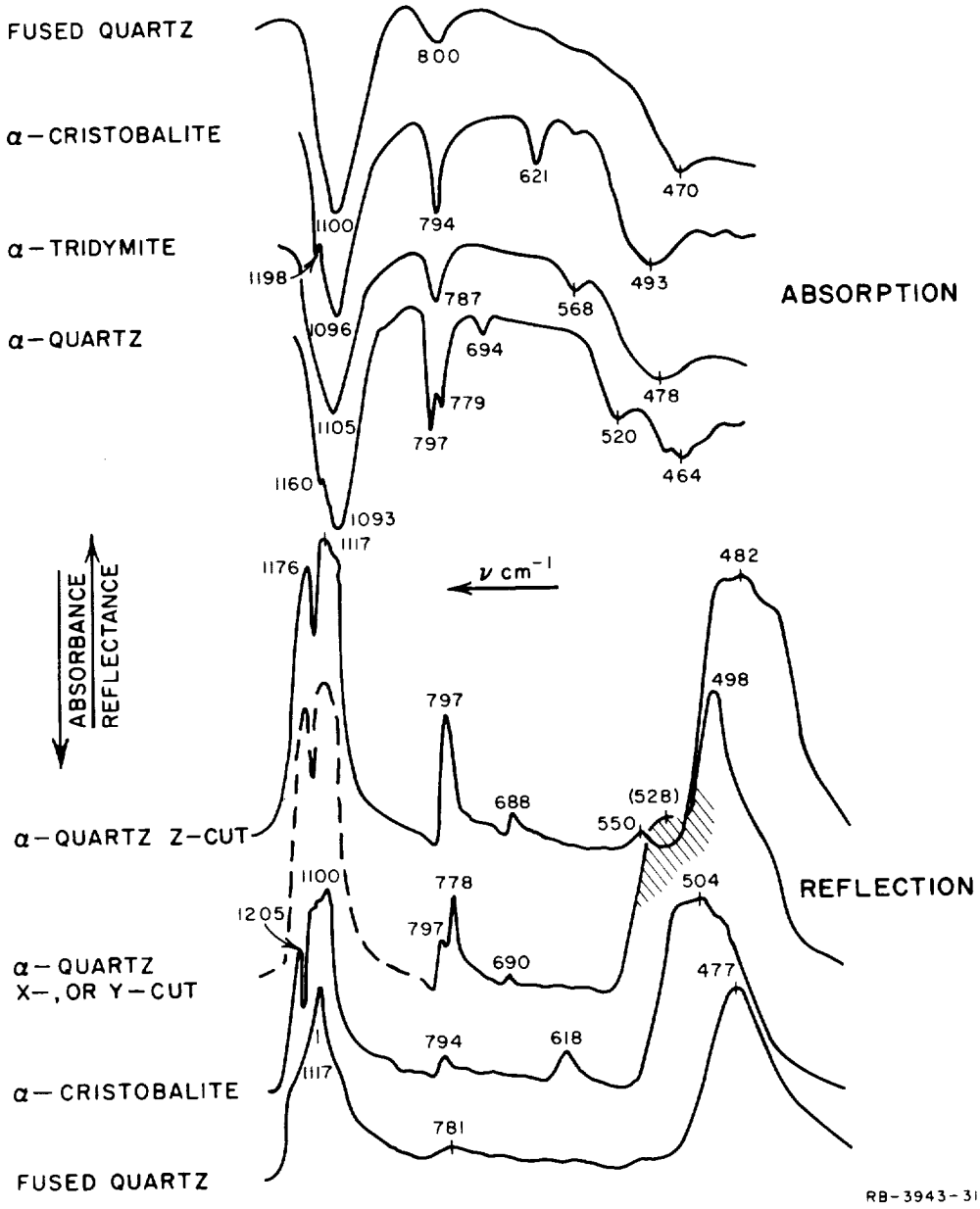

Fig. 48 Comparison of absorption and reflection spectra for various silica modifications. The curves are displaced vertically. The figure is redrawn from Figs. 1 and 2 of a paper by Sevchenko and Florinskaya, 1956.[37]

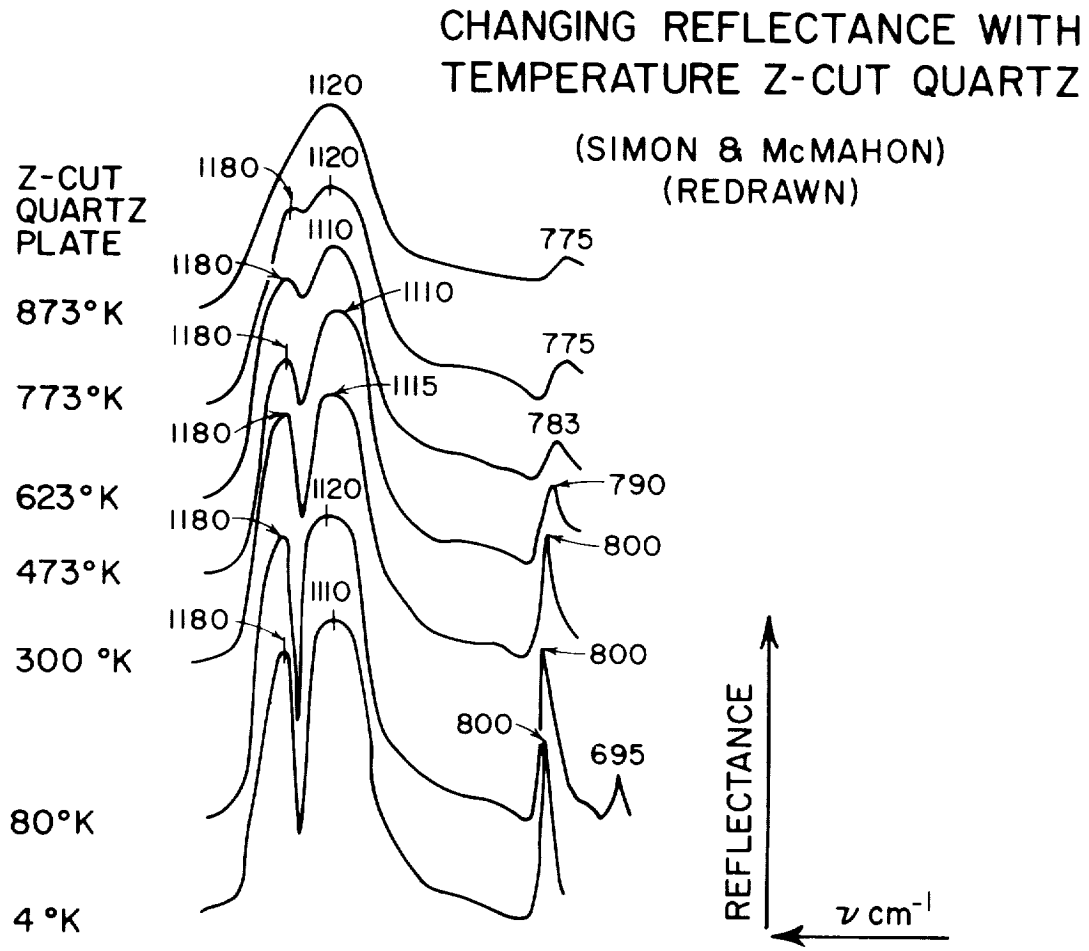

Fig. 49 Variation in reflectance with temperature for a Z-cut quartz plate. The angle of incidence of radiation is 20 deg, and the radiation was not polarized. The curves are displaced vertically. The figure is redrawn from Fig. 8 in Simon and McMahon, 1953. [10]

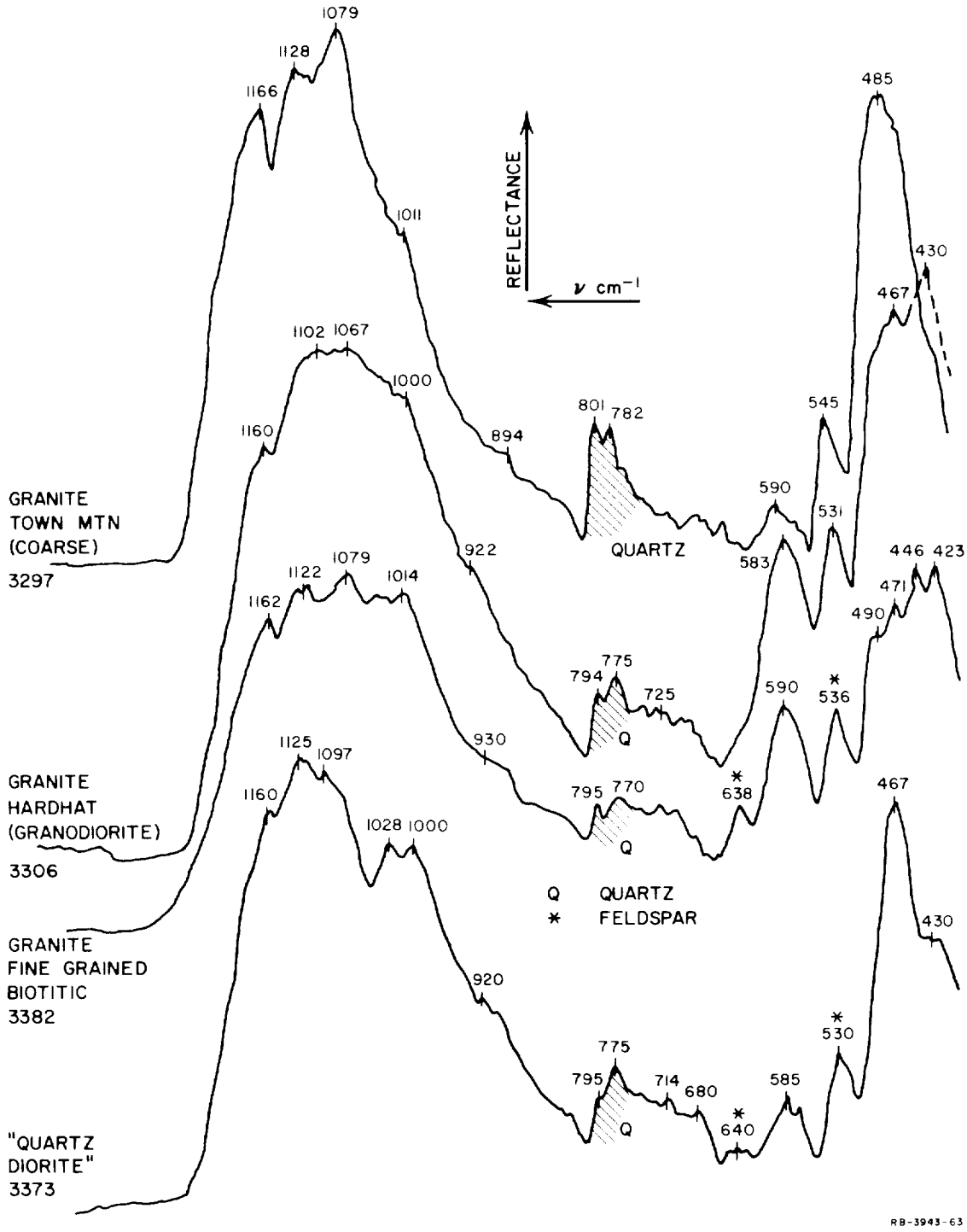

Fig. 50 Reflection spectra for granites. Note the quartz doublets at approximately 800 and 775 cm^{-1}.

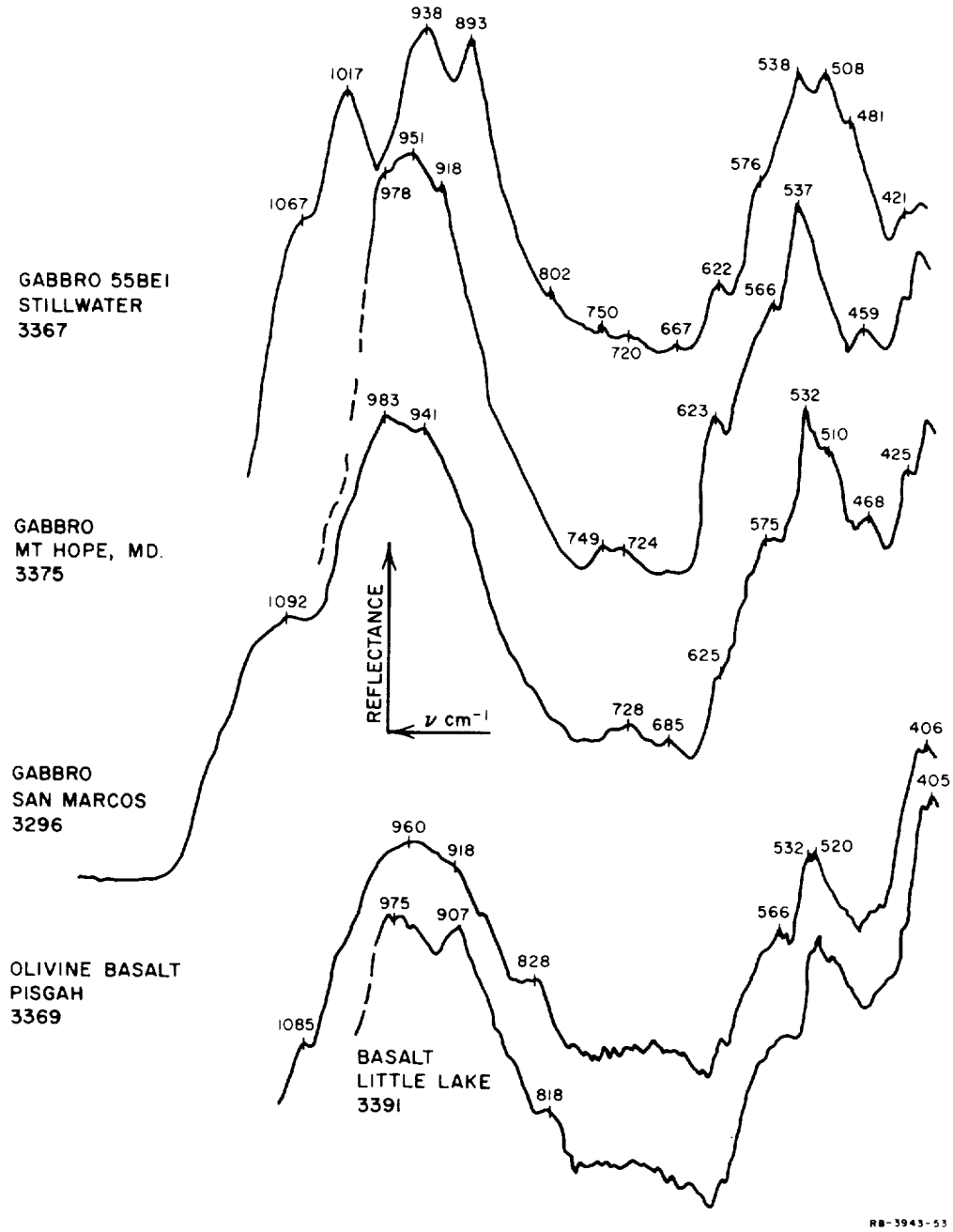

Fig. 51 Reflection spectra for gabbro and basalt. The reference beam was attenuated 40%.

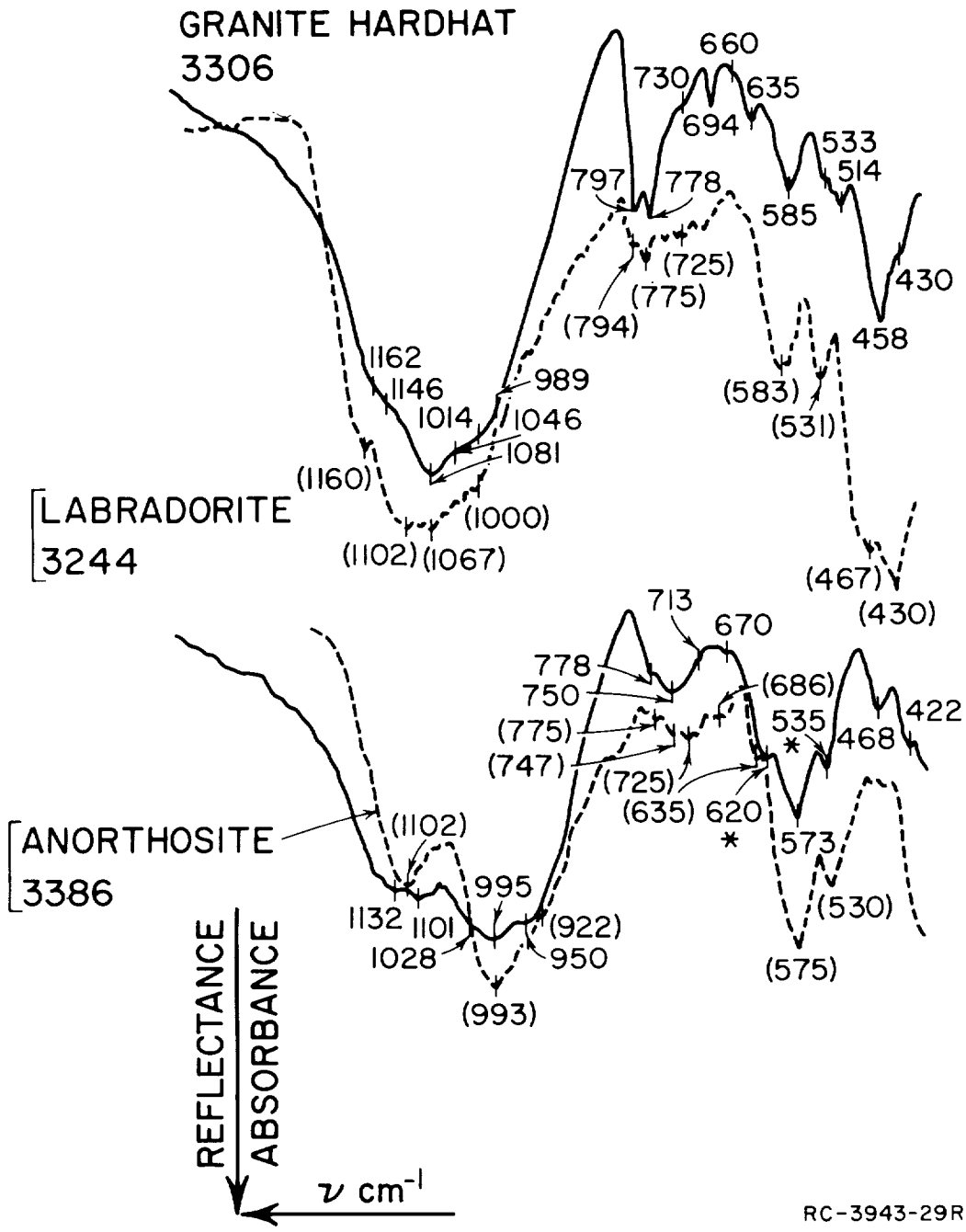

Fig. 52 Comparison between absorption (solid line) and reflection (dashed line) spectra for (a) granite from the Nevada Test Site, Mercury, Nevada, and (b) anorthosite and labradorite. The anorthosite is from the San Gabriel mountains, California. The reflection spectra have been inverted for comparison.

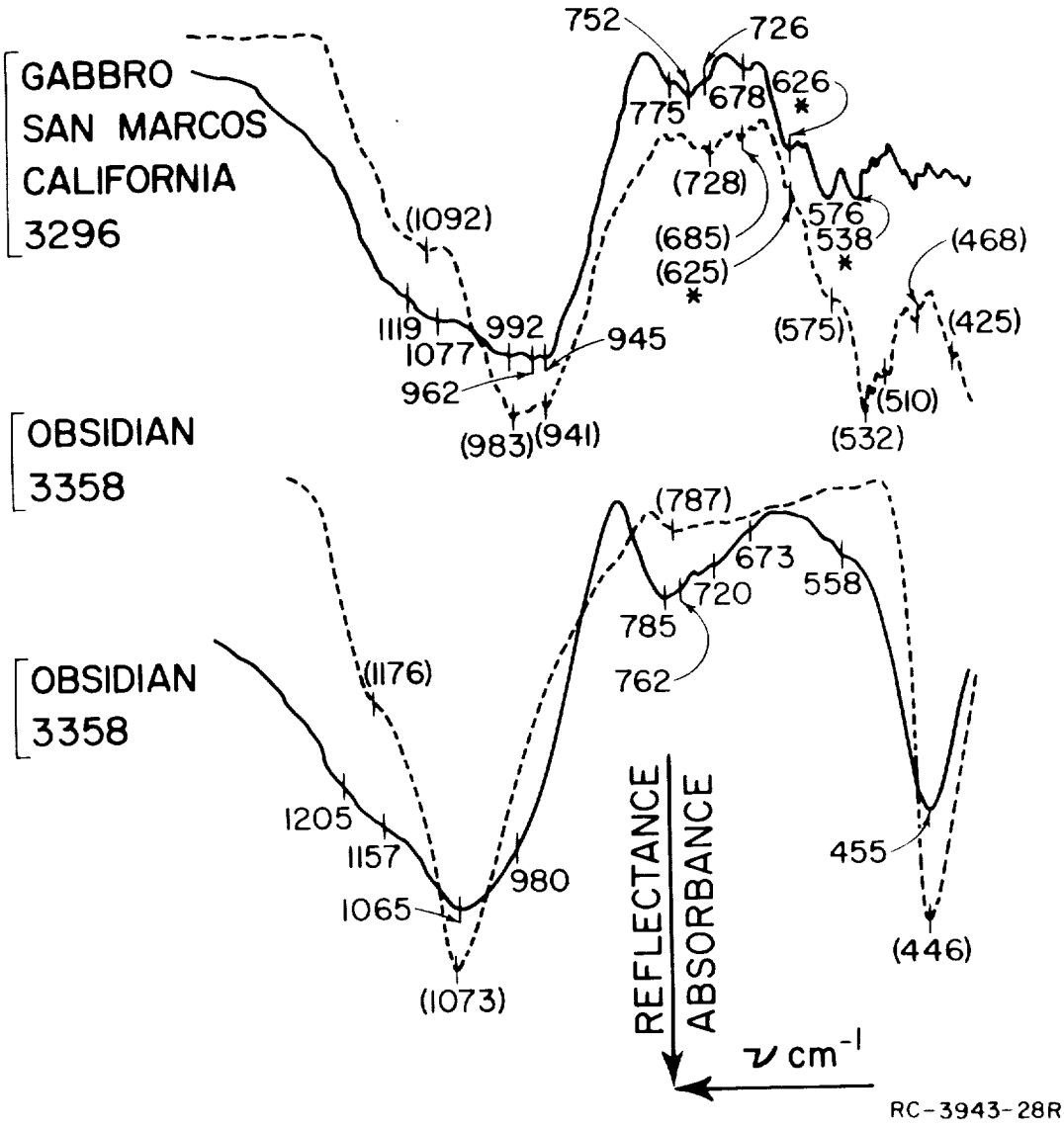

Fig. 53 Comparison between absorption (solid line) and reflection (dashed line) spectra for (a) gabbro from San Marcos, California, and (b) obsidian from Clear Lake, California. The reflection spectra have been inverted for comparison.

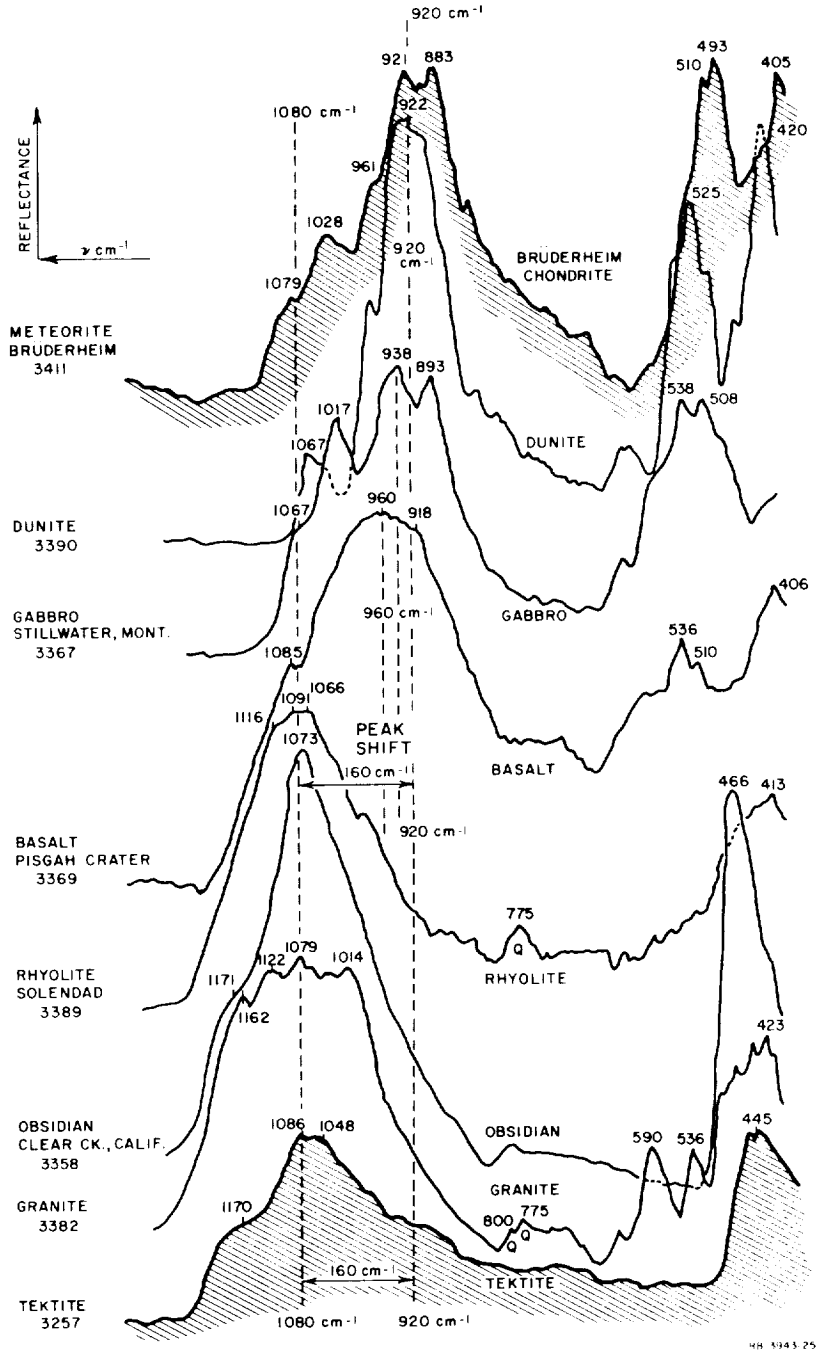

Fig. 54 Peak shift of 160 cm^{-1} for the reflection spectra for rock compositions between tektite and chondritic meteorites. Samples are chondrite from Bruderheim, Alberta: dunite from Twin Sisters, California; gabbro from Stillwater, Montana; basalt from Pisgah crater, California; rhyolite from Soledad, California; and others as noted. The reference beam was attenuated about 40%. The curves are displaced vertically.

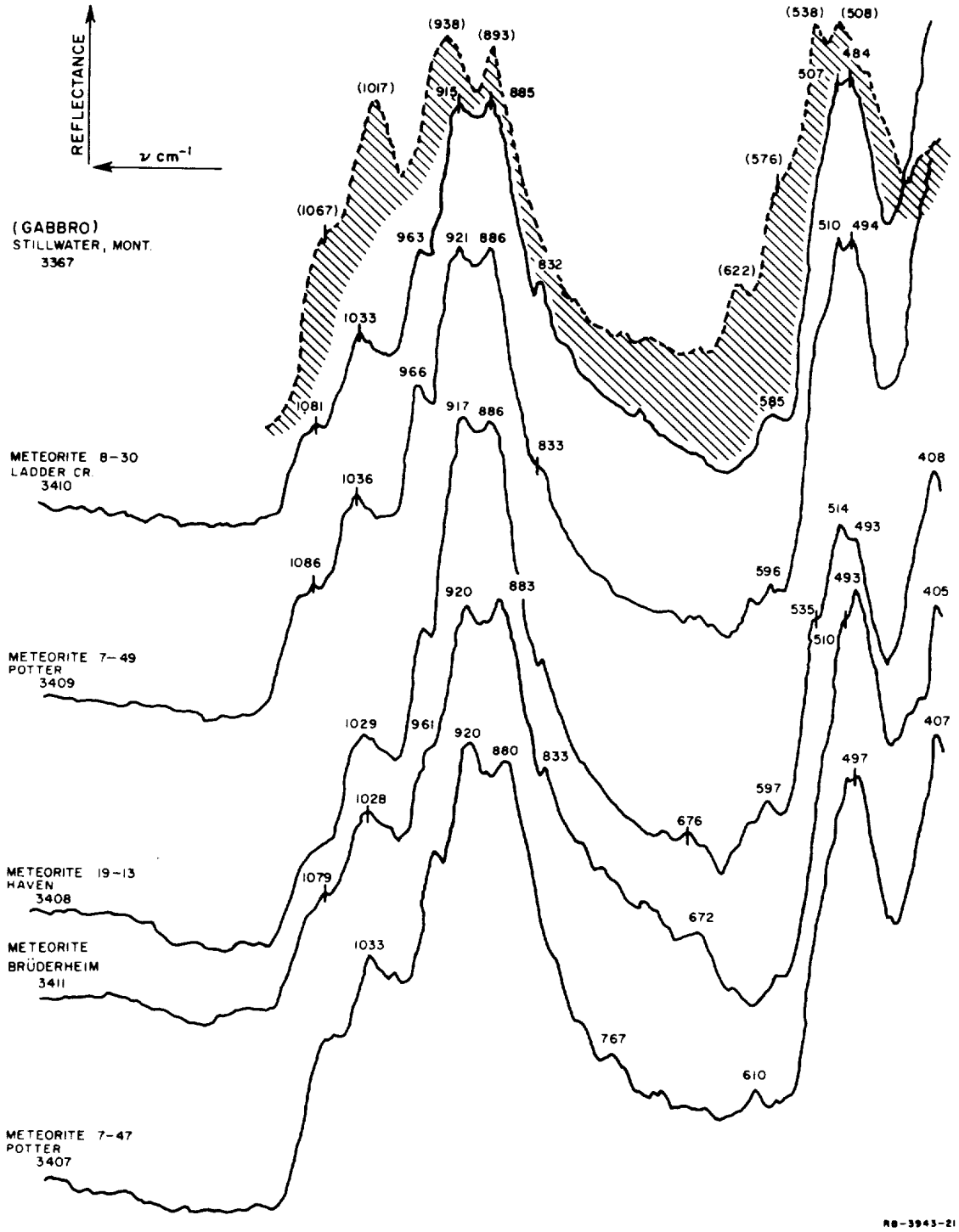

Fig. 55 Reflection spectra for chondritic meteorites compared with Stillwater gabbro. Meteorite samples are from various falls as noted. The reference beam was about 40% attenuated. The curves are displaced vertically.

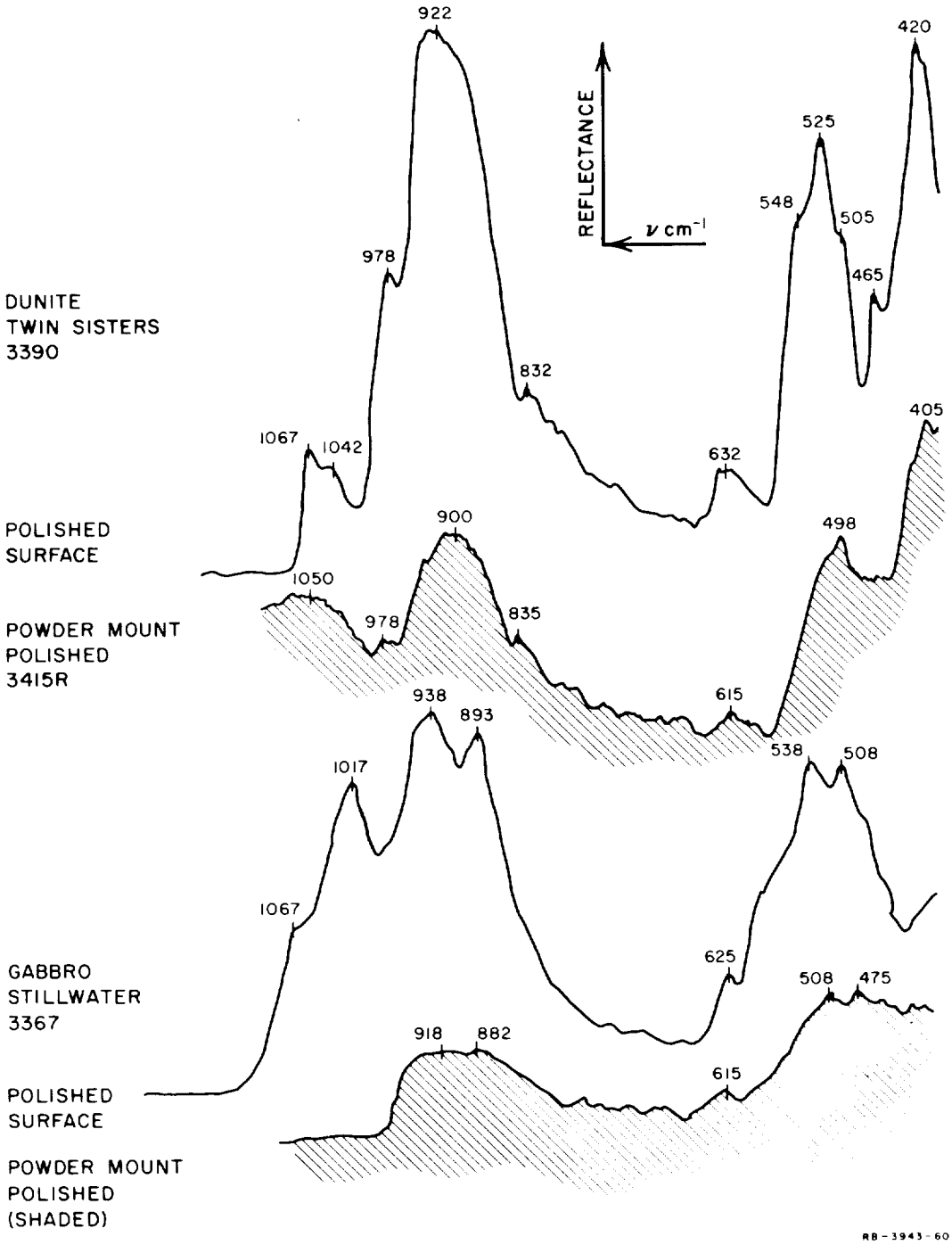

Fig. 56 Comparison of reflection spectra for rock surfaces and rock powders mounted in lucite plastic mounts. The reference beam was attenuated about 40% for both powder-mount samples.

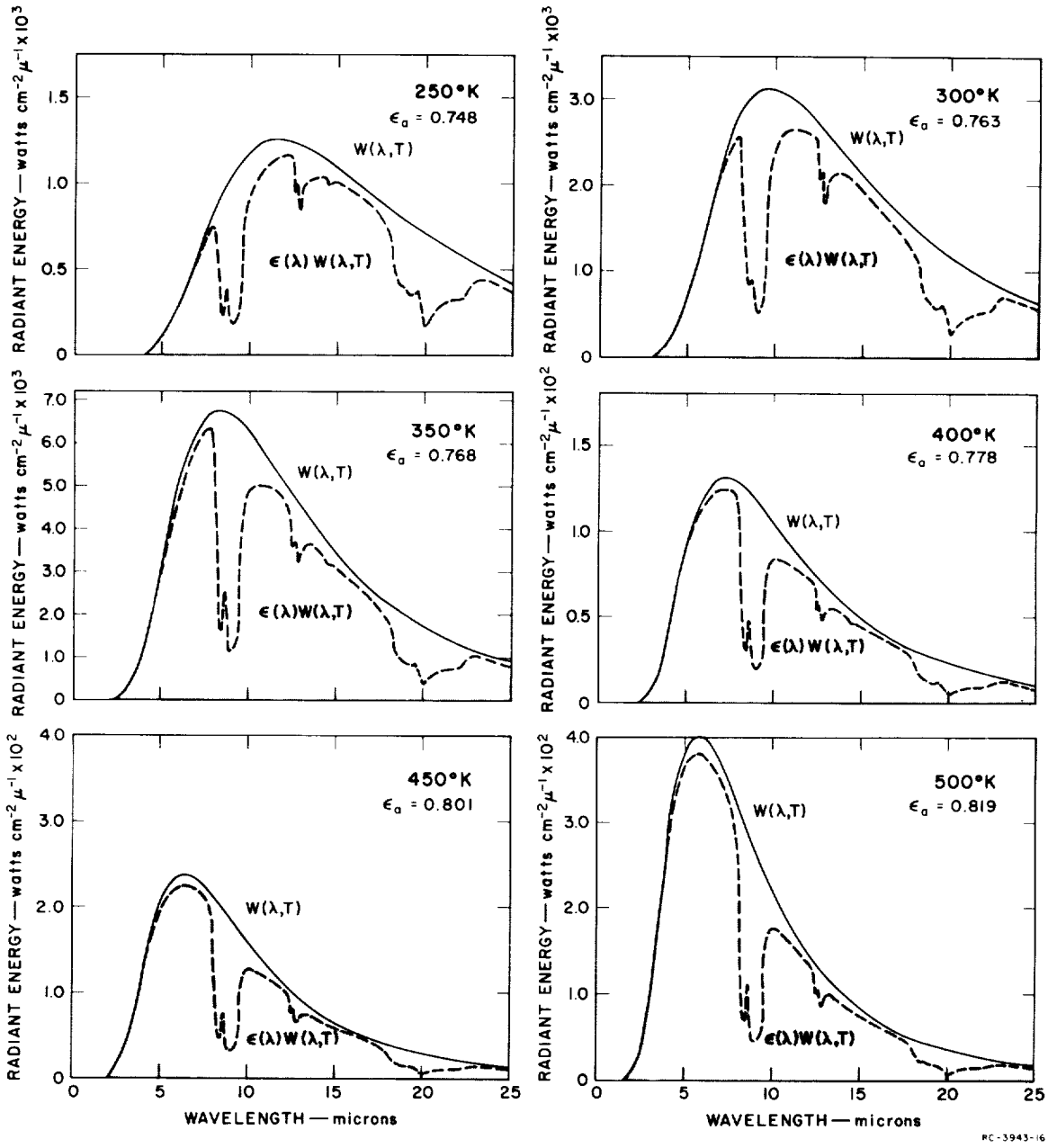

Fig. 57 Emittance of quartz and a blackbody as a function of wavelength and temperature

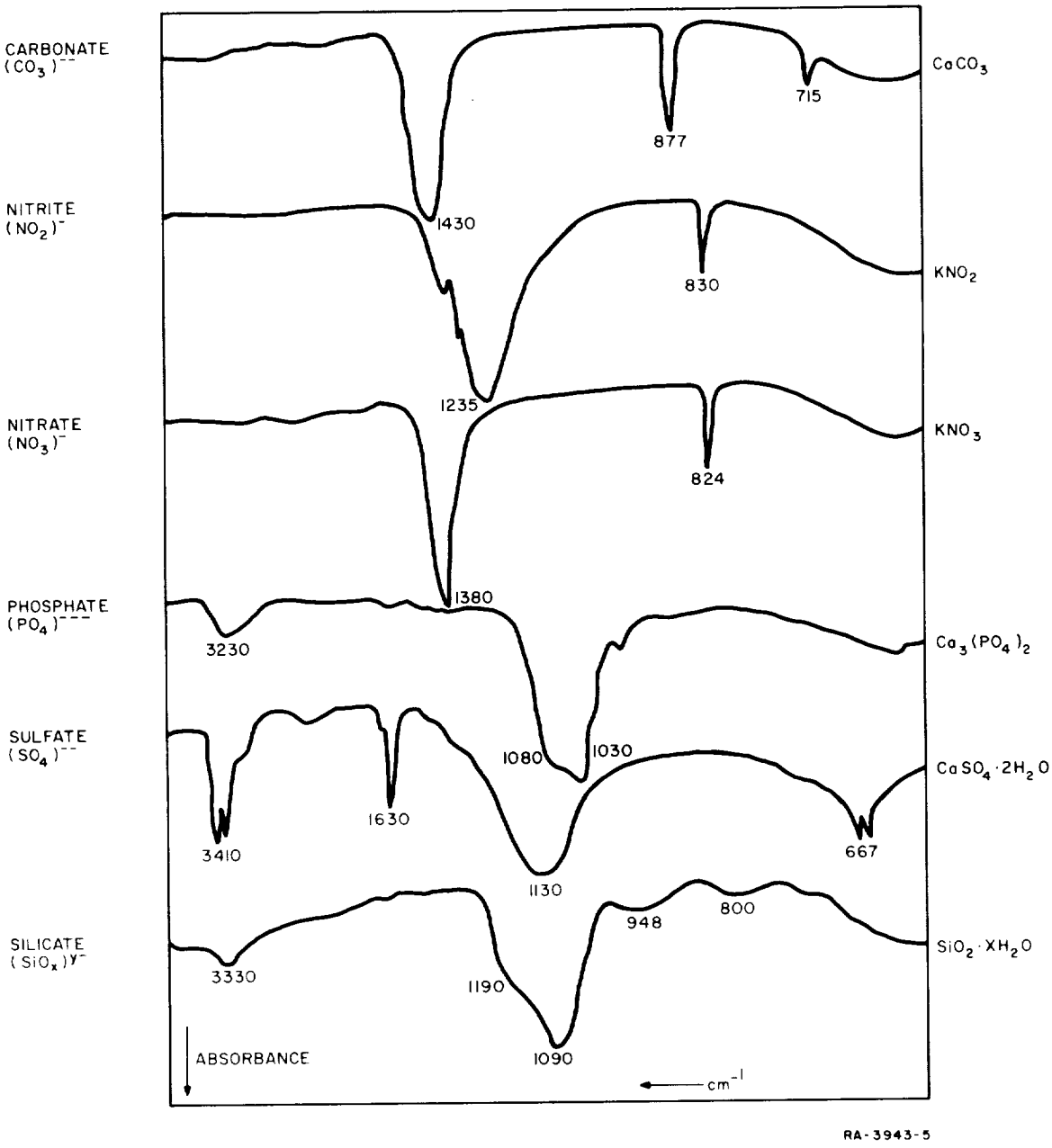

Fig. 58 Absorption spectra of the principal inorganic anions. This figure is redrawn from Miller and Wilkins, 1952.[18]

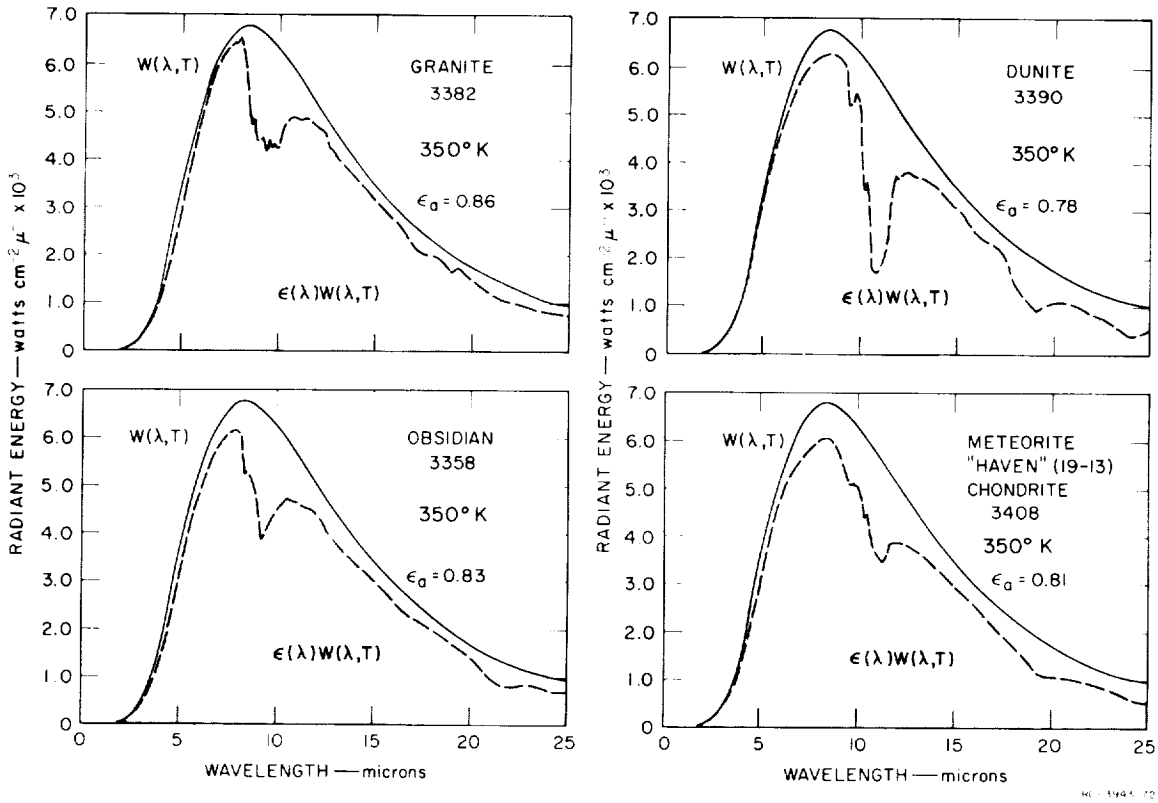

Fig. C.1 Emittance of granite, obsidian, dunite, and a stony chondritic meteorite as a function of wavelength at 350°K. Curves were calculated from reflectance data for the samples.

NASA-Langley, 1963 D-1871

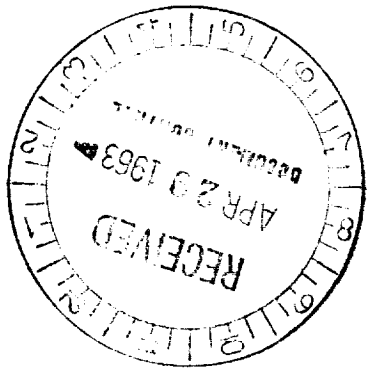
RECEIVED
APR 29 1953